Electronic Supplementary Material (ESI) for Dalton Transactions.

Supplementary Information

Phosphinoborenium cations stabilized by *N*-heterocyclic carbenes: synthesis, structure, and reactivity

Kinga Kaniewska-Laskowska,[a]* Anna Ordyszewska, [a] Tomasz Wojnowski,[a] Hanna Halenka,[a] Marcin Czapla,[b] Jarosław Chojnacki,[a] and Rafał Grubba[a]*

**corresponding author: kinga.kaniewska-laskowska@pg.edu.pl, rafal.grubba@pg.edu.pl*

[a]*Department of Inorganic Chemistry, Faculty of Chemistry and Advanced Materials Center, Gdańsk University of Technology, Narutowicza 11/12, 80-233 Gdańsk, Poland*

[b]*Laboratory of Quantum Chemistry, Department of Theoretical Chemistry, Faculty of Chemistry, University of Gdańsk, Wita Stwosza 63, 80-308 Gdańsk, Poland*

Table of Contents

Experimental section

Experimental details

All manipulations were performed under a dry argon atmosphere employing flame-dried Schlenk-type glassware on a vacuum line or in a glovebox. Solvents, dichloromethane and dichloromethane-d_2 were dried over P_2O_5 and distilled under argon. Pentane and petroleum ether were dried with sodium-potassium alloy and distilled under argon. Toluene was dried with K/benzophenone and also distilled under argon. C_6D_6, was purified with metallic sodium. 1D (^{1}H, ^{11}B, ^{31}P{^{1}H}, ^{31}P, ^{13}C, ^{27}Al, ^{19}F {^{1}H}, ^{19}F) and 2D NMR spectra were recorded on a Bruker AV400 MHz spectrometer (external standard TMS for ^{1}H and ^{13}C; $BF_3{\cdot}Et_2O$ for ^{11}B, 85% H_3PO_4 for ^{31}P; $[Al(H_2O)_6]^{3+}$ for ^{27}Al, $CFCl_3$ for ^{19}F) at ambient temperature. Reaction progress was monitored by ^{11}B, ^{31}P{^{1}H} and ^{31}P NMR spectra of reaction mixtures. Data were processed using Bruker's Topspin 3.5 software. Elemental analyses of all compounds were performed using Elementar Vario El Cube CHNS micro elemental analyzer. The principle of quantitative CHNS analysis is based on complete combustion of sample within high-temperature reactor, followed by an accurate and precise determination of produced elemental gases by TCD detector (thermal conductivity detector). $(Ph_2N)BBr_2$[1], $(iPr_2N)B(Br)PtBu_2$[1], $(Cy_2N)B(Br)PtBuPh$[2], $Li[Al(OC(CF_3)_3)_4]$[3], IMe_2[4,5] and $IiPr_2$[6] were prepared according to literature procedures.

Preparation of phosphinoborenium cations stabilized by NHC

Preparation of 2

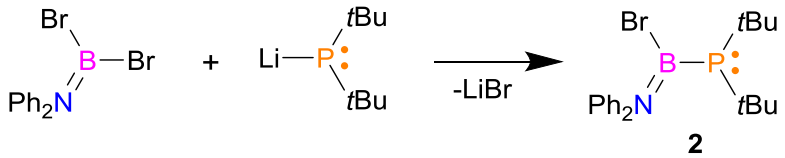

Scheme S 1. Synthesis of **2**

A solution of $(Ph_2N)BBr_2$ (0.678 g, 2 mmol) in toluene (6 mL) was added dropwise to a stirred suspension of tBu_2PLi (0.344 g, 2 mmol) in toluene (5 mL) at -30 °C. The mixture was allowed to warm to room temperature and stirred overnight. Afterwards, the solvent was removed under reduced pressure and obtained crude product was extracted with 30 mL of petroleum ether. Filtration to separate the white precipitate of LiCl, followed by the evaporation of the solvent under reduced pressure, afforded a light yellow oily residue. Slow cooling of the resulting oil layered with 3 mL of petroleum ether to -20°C gave suitable crystals for X-ray diffraction. Yield: 63% (0.512 g, 1.267 mmol).

Elemental analysis calc. for $C_{20}H_{28}BBrNP$ (404.13 g/mol): C, 59.44; H, 6.983; N, 3.47. Found: C, 59.27; H, 6.916; N, 3.43.

NMR data of 2

^{11}B NMR (C_6D_6): δ 43.6 (s).

^{31}P{^{1}H} NMR (C_6D_6): δ -14.7 (s).

^{1}H NMR (C_6D_6): δ 7.14 – 6.80 (10 H, m, overlapped signals of *o*-C***H***, *m*-C***H*** and *p*-C***H*** of Ph); 1.37 (18 H, d, $^3J_{P\text{-}H}$ = 11.7 Hz, C(C***H***$_3$)$_3$).

^{13}C{^{1}H} NMR (C_6D_6): δ 149.3 (bs, *ipso*-***C*** of Ph); 148.6 (bs, *ipso*-***C*** of Ph); 129.0 (bs, ***C***H of Ph); 128.8 (bs, ***C***H of Ph); 128.6 (s, ***C***H of Ph); 128.5 (bs, ***C***H of Ph); 126.2 (bs, ***C***H of Ph); 126.1 (s, ***C***H of Ph); 32.3 (d, $^1J_{CP}$ = 21.9 Hz, ***C***(CH$_3$)$_3$); 31.9 (d, $^2J_{CP}$ = 14.0 Hz, C(***C***H$_3$)$_3$).

General procedure of synthesis of phosphinoborenium salts

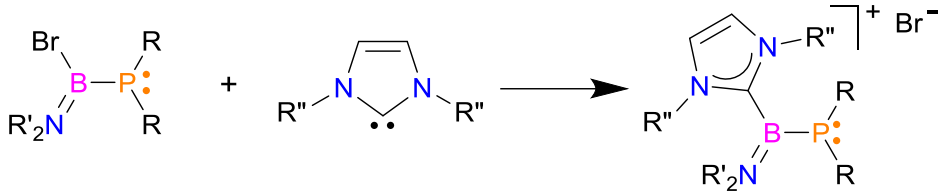

1 (PR_2= P*t*Bu$_2$, R'= *i*Pr) **a** (R"= *i*Pr) **1a** (PR_2= P*t*Bu$_2$, R'= *i*Pr, R"= *i*Pr)
2 (PR_2= P*t*Bu$_2$, R'= Ph) **b** R"= Me) **1b** (PR_2= P*t*Bu$_2$, R'= *i*Pr, R"= Me)
3 (PR_2= *t*BuPhP, R'= Cy) **2a** (PR_2= P*t*Bu$_2$, R'= Ph, R"= *i*Pr)
2b (PR_2= P*t*Bu$_2$, R'= Ph, R"= Me)
3a (PR_2= *t*BuPhP, R'= Cy, R"= *i*Pr)
3b (PR_2= *t*BuPhP, R'= Cy, R"= Me)

Scheme S 2. Synthesis of NHC-stabilized borenium cations

A solution of *N*-heterocyclic carbene NHC (**a** in petroleum ether, and **b** in toluene, 2 eq, 0.25 M, 2 mL) was added dropwise to a stirred solution of (bromo)phosphinoborane **1**-**3** (1 eq, 0.250 mmol) in petroleum ether (4 mL) at -30°C. The mixture was allowed to warm to room temperature and stirred overnight. Filtration to separate the colour (orange for reaction with **a**, yellow for reaction with **a**) precipitate of borenium cations, followed by the evaporation of all the volatiles of the remaining solid under reduced pressure, yielded 67 to 90% crude phosphinoborenium salt (**1a**-**3a**, **1b**-**3b**). Equimolar reactions of starting materials also lead to the desired borenium cations, however, with much lower yields.

Details for 1a

Single crystals suitable for X-ray diffraction were obtained from CH_2Cl_2 solution (1 mL) of **1a** layered with pentane (2 mL) stored at room temperature.

Yield: 78% (0.095 g, 0.195 mmol). **Elemental analysis** calc. for $C_{23}H_{48}BBrN_3P \cdot CH_2Cl_2$ (573.27 g/mol): C, 50.28; H, 8.791; N, 7.33. Found: C, 50.42 ; H, 8.721; N, 7.46.

NMR data of 1a

^{11}B NMR (CD_2Cl_2): δ 40.2 (s).

^{31}P{^{1}H} NMR (CD_2Cl_2): δ 24.2 (s).

^{1}H NMR (CD_2Cl_2): δ 8.07 (s, 2 H, ***H***C=C***H*** of I*i*Pr$_2$); 4.73 (dsept, 1 H, $^3J_{HH}$ = 7.2 Hz, $^4J_{PH}$ = 2.0 Hz, C***H***(CH$_3$)$_2$); 4.62 (dsept, 2 H, $^3J_{HH}$ = 6.7 Hz, $^5J_{PH}$ = 1.9 Hz, C***H***(CH$_3$)$_2$ of I*i*Pr$_2$); 3.47 (sept, 1 H, $^3J_{HH}$ = 7.0 Hz, C***H***(CH$_3$)$_2$); 1.60 (d, 6 H, $^3J_{HH}$ = 6.7 Hz, CH(C***H***$_3$)$_2$ of I*i*Pr$_2$); 1.50 (d, 6 H, $^3J_{HH}$ = 6.7 Hz, CH(C***H***$_3$)$_2$ of I*i*Pr$_2$); 1.48 (d, 6 H, $^3J_{HH}$ = 7.2 Hz, CH(C***H***$_3$)$_2$); 1.32 (d, 6 H, $^3J_{HH}$ = 7.0 Hz, CH(C***H***$_3$)$_2$); 1.19 (d, 18 H, $^3J_{PH}$ = 12.7 Hz, C(C***H***$_3$)$_3$).

^{13}C{^{1}H} NMR (CD_2Cl_2): δ 122.0 (s, H***C***=***C***H of I*i*Pr$_2$); 56.2 (s, ***C***H(CH$_3$)$_2$); 55.8 (d, $^3J_{CP}$ = 6.0 Hz, ***C***H(CH$_3$)$_2$); 52.4 (d, $^4J_{CP}$ = 7.6 Hz, ***C***H(CH$_3$)$_2$ of I*i*Pr$_2$); 33.3 (d, $^1J_{CP}$ = 19.4 Hz, ***C***(CH$_3$)$_3$); 32.8 (d, $^2J_{CP}$ = 11.8 Hz, C(***C***H$_3$)$_3$); 25.4 (s, CH(***C***H$_3$)$_2$); 24.9 (s, CH(***C***H$_3$)$_2$ of I*i*Pr$_2$); 24.5 (s, CH(***C***H$_3$)$_2$); 22.5 (d, $^5J_{CP}$ = 2.7 Hz, CH(***C***H$_3$)$_2$ of I*i*Pr$_2$). The carbene carbon atom was not detected at the ^{13}C{^{1}H} spectrum; however, chemical shift of carbene carbon atom was identified at 149.1 ppm based on ^{13}C ^{1}H HMBC spectrum (a coupling of ***H***C=C***H*** of I*i*Pr$_2$ protons with carbene carbon atom).

Details for 1b

Yield: 82% (0.089 g, 0.206 mmol).

NMR data of 1b

^{11}B NMR (CD_2Cl_2): δ 40.9 (s).

^{31}P{^{1}H} NMR (CD_2Cl_2): δ 5.1 (s).

^{1}H NMR (CD_2Cl_2): δ 7.96 (s, 2 H, ***H***C=C***H*** of IMe$_2$); 5.02 (bm, 1 H, C***H***(CH$_3$)$_2$); 3.87 (s, 6 H, C***H***$_3$ of IMe$_2$); 3.43 (sept, 1 H, $^3J_{HH}$ = 6.9 Hz, C***H***(CH$_3$)$_2$); 1.38 (d, 6 H, $^3J_{HH}$ = 6.9 Hz, CH(C***H***$_3$)$_2$); 1.15 (d, 18 H, $^3J_{PH}$ = 12.4 Hz, C(C***H***$_3$)$_3$, overlapped with CH(C***H***$_3$)$_2$); 1.14 (d, 6 H, $^3J_{HH}$ = 6.9 Hz, CH(C***H***$_3$)$_2$, overlapped with C(C***H***$_3$)$_3$).

$^{13}C\{^1H\}$ NMR (CD_2Cl_2): δ 125.5 (s, H***C***=***C***H of IMe_2); 55.2 (d, $^3J_{CP}$ = 20.4 Hz, ***C***H$(CH_3)_2$); 53.6 (s, ***C***H$(CH_3)_2$, overlapped with solvent); 38.4 (d, $^4J_{CP}$ = 2.7 Hz, ***C***H_3 of IMe_2); 32.8 (d, $^1J_{CP}$ = 18.1 Hz, ***C***$(CH_3)_3$, overlapped with C(***C***$H_3)_3$); 32.8 (d, $^2J_{CP}$ = 12.7 Hz, C(***C***$H_3)_3$, overlapped with ***C***$(CH_3)_3$); 24.7 (s, CH(***C***$H_3)_2$); 23.2 (d, $^4J_{CP}$ = 4.0 Hz, CH(***C***$H_3)_2$). The carbene carbon atom was not detected at the $^{13}C\{^1H\}$ spectrum; however, chemical shift of carbene carbon atom was identified at 151.8 ppm based on ^{13}C ^1H HMBC spectrum (couplings of ***H***C=C***H*** of IMe_2 and C***H***$_3$ of IMe_2 protons with carbene carbon atom).

Details for 2a

Yield: 90% (0.126 g, 0.226 mmol).

NMR data of 2a

^{11}B NMR (CD_2Cl_2): δ 40.7 (s).

$^{31}P\{^1H\}$ NMR (CD_2Cl_2): δ 47.1 (s).

^1H NMR (CD_2Cl_2): δ 7.86 (s, 2 H, ***H***C=C***H*** of I*i*Pr_2); 7.42 – 7.30 (m, 2 H, overlapped signals of C***H*** of Ph); 7.23 – 7.07 (m, 6 H, overlapped signals of C***H*** of Ph); 6.80 – 6.75 (m, 2 H, overlapped signals of C***H*** of Ph); 5.04 (bm, 2 H, C***H***$(CH_3)_2$ of I*i*Pr_2); 1.62 (d, 6 H, $^3J_{HH}$ = 6.6 Hz, CH(C***H***$_3)_2$ of I*i*Pr_2); 1.24 (bd, 6 H, $^3J_{HH}$ = 6.0 Hz, CH(C***H***$_3)_2$ of I*i*Pr_2); 0.99 (d, 18 H, $^3J_{PH}$ = 13.5 Hz, C(C***H***$_3)_3$).

$^{13}C\{^1H\}$ NMR (CD_2Cl_2): δ 148.5 (s, *ipso*-***C*** of Ph); 148.3 (s, *ipso*-***C*** of Ph); 129.7 (s, ***C***H of Ph); 129.6 (s, ***C***H of Ph); 128.4 (s, ***C***H of Ph); 128.0 (s, ***C***H of Ph); 127.5 (s, ***C***H of Ph); 126.0 (s, ***C***H of Ph); 122.1 (s, H***C***=***C***H of I*i*Pr_2); 52.5 (d, $^4J_{CP}$ = 10.3 Hz, ***C***H$(CH_3)_2$ of I*i*Pr_2); 34.7 (d, $^1J_{CP}$ = 9.5 Hz, ***C***$(CH_3)_3$); 32.1 (d, $^2J_{CP}$ = 9.1 Hz, C(***C***$H_3)_3$); 23.7 (s, CH(***C***$H_3)_2$ of I*i*Pr_2); 23.4 (d, $^5J_{CP}$ = 2.2 Hz, CH(***C***$H_3)_2$ of I*i*Pr_2). The carbene carbon atom was not detected at the $^{13}C\{^1H\}$ spectrum; however, chemical shift of carbene carbon atom was identified at 149.2 ppm based on ^{13}C ^1H HMBC spectrum (a coupling of ***H***C=C***H*** of I*i*Pr_2 protons with carbene carbon atom).

Details for 2b

Yield: 70% (0.087 g, 0.174 mmol).

NMR data of 2b

^{11}B NMR (CD_2Cl_2): δ 41.2 (s).

$^{31}P\{^1H\}$ NMR (CD_2Cl_2): δ 35.1 (s).

^{1}H NMR (CD_2Cl_2): δ 7.63 (s, 2 H, ***H***C=C***H*** of I*i*Pr$_2$); 7.40 – 7.04 (m, 10 H, overlapped signals of C***H*** of Ph); 4.00 (s, 6 H, C***H***$_3$ of IMe$_2$); 1.02 (d, 18 H, $^{3}J_{PH}$ = 13.4 Hz, C(C***H***$_3$)$_3$).

^{13}C{^{1}H} NMR (CD_2Cl_2): δ 148.5 (s, *ipso*-***C*** of Ph); 129.7 (bs, ***C***H of Ph); 128.1 (bs, ***C***H of Ph); 127.5 (bs, ***C***H of Ph); 125.3 (s, H***C***=***C***H of IMe$_2$); 37.7 (d, $^{4}J_{CP}$ = 9.4 Hz, ***C***H$_3$ of IMe$_2$); 34.6 (d, $^{1}J_{CP}$ = 10.0 Hz, ***C***(CH$_3$)$_3$); 32.3 (d, $^{2}J_{CP}$ = 10.0 Hz, C(***C***H$_3$)$_3$). The carbene carbon atom was not detected at the ^{13}C{^{1}H} spectrum; however, chemical shift of carbene carbon atom was identified at 151.7 ppm based on ^{13}C ^{1}H HMBC spectrum (couplings of ***H***C=C***H*** of IMe$_2$ and C***H***$_3$ of IMe$_2$ protons with carbene carbon atom).

Details for 3a

Yield: 83% (0.122 g, 0.207 mmol).

NMR data of 3a

^{11}B NMR (CD_2Cl_2): δ 41.0 (s).

^{31}P{^{1}H} NMR (CD_2Cl_2): δ -3.7 (s).

^{1}H NMR (CD_2Cl_2): δ 8.04 (s, 2 H, ***H***C=C***H*** of I*i*Pr$_2$); 7.29 (m, 1 H, *p*-C***H*** of Ph); 7.27 – 7.17 (m, 4 H, overlapped signals of *o*-C***H*** and *m*-C***H*** of Ph); 4.26 (sept, 2 H, $^{3}J_{HH}$ = 6.6 Hz, C***H***(CH$_3$)$_2$ of I*i*Pr$_2$); 4.16 (bm, 1 H, C***H*** of Cy); 2.78 (m, 1 H, C***H*** of Cy); 1.90 – 1.57 (m, 14 H, overlapped signals of C***H***$_2$ of Cy); 1.47 (d, $^{3}J_{HH}$ = 6.6 Hz, CH(C***H***$_3$)$_2$ of I*i*Pr$_2$); 1.29 (d, $^{3}J_{HH}$ = 6.6 Hz, CH(C***H***$_3$)$_2$ of I*i*Pr$_2$); 1.01 (d, 9 H, $^{3}J_{P\text{-}H}$ = 13.1 Hz, C(C***H***$_3$)$_3$); 0.99 – 0.83 (m, 6 H, overlapped signals of C***H***$_2$ of Cy).

^{13}C{^{1}H} NMR (CD_2Cl_2): δ 137.7 (d, $^{2}J_{CP}$ = 19.4 Hz, *o*-***C***H of Ph); 133.2 (d, $^{1}J_{CP}$ = 5.8 Hz, *ipso*-***C***P of Ph); 129.6 (s, *p*-***C***H of Ph); 128.6 (d, $^{3}J_{CP}$ = 9.1 Hz, *m*-***C***H of Ph); 121.7 (s, H***C***=***C***H of I*i*Pr$_2$); 65.9 (s, ***C***H of Cy); 63.9 (d, $^{3}J_{CP}$ = 20.1 Hz, ***C***H of Cy); 53.0 ($^{4}J_{CP}$ = 2.6 Hz, ***C***H(CH$_3$)$_2$ of I*i*Pr$_2$, overlapped with solvent); 36.0 (s, ***C***H$_2$ of Cy); 34.6 (s, s, ***C***H$_2$ of Cy); 33.3 (d, $^{1}J_{CP}$ = 11.9 Hz, ***C***(CH$_3$)$_3$); 31.6 (d, $^{2}J_{CP}$ = 11.5 Hz, C(***C***H$_3$)$_3$); 26.8 (s, ***C***H$_2$ of Cy); 26.7 (s, ***C***H$_2$ of Cy); 25.2 (s, ***C***H$_2$ of Cy); 25.0 (s, ***C***H$_2$ of Cy); 24.4 (s, CH(***C***H$_3$)$_2$ of I*i*Pr$_2$); 22.5 (s, CH(***C***H$_3$)$_2$ of I*i*Pr$_2$). The carbene carbon atom was not detected at the ^{13}C{^{1}H} spectrum; however, chemical shift of carbene carbon atom was identified at 147.6 ppm based on ^{13}C ^{1}H HMBC spectrum (couplings of ***H***C=C***H*** of I*i*Pr$_2$ protons with carbene carbon atom).

Details for 3b

Yield: 67% (0.089 g, 0.167 mmol).

NMR data of 3b

^{11}B NMR (CD_2Cl_2): δ 39.8 (s).

^{31}P{^{1}H} NMR (CD_2Cl_2): δ -4.4 (s).

^{1}H NMR (CD_2Cl_2): δ 7.94 (s, 2 H, ***H***C=C***H*** of IMe_2); 7.39 (m, 2 H, *m*-C***H*** of Ph); 7.35 – 7.25 (m, 3 H, overlapped signals of *o*-C***H*** and *p*-C***H*** of Ph); 3.81 (s, 6 H, C***H***$_3$ of IMe_2); 3.69 (m, 1 H, C***H*** of Cy); 2.90 (m, 1 H, C***H*** of Cy); 1.72 – 1.59 (m, 4 H, overlapped signals of C***H***$_2$ of Cy); 1.59 – 1.43 (m, 4 H, overlapped signals of C***H***$_2$ of Cy); 1.43 – 1.30 (m, 4 H, overlapped signals of C***H***$_2$ of Cy); 1.25 – 1.08 (m, 2 H, overlapped signals of C***H***$_2$ of Cy); 0.87 (d, 9 H, $^3J_{P\text{-}H}$ = 13.3 Hz, C(C***H***$_3$)$_3$); 0.82 – 0.62 (m, 4 H, overlapped signals of C***H***$_2$ of Cy).

^{13}C{^{1}H} NMR (CD_2Cl_2): δ 138.2 (d, $^3J_{CP}$ = 18.0 Hz, *m*-***C***H of Ph); 134.1 (d, $^1J_{CP}$ = 3.6 Hz, *ipso*-***C***P of Ph); 129.5 (s, *p*-***C***H of Ph); 128.6 (d, $^2J_{CP}$ = 9.1 Hz, *o*-***C***H of Ph); 125.3 (s, H***C***=***C***H of IMe_2); 64.5 (d, $^3J_{CP}$ = 18.4 Hz, ***C***H of Cy); 59.6 (bs, ***C***H of Cy); 38.3 (d, $^4J_{CP}$ = 2.6 Hz, ***C***H$_3$ of IMe_2); 35.8 (s, ***C***H$_2$ of Cy); 31.8 (d, $^1J_{CP}$ = 9.3 Hz, ***C***(CH$_3$)$_3$); 31.3 (s, ***C***H$_2$ of Cy); 30.7 (d, $^2J_{CP}$ = 11.7 Hz, C(***C***H$_3$)$_3$); 26.6 (s, ***C***H$_2$ of Cy); 25.4 (s, ***C***H$_2$ of Cy); 25.1 (s, ***C***H$_2$ of Cy); 25.0 (s, ***C***H$_2$ of Cy). The carbene carbon atom was not detected at the ^{13}C{^{1}H} spectrum; however, chemical shift of carbene carbon atom was identified at 150.7 ppm based on ^{13}C ^{1}H HMBC spectrum (couplings of ***H***C=C***H*** of IMe_2 and C***H***$_3$ of IMe_2 protons with carbene carbon atom).

NMR spectra of phosphinoborenium salts (including precursor 2)

Abbreviations

s	deuterated solvent (residual signal)
g	grease
★	impurity
●	imidazolium salt
●	R_2PH
t	toluene

NMR spectra of 2

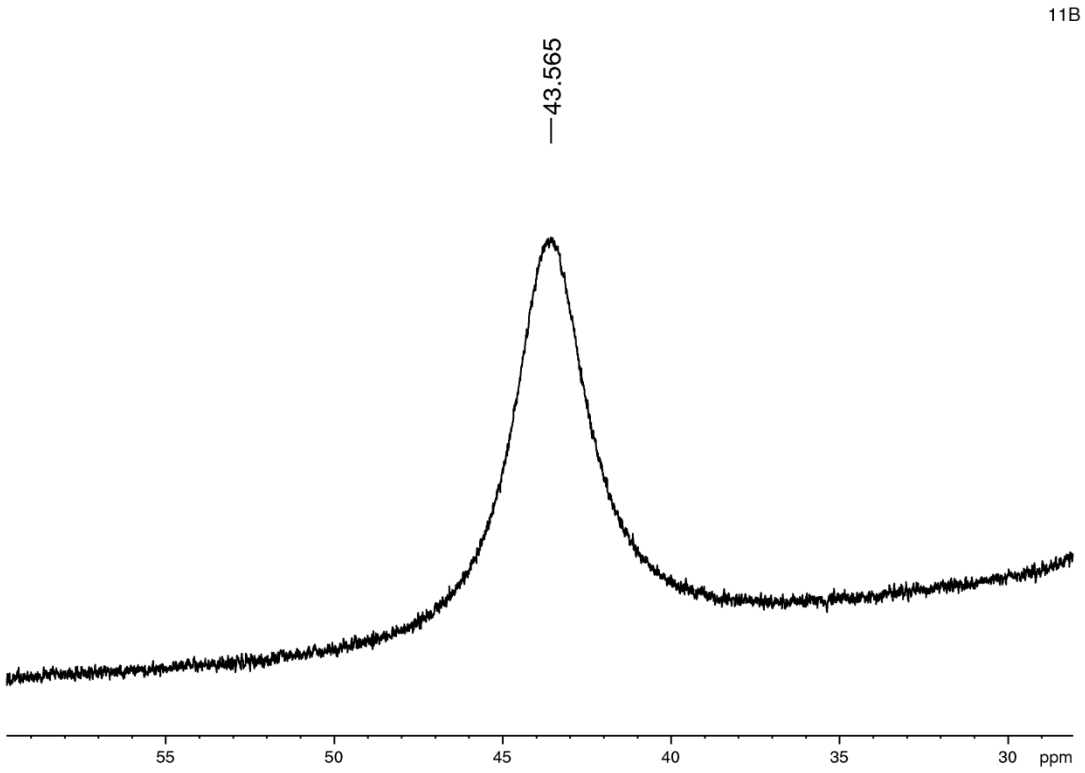

Figure S 1. ^{11}B spectrum (C_6D_6) of **2**

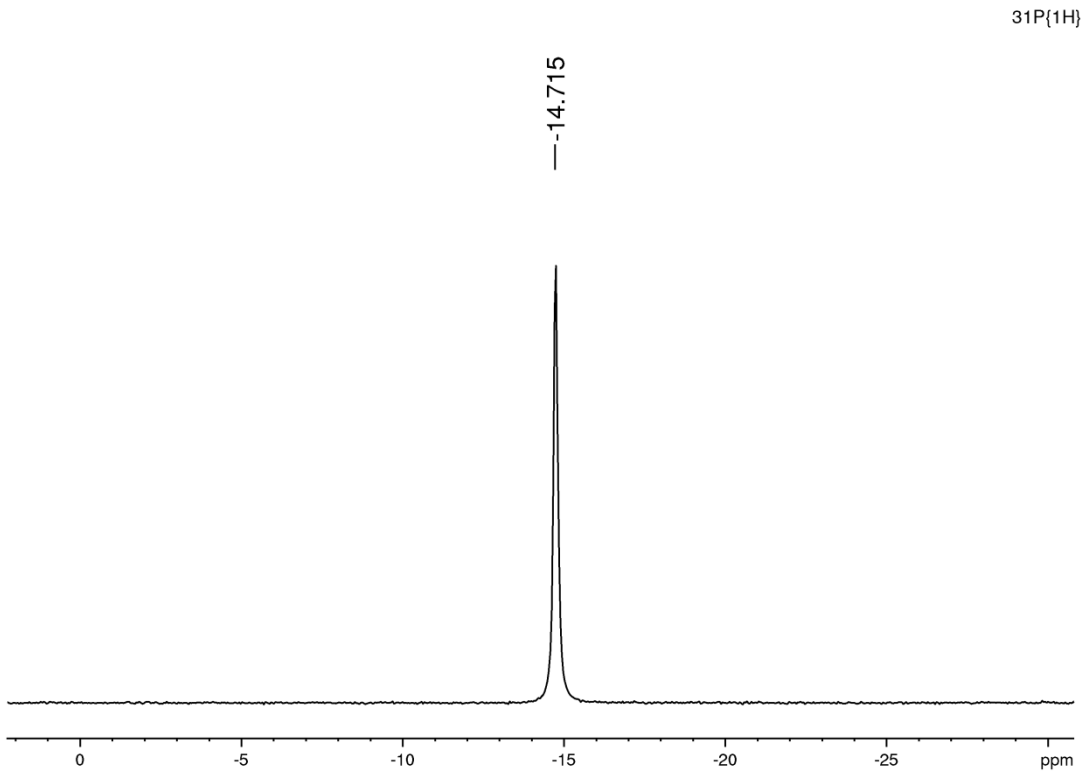

Figure S 2. $^{31}P\{^{1}H\}$ spectrum (C_6D_6) of **2**

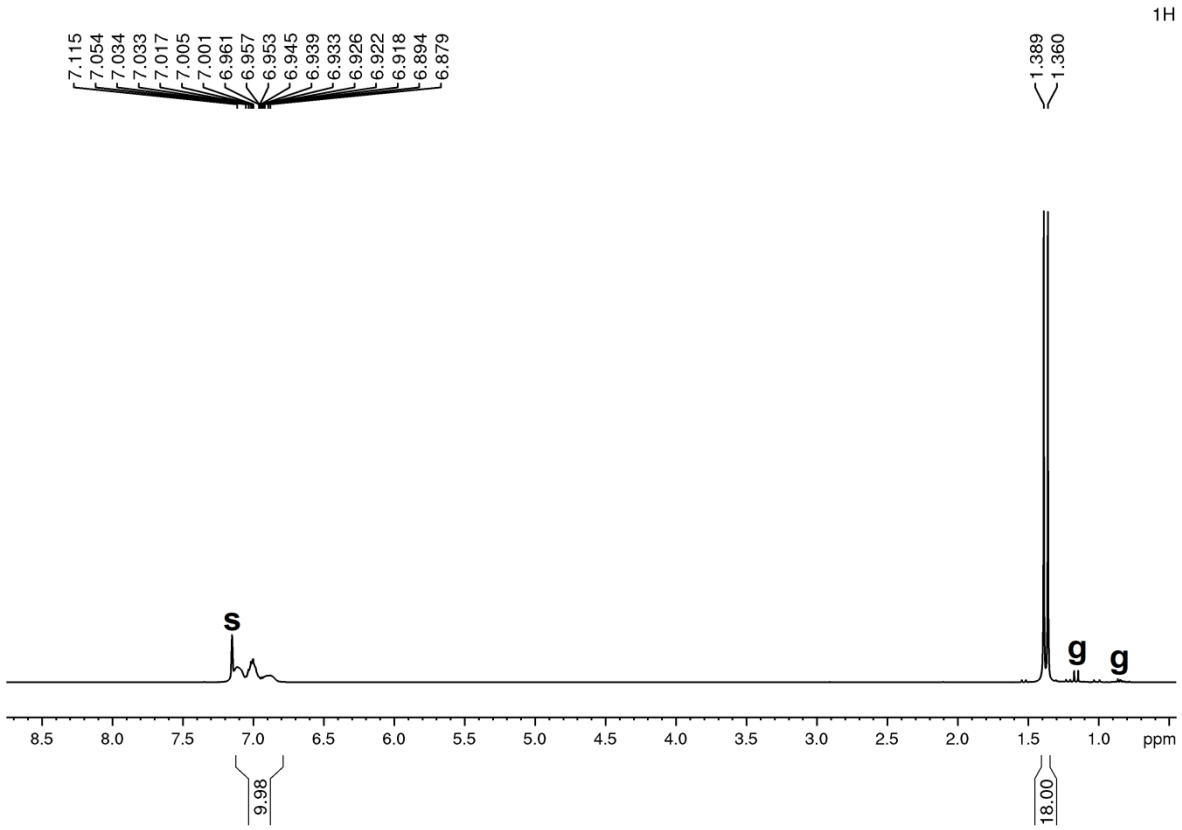

Figure S 3. ^{1}H spectrum (C_6D_6) of **2**

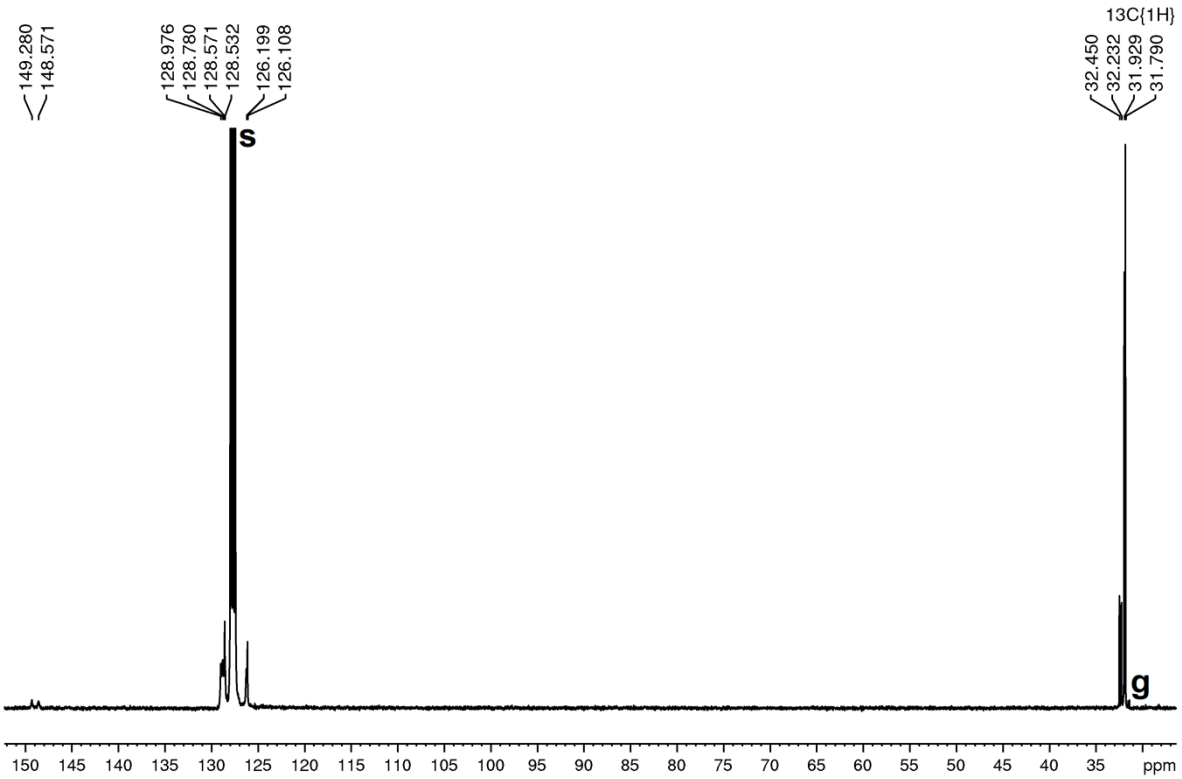

Figure S 4. $^{13}C\{^{1}H\}$ spectrum (C_6D_6) of **2**

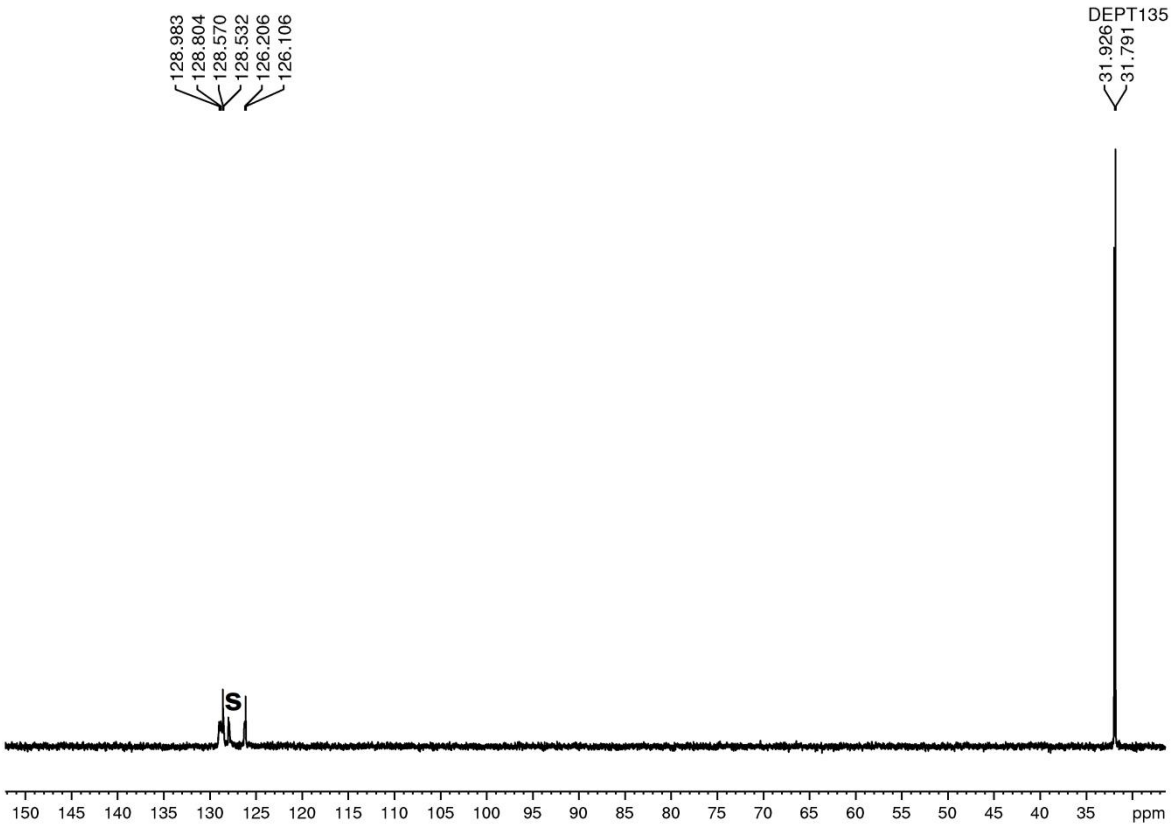

Figure S 5. ^{135}DEPT spectrum (C_6D_6) of **2**

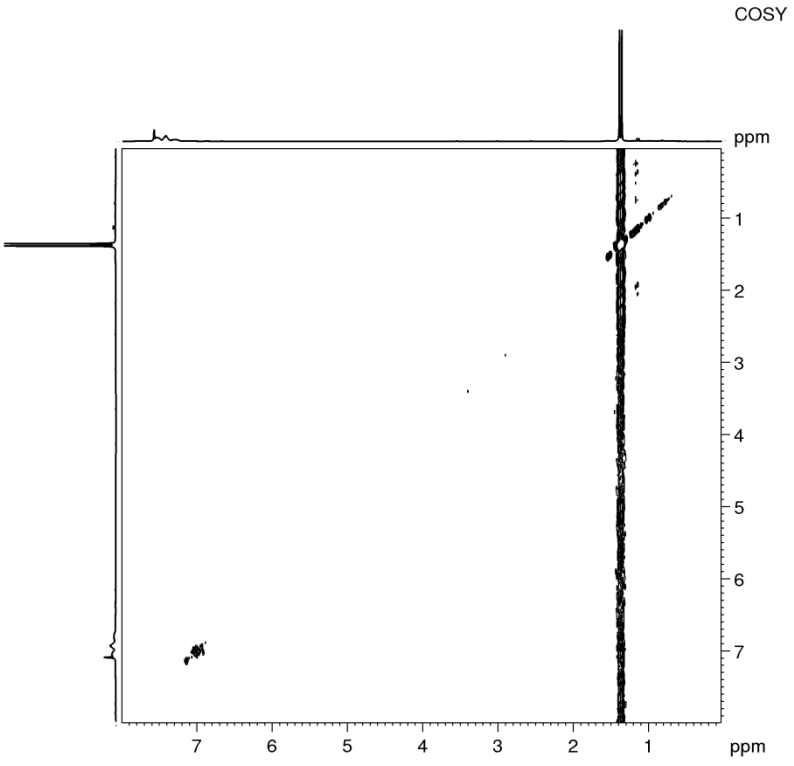

Figure S 6. COSY spectrum (C_6D_6) of **2**

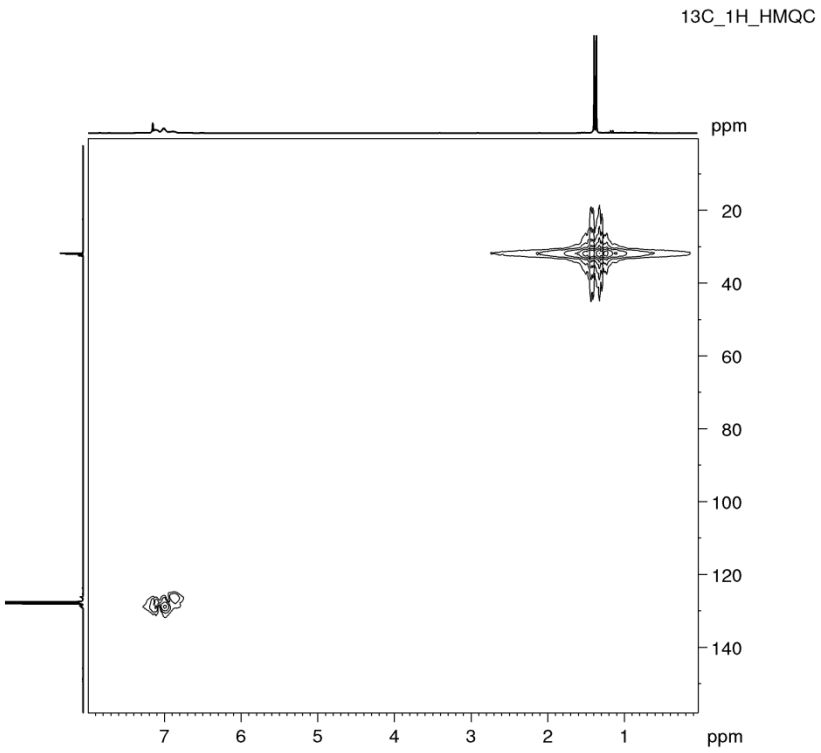

Figure S 7. ^{13}C ^{1}H HMQC spectrum (C_6D_6) of **2**

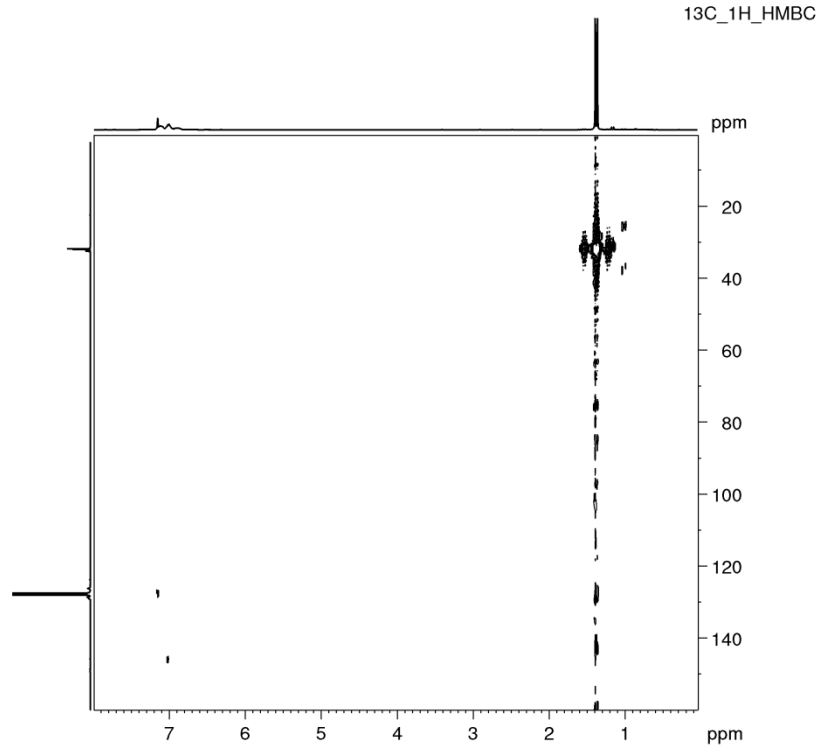

Figure S 8. ^{13}C ^{1}H HMBC spectrum (C_6D_6) of **2**

NMR spectra of 1a

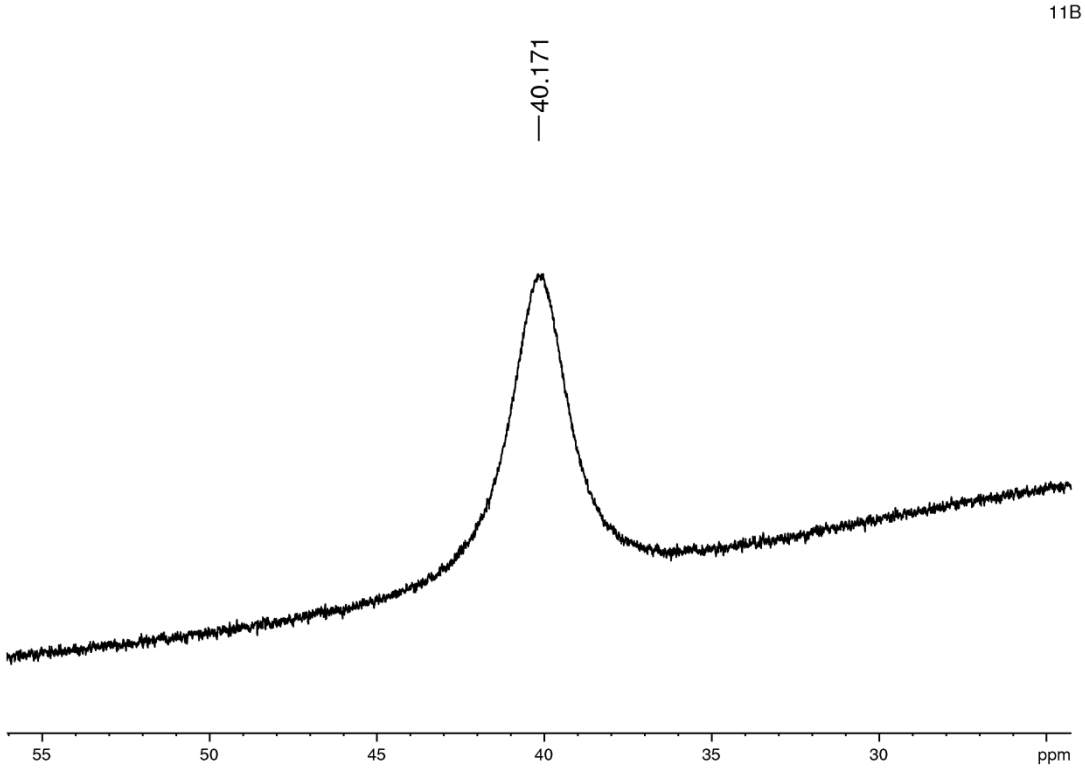

Figure S 9. ^{11}B spectrum (CD_2Cl_2) of **1a**

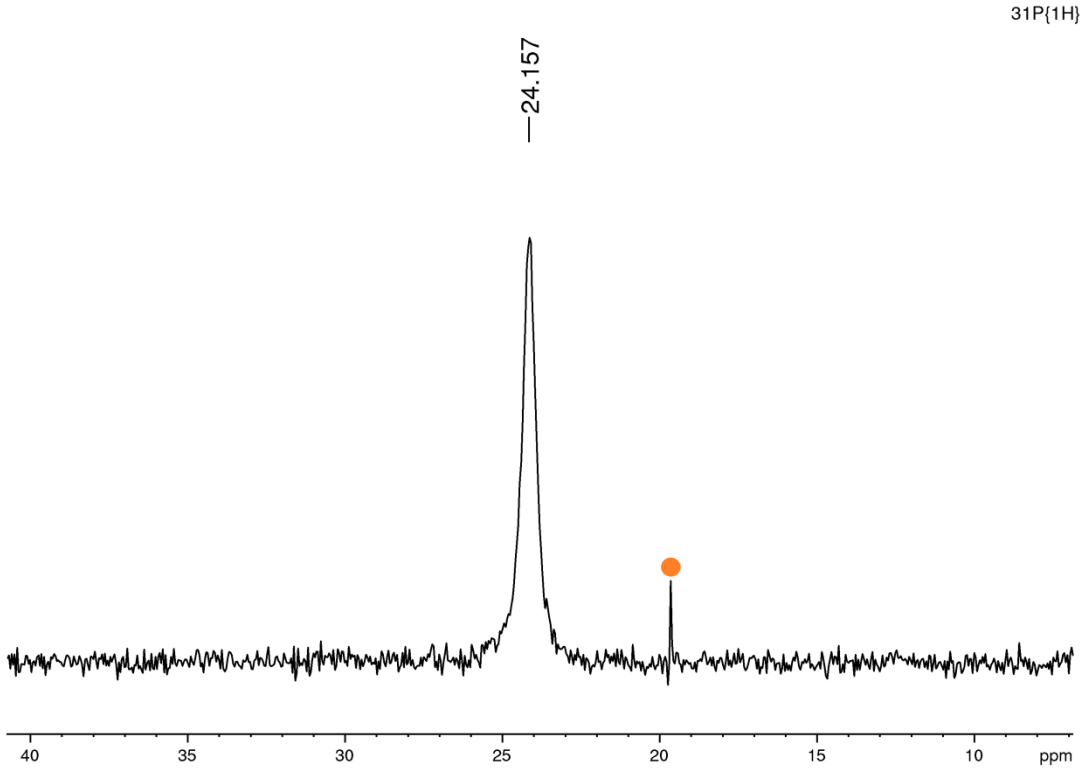

Figure S 10. $^{31}P\{^{1}H\}$ spectrum (CD_2Cl_2) of **1a**

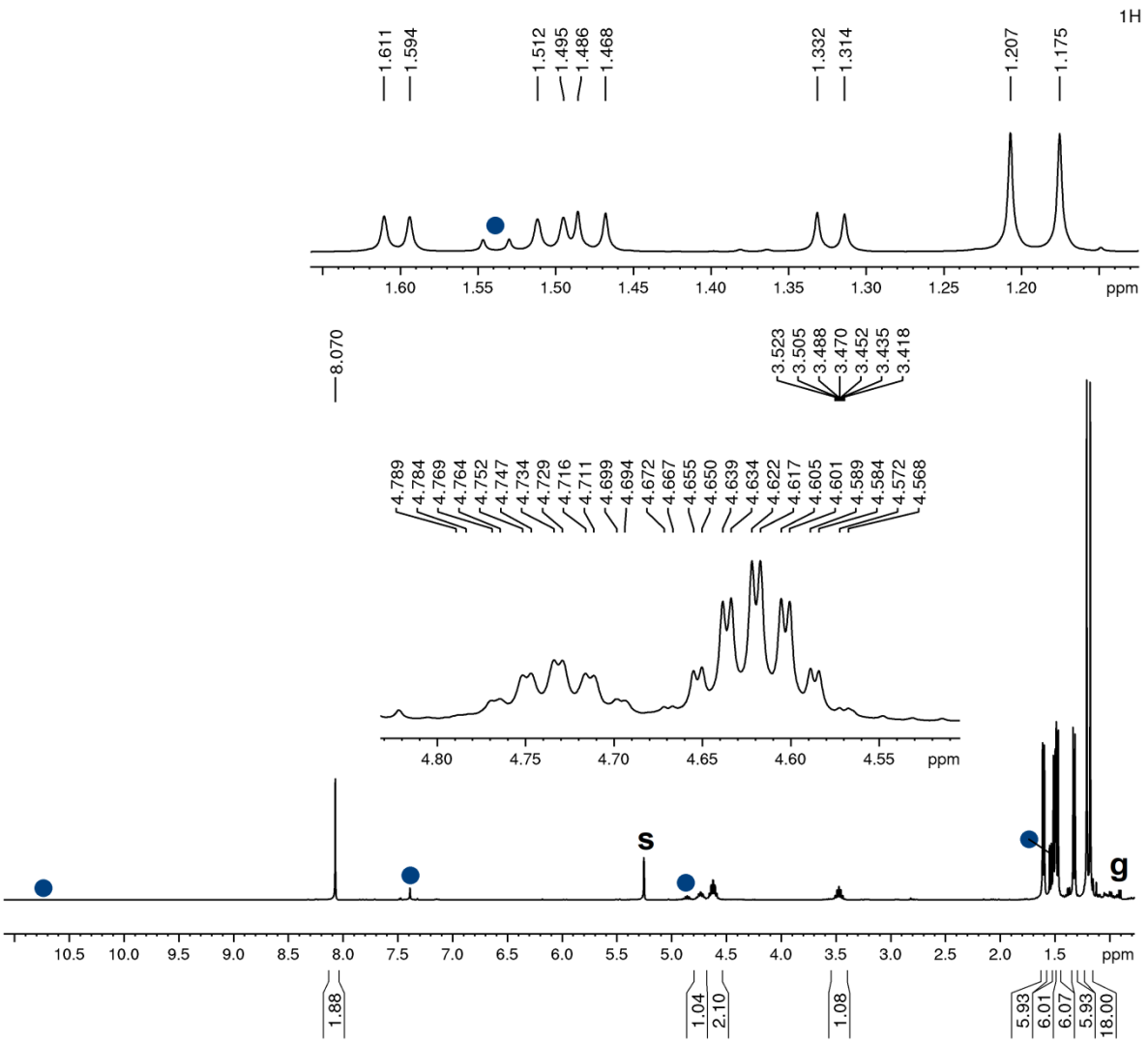

Figure S 11. ^{1}H spectrum (CD_2Cl_2) of **1a**

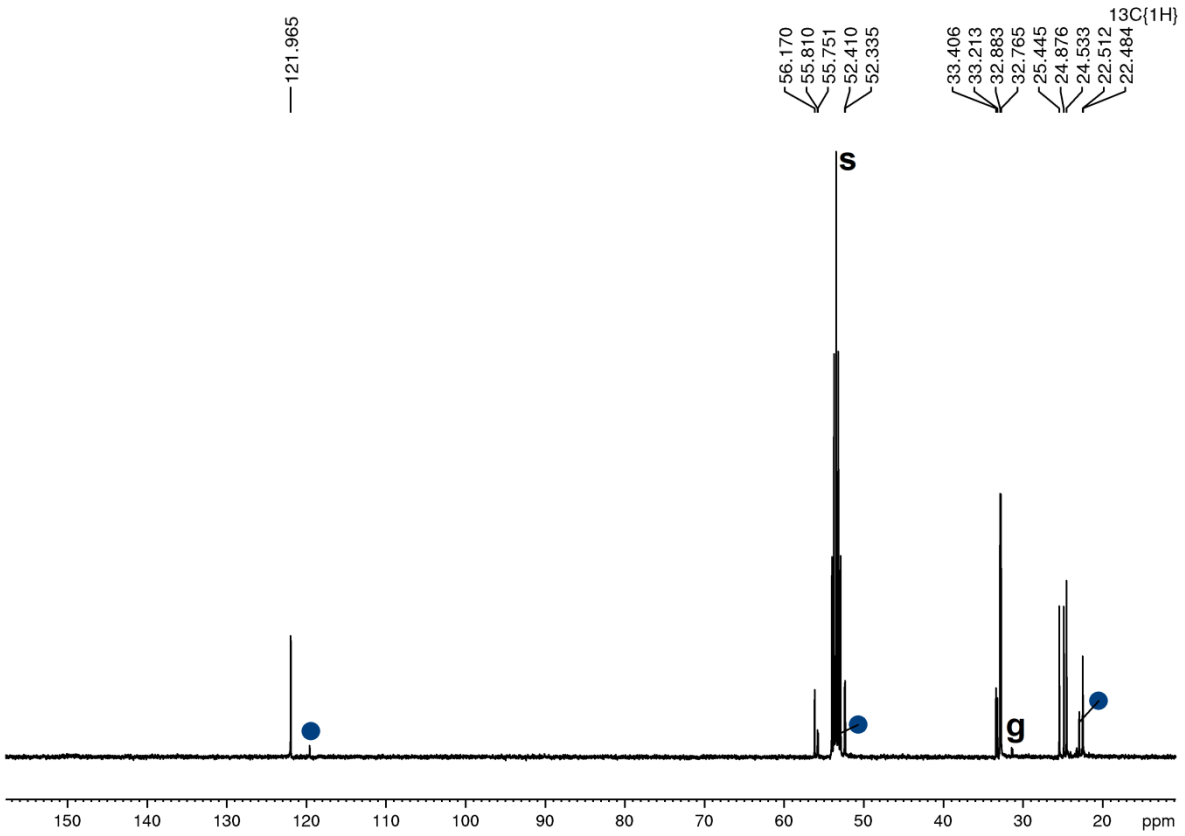

Figure S 12. $^{13}C\{^{1}H\}$ spectrum (CD_2Cl_2) of **1a**

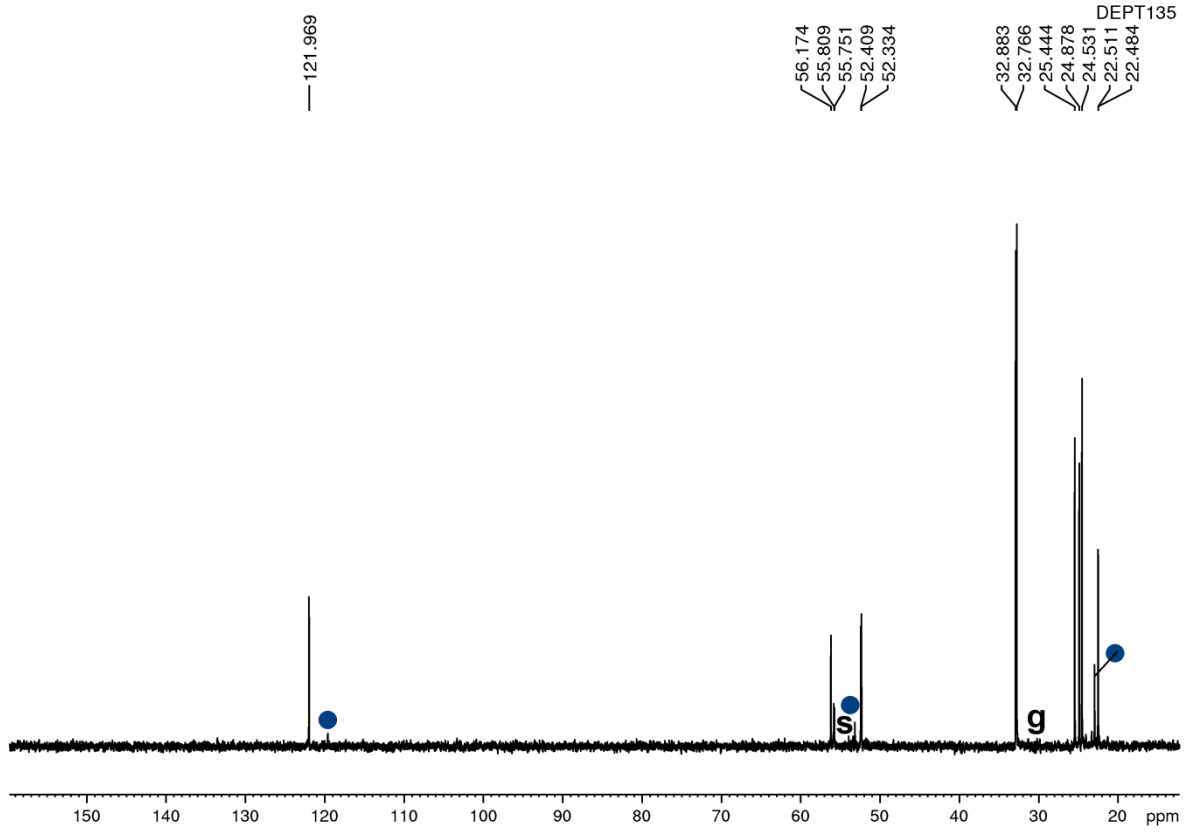

Figure S 13. ^{135}DEPT spectrum (CD_2Cl_2) of **1a**

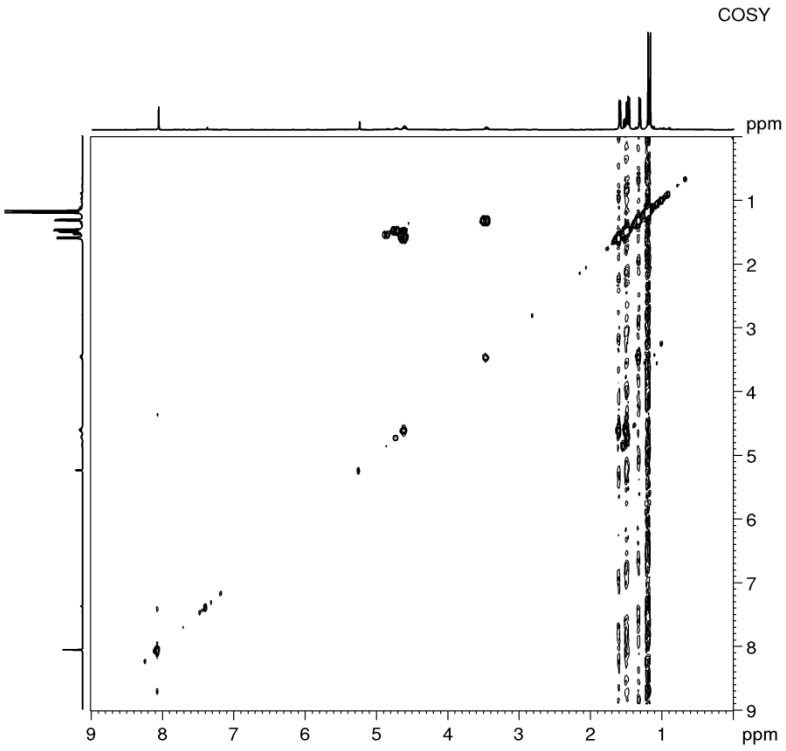

Figure S 14. COSY spectrum (CD_2Cl_2) of **1a**

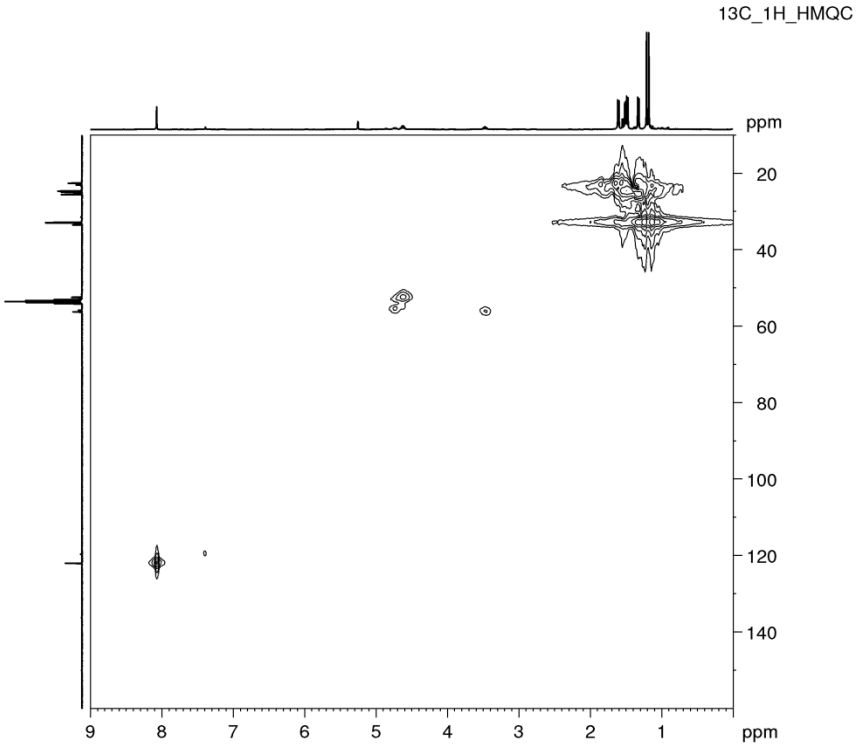

Figure S 15. ^{13}C ^{1}H HMQC spectrum (CD_2Cl_2) of **1a**

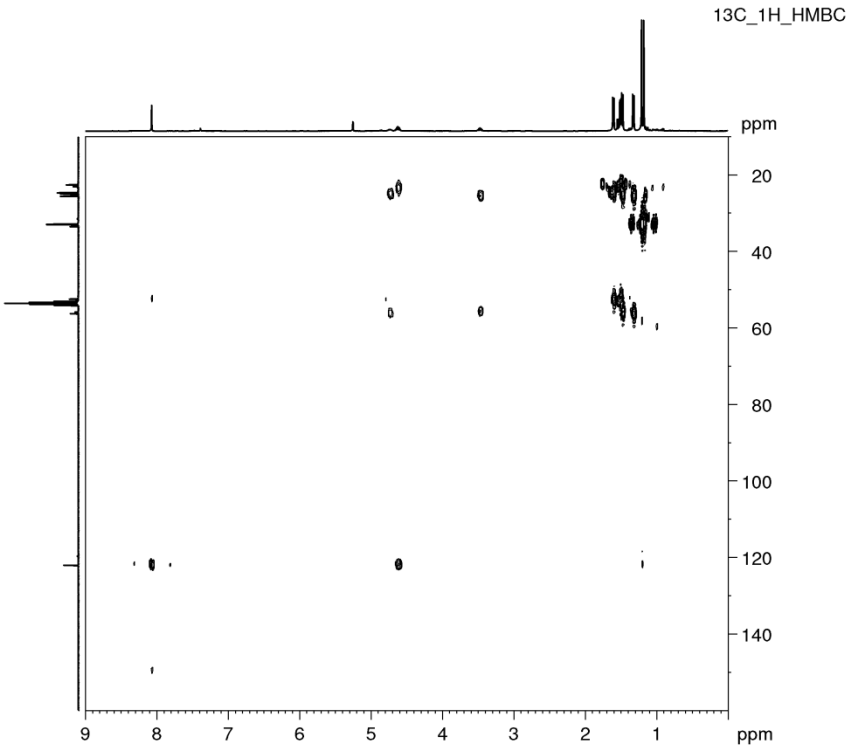

Figure S 16. ^{13}C ^{1}H HMBC spectrum (CD_2Cl_2) of **1a**

NMR spectra of 1b

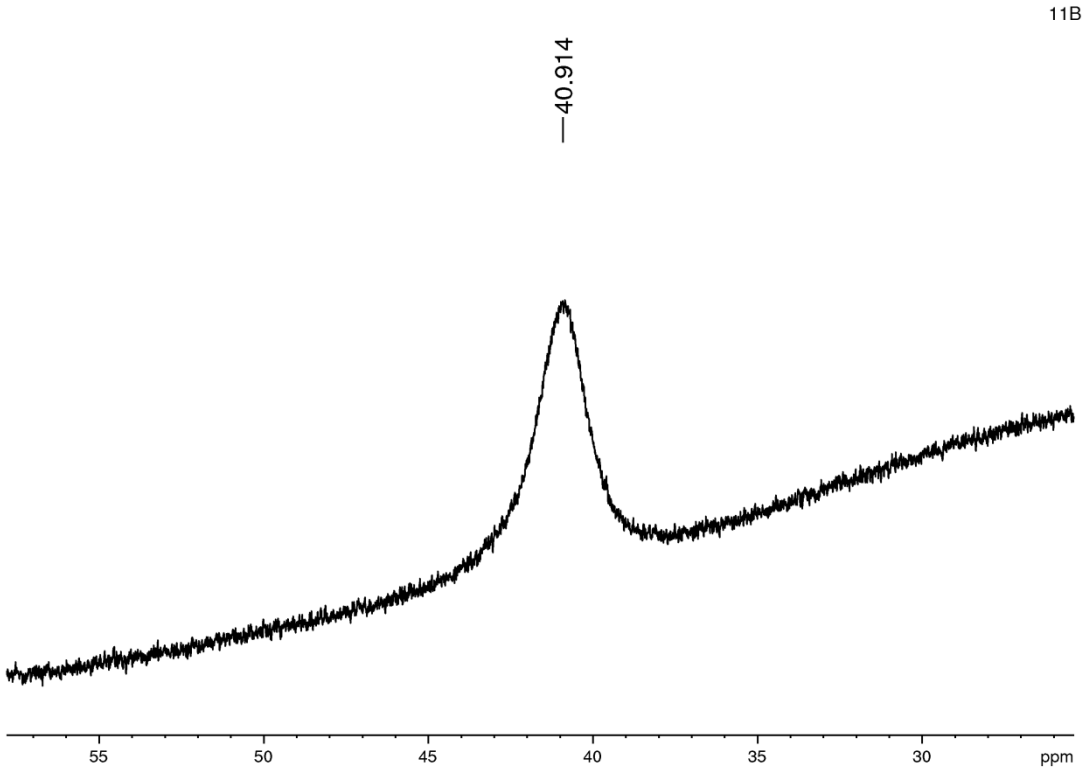

Figure S 17. ^{11}B spectrum (CD_2Cl_2) of **1b**

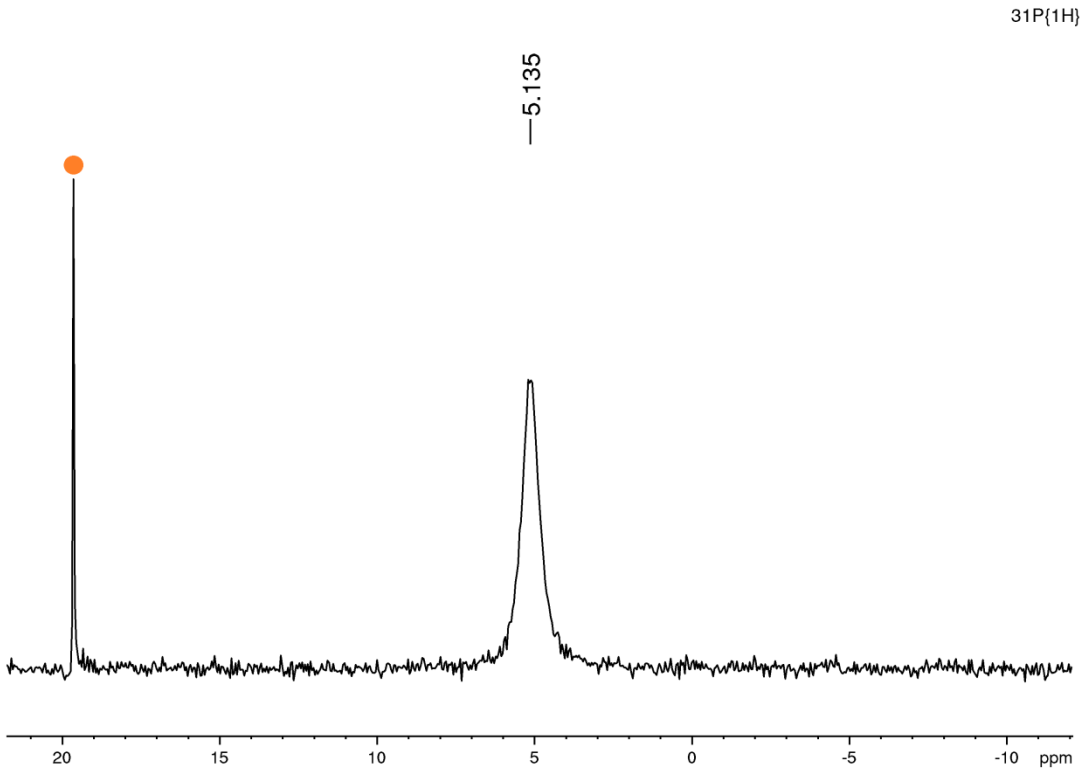

Figure S 18. $^{31}P\{^{1}H\}$ spectrum (CD_2Cl_2) of **1b**

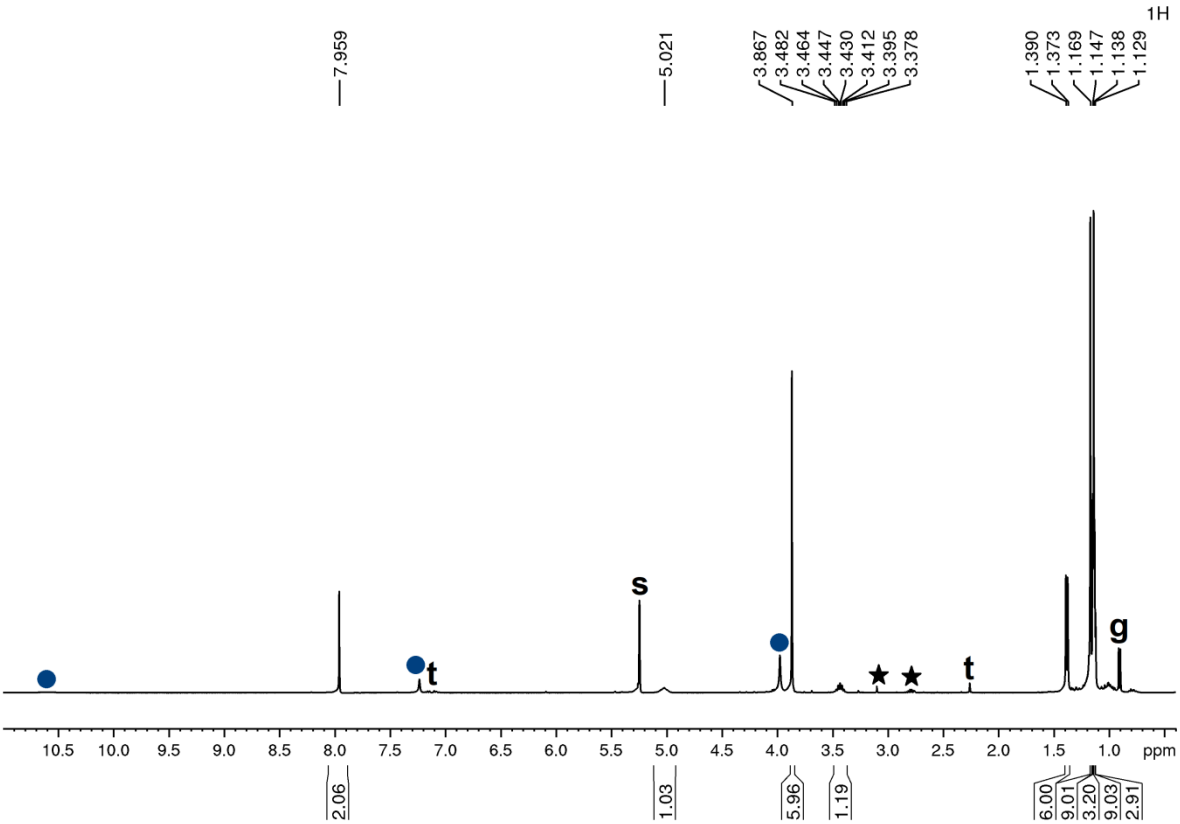

Figure S 19. ^{1}H spectrum (CD_2Cl_2) of **1b**

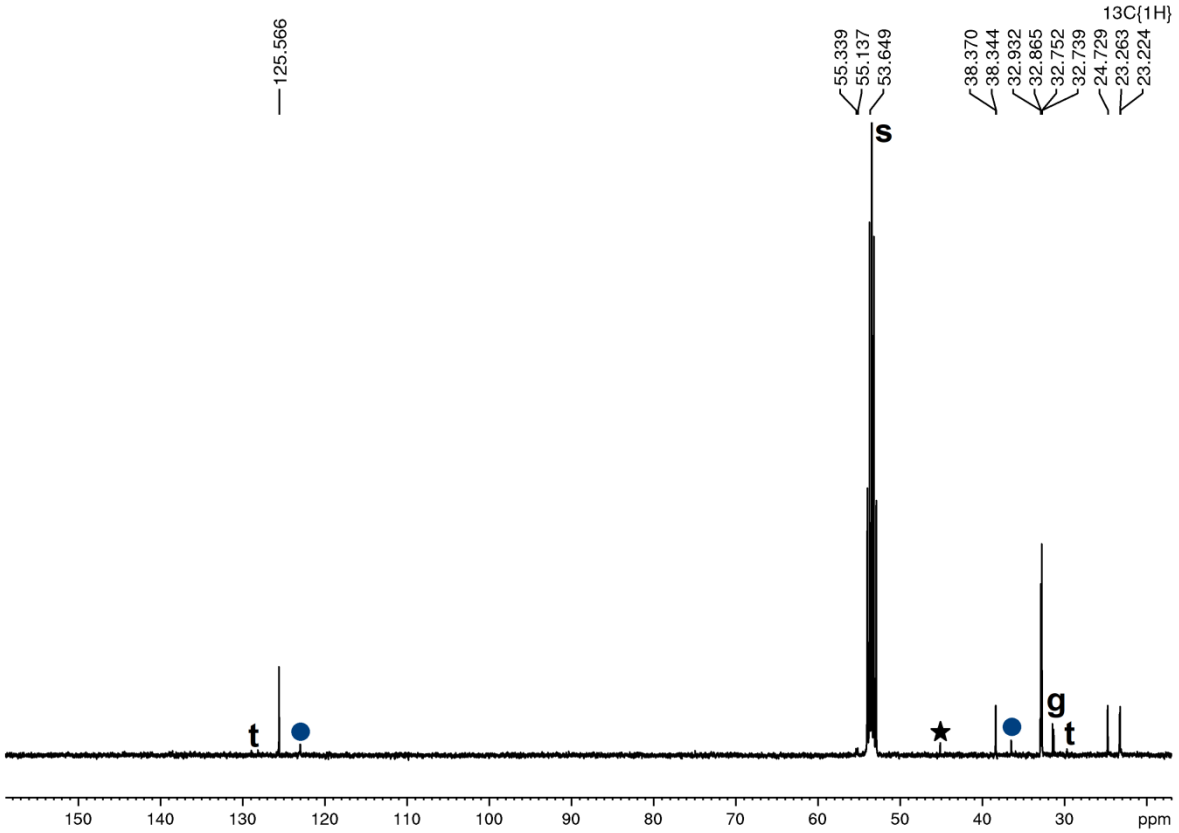

Figure S 20. $^{13}C\{^{1}H\}$ spectrum (CD_2Cl_2) of **1b**

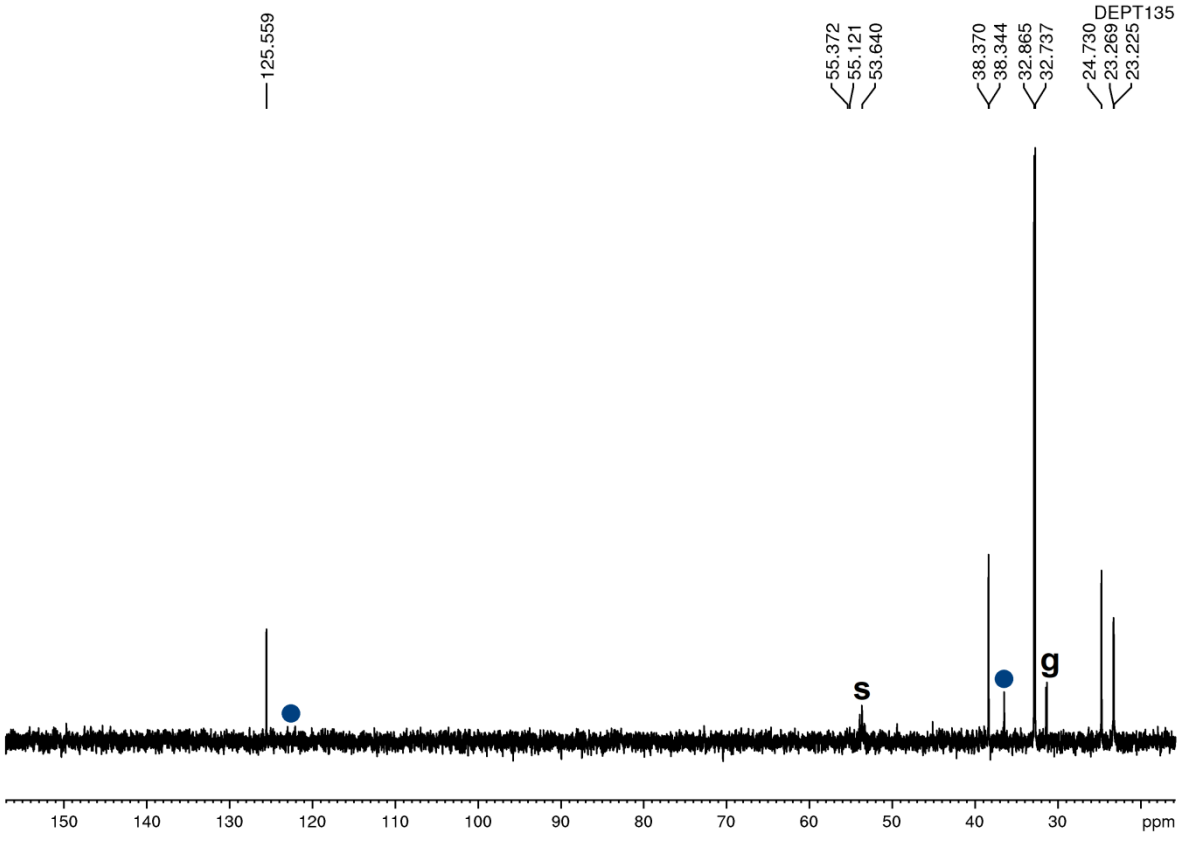

Figure S 21. ^{135}DEPT spectrum (CD_2Cl_2) of **1b**

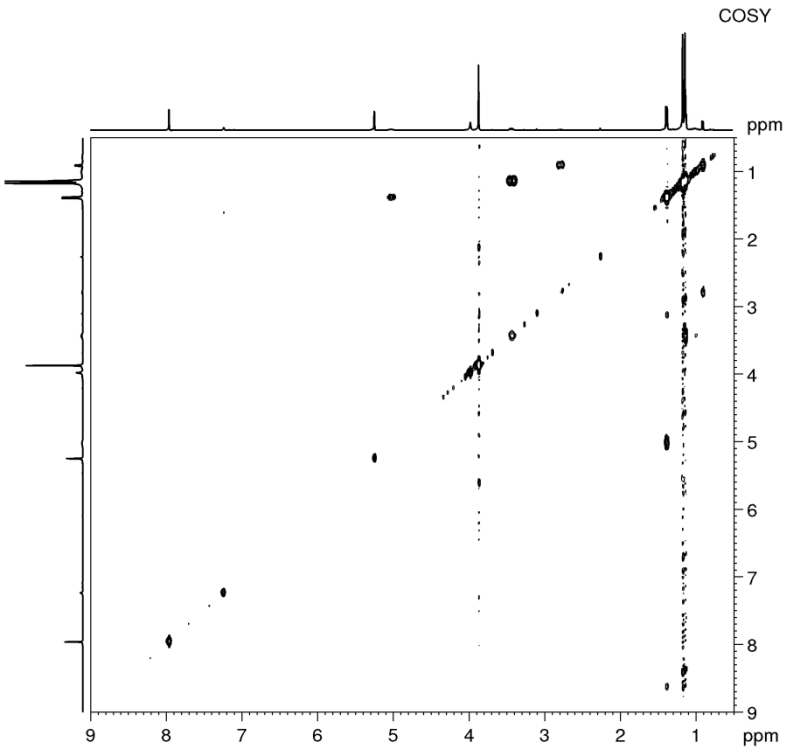

Figure S 22. COSY spectrum (CD_2Cl_2) of **1b**

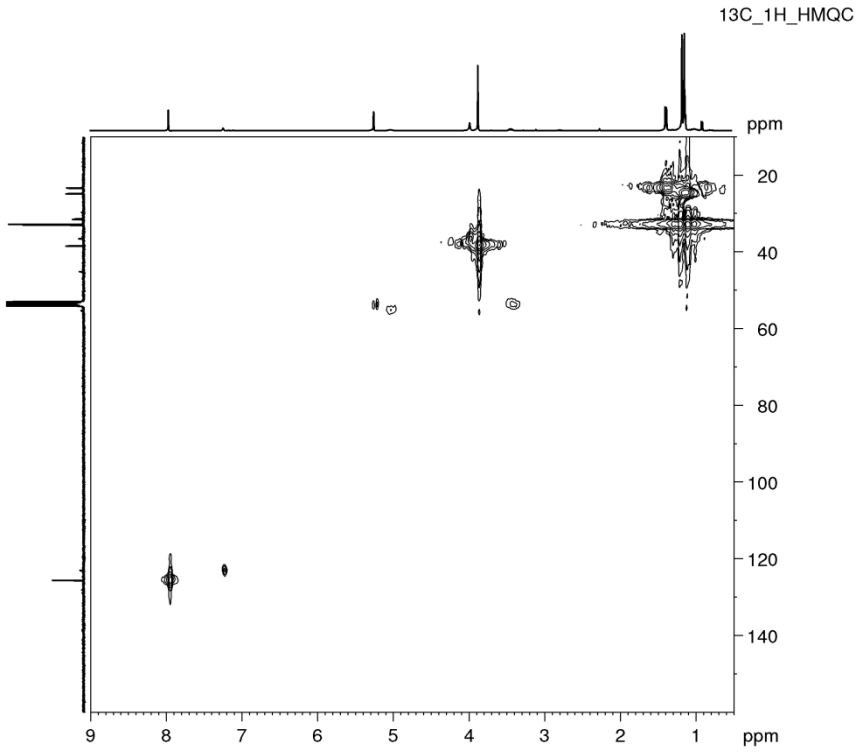

Figure S 23. ^{13}C ^{1}H HMQC spectrum (CD_2Cl_2) of **1b**

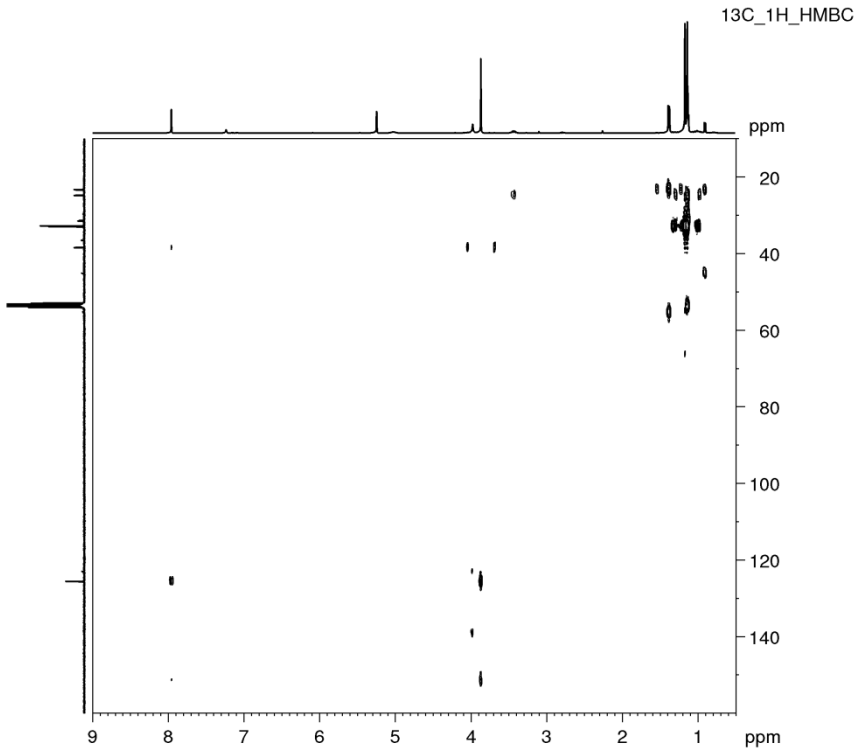

Figure S 24. ^{13}C ^{1}H HMBC spectrum (CD_2Cl_2) of **1b**

NMR spectra of 2a

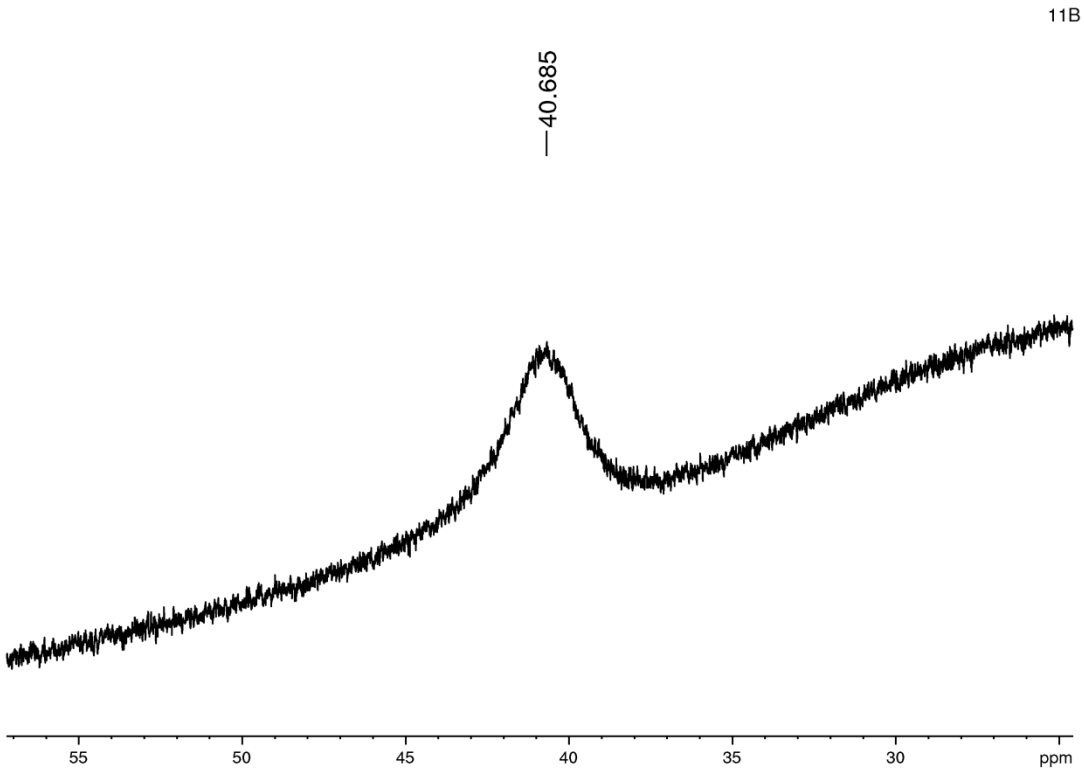

Figure S 25. ^{11}B spectrum (CD_2Cl_2) of **2a**

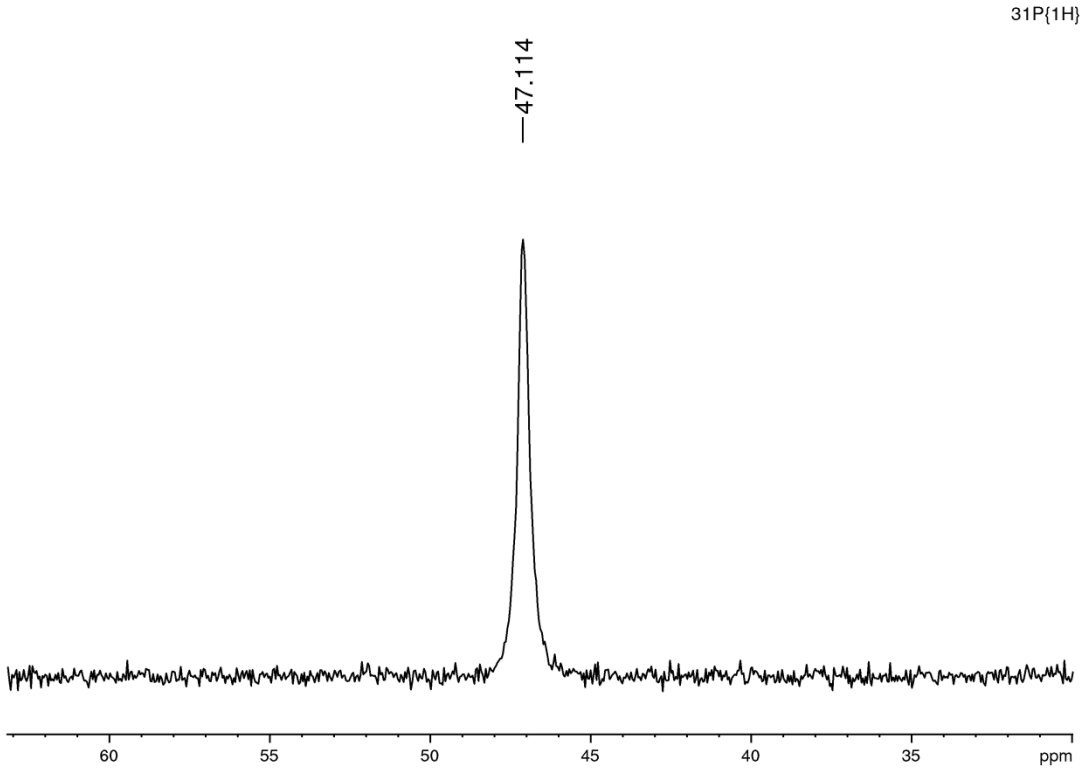

Figure S 26. $^{31}P\{^{1}H\}$ spectrum (CD_2Cl_2) of **2a**

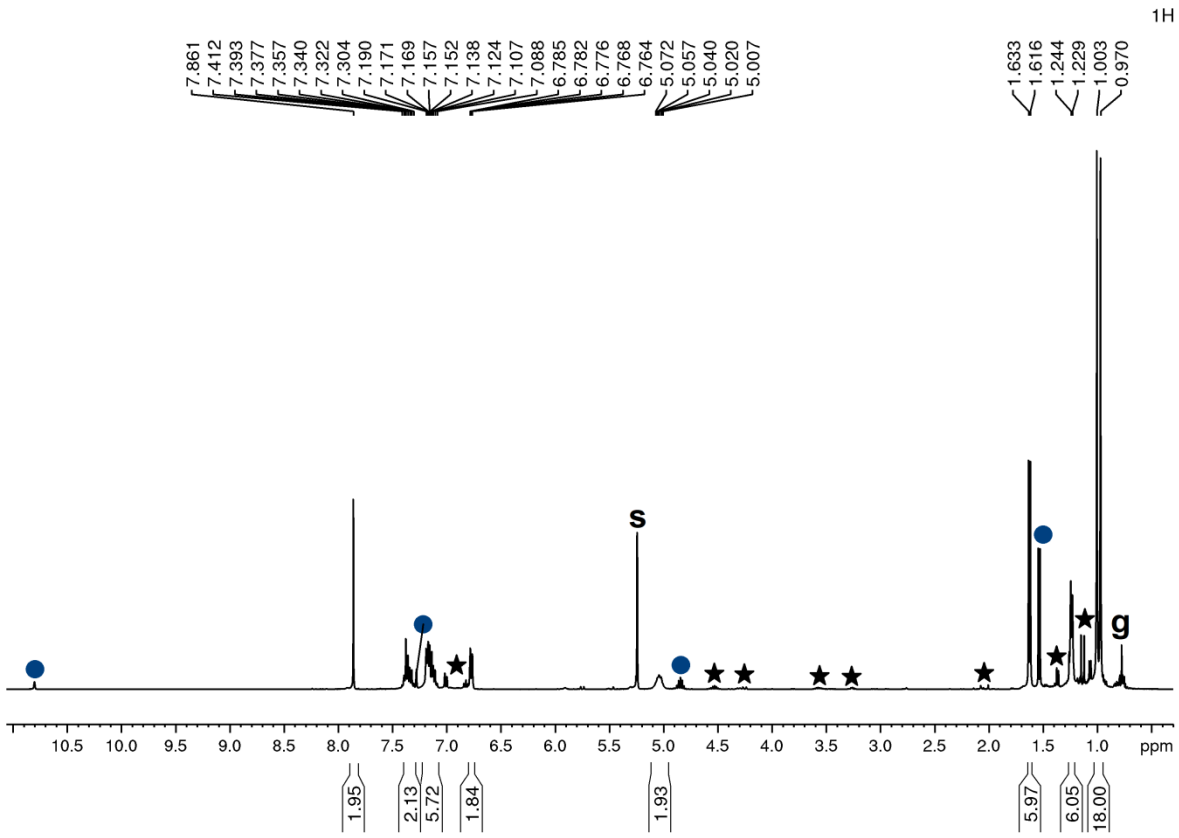

Figure S 27. ^{1}H spectrum (CD_2Cl_2) of **2a**

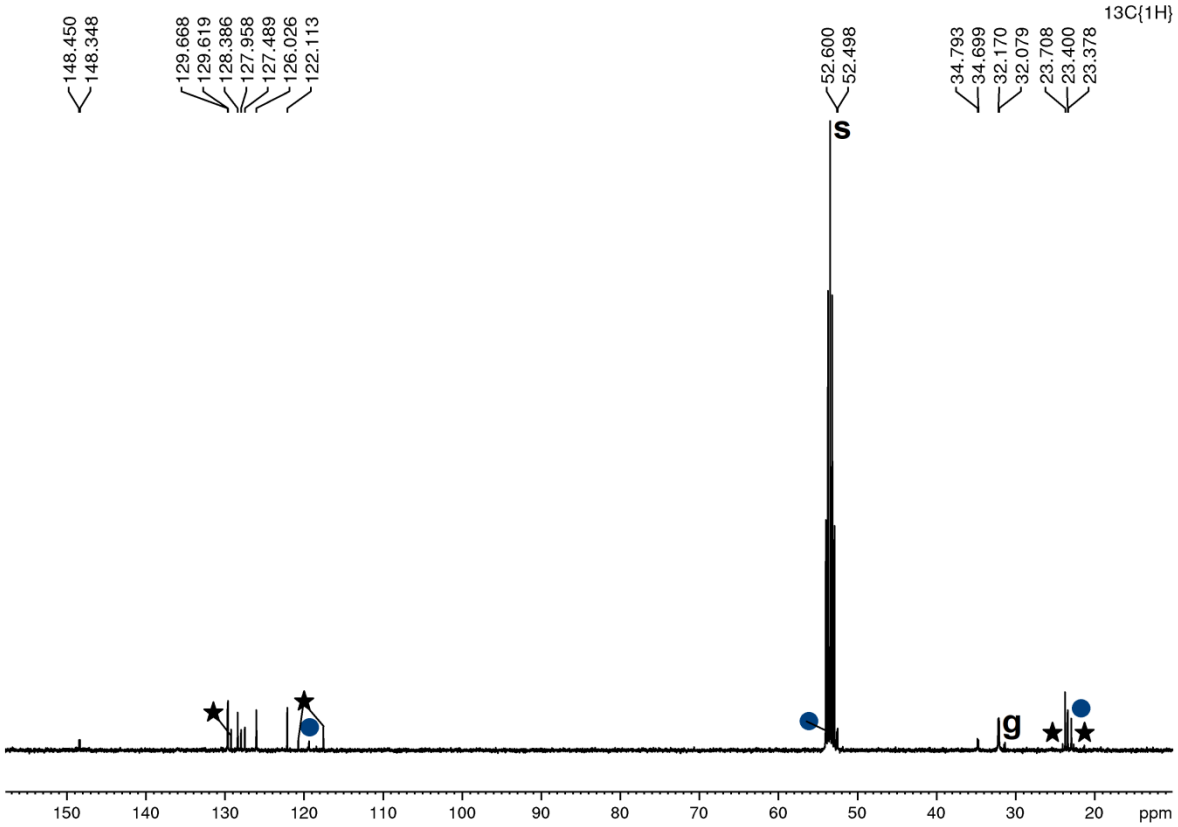

Figure S 28. $^{13}C\{^{1}H\}$ spectrum (CD_2Cl_2) of **2a**

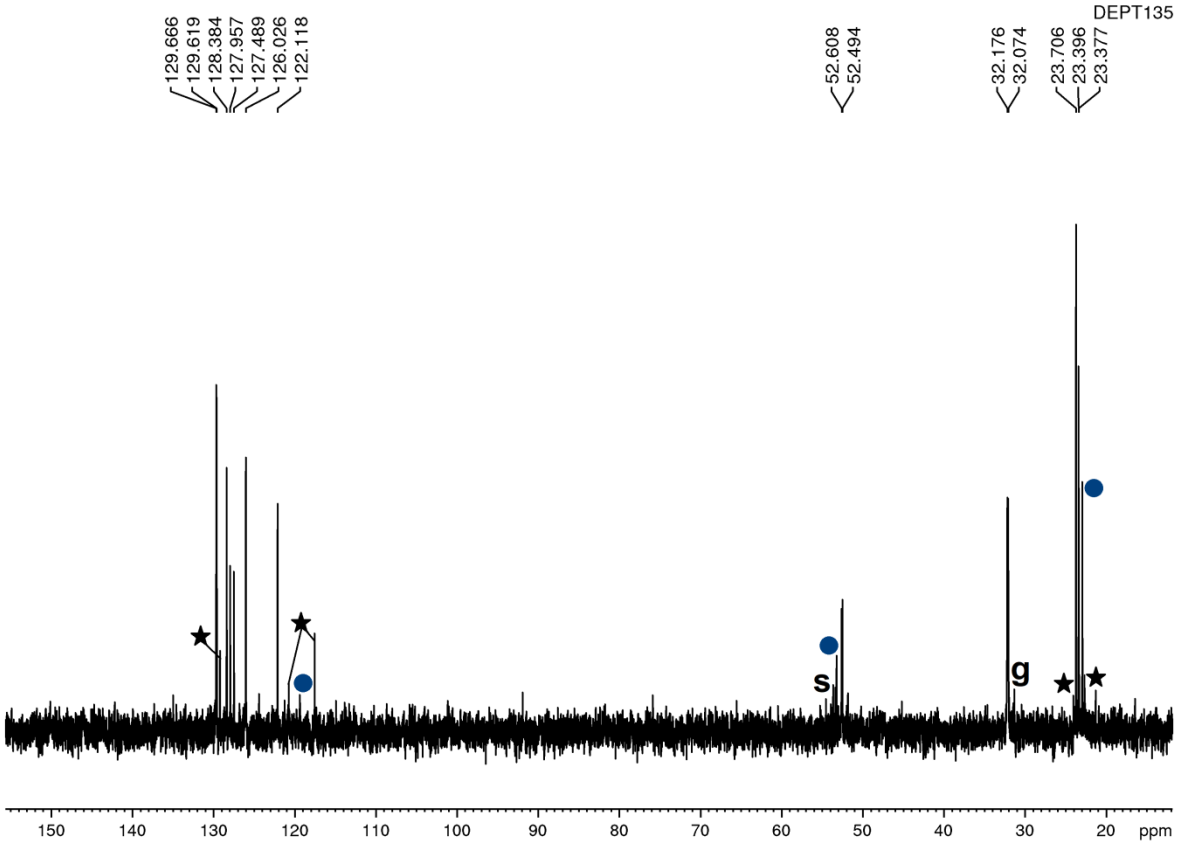

Figure S 29. ^{135}DEPT spectrum (CD_2Cl_2) of **2a**

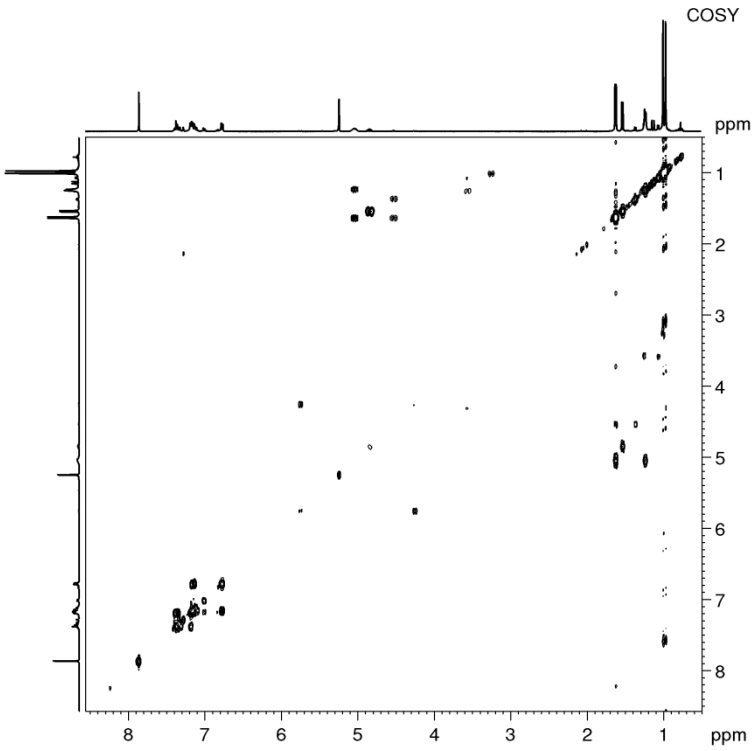

Figure S 30. COSY spectrum (CD_2Cl_2) of **2a**

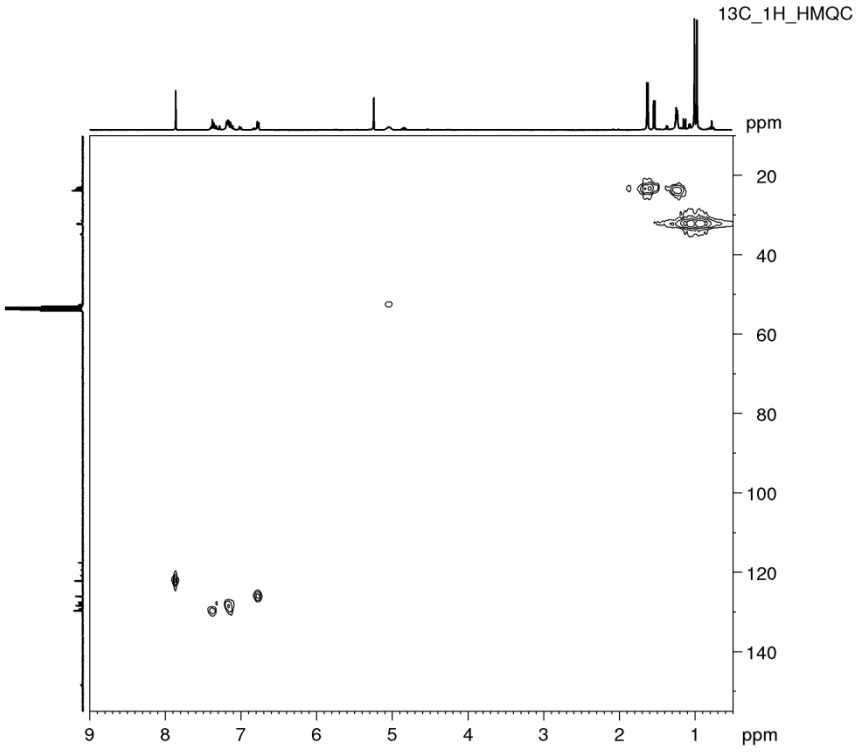

Figure S 31. ^{13}C ^{1}H HMQC spectrum (CD_2Cl_2) of **2a**

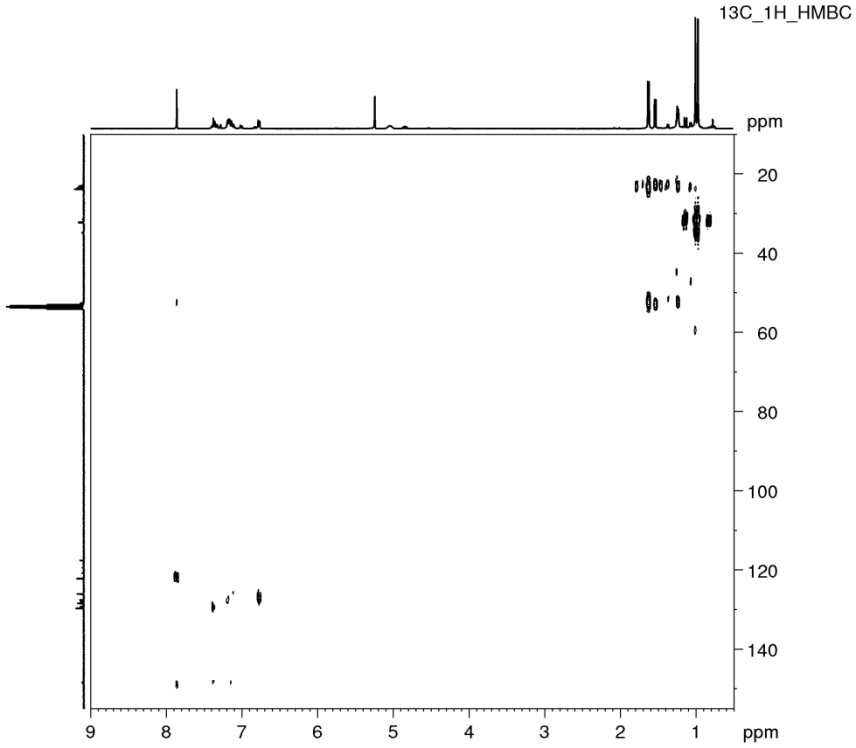

Figure S 32. ^{13}C ^{1}H HMBC spectrum (CD_2Cl_2) of **2a**

NMR spectra of 2b

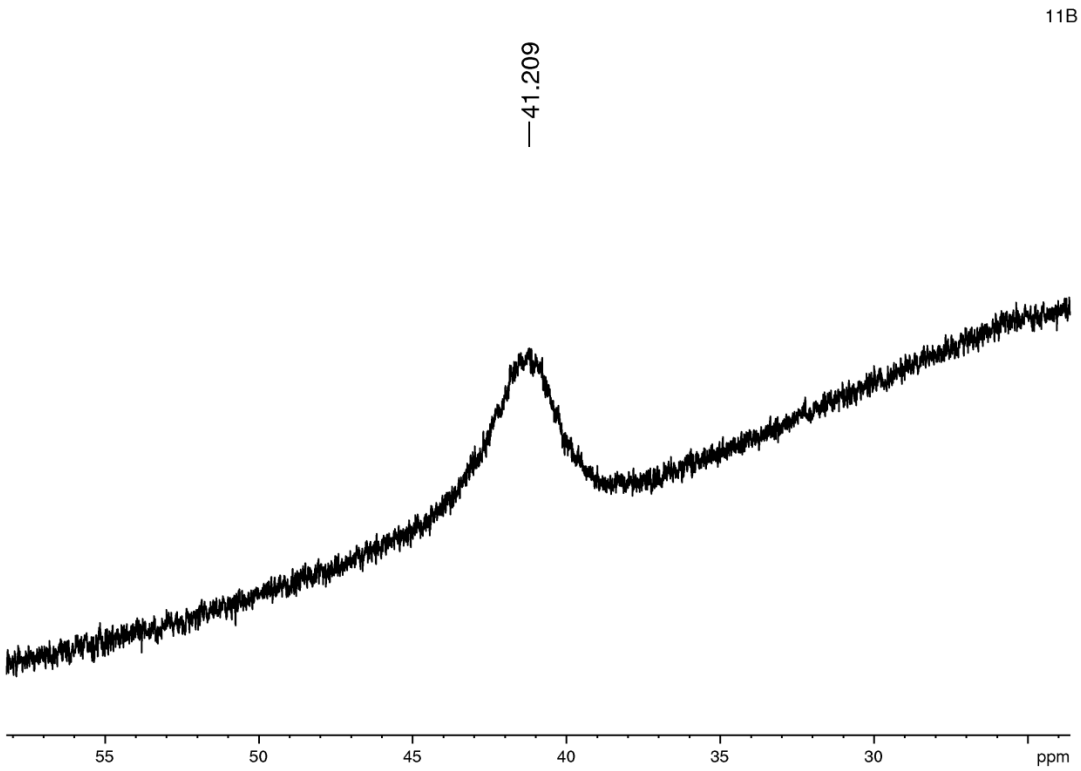

Figure S 33. ^{11}B spectrum (CD_2Cl_2) of **2b**$^{-}$

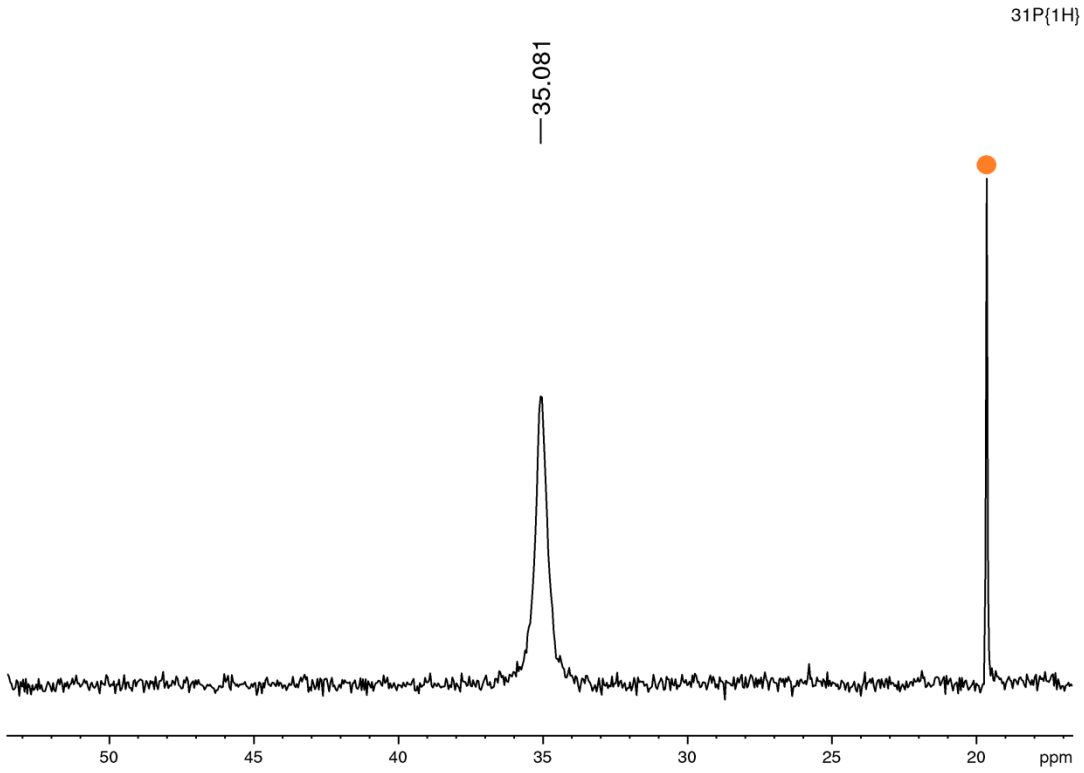

Figure S 34. $^{31}P\{^{1}H\}$ spectrum (CD_2Cl_2) of **2b**

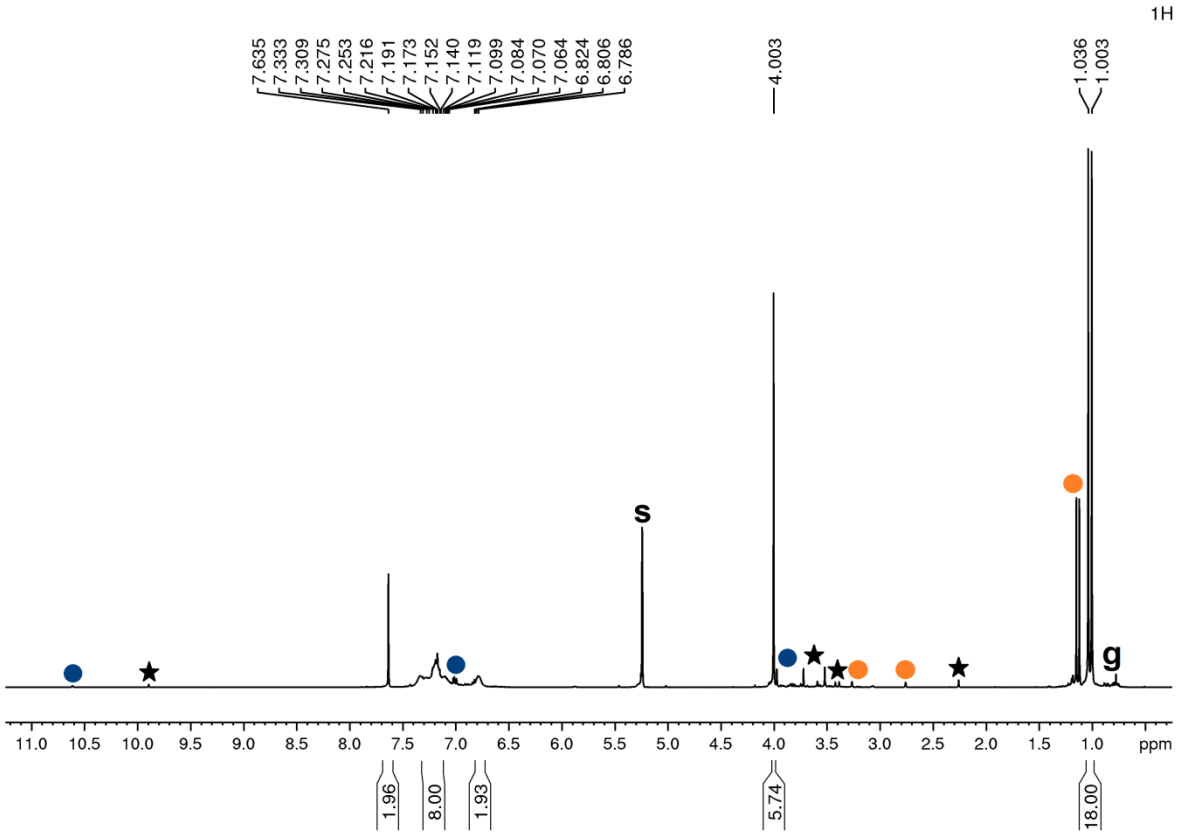

Figure S 35. ^{1}H spectrum (CD_2Cl_2) of **2b**

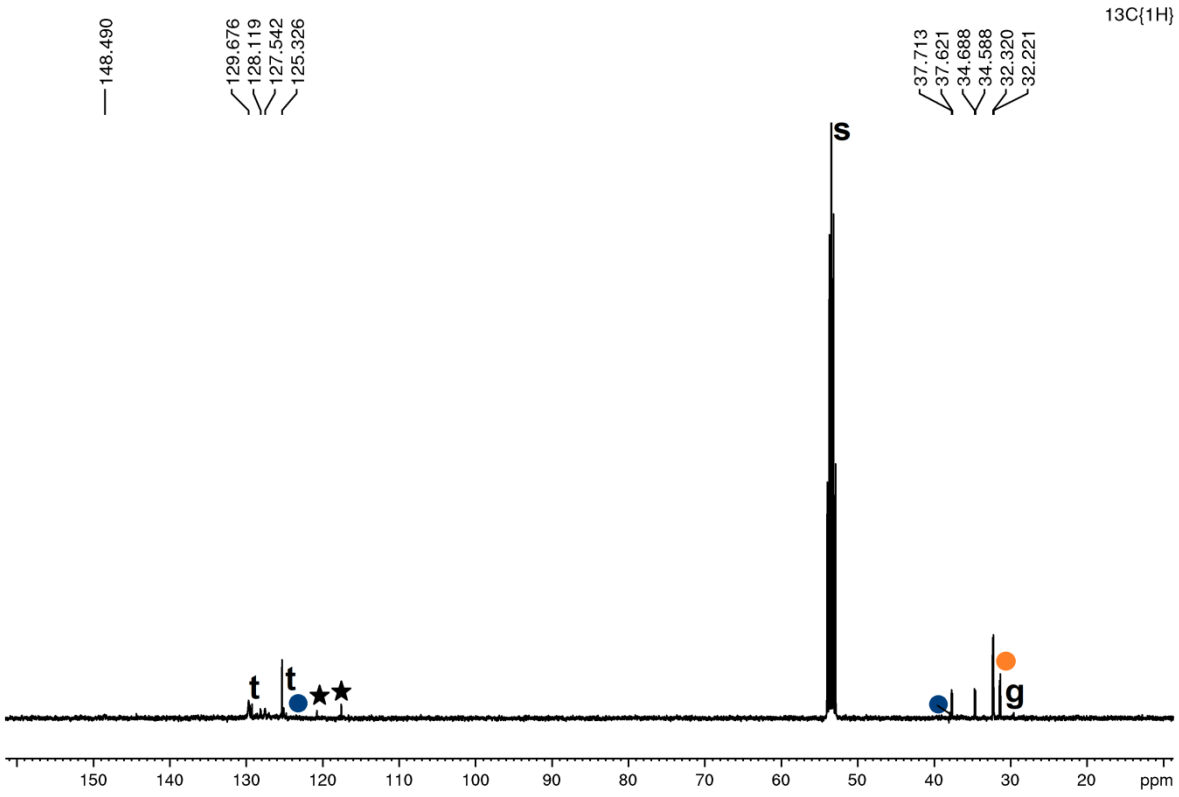

Figure S 36. $^{13}C\{^{1}H\}$ spectrum (CD_2Cl_2) of **2b**

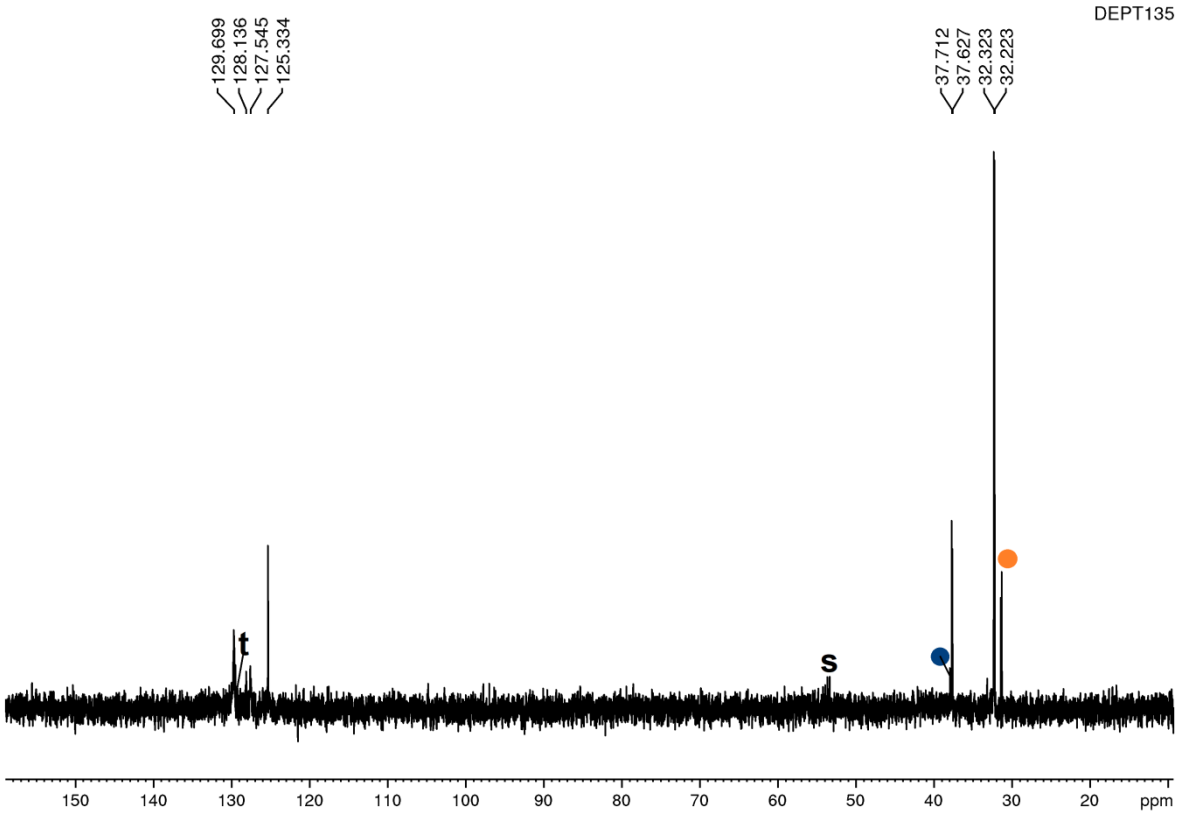

Figure S 37. ^{135}DEPT spectrum (CD_2Cl_2) of **2b**

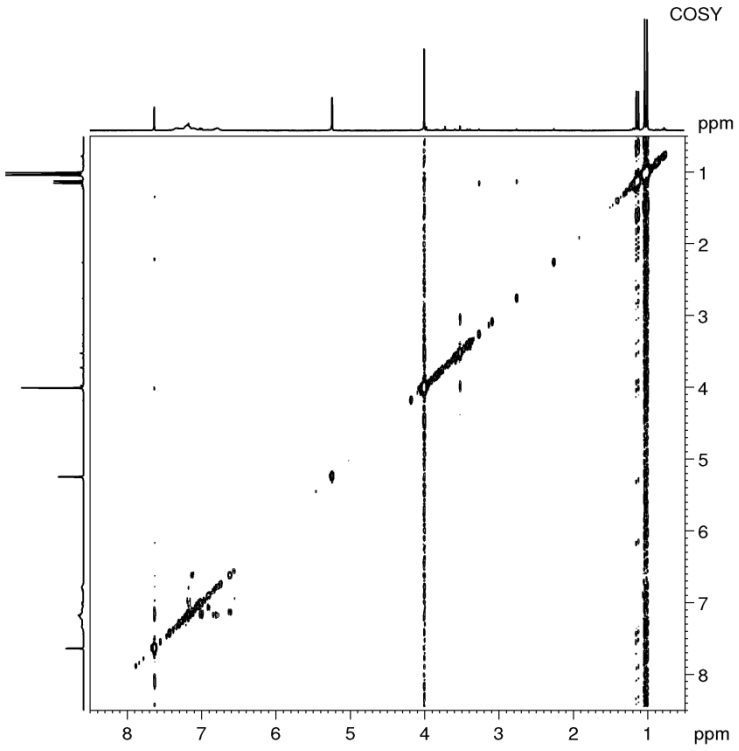

Figure S 38. COSY spectrum (CD_2Cl_2) of **2b**

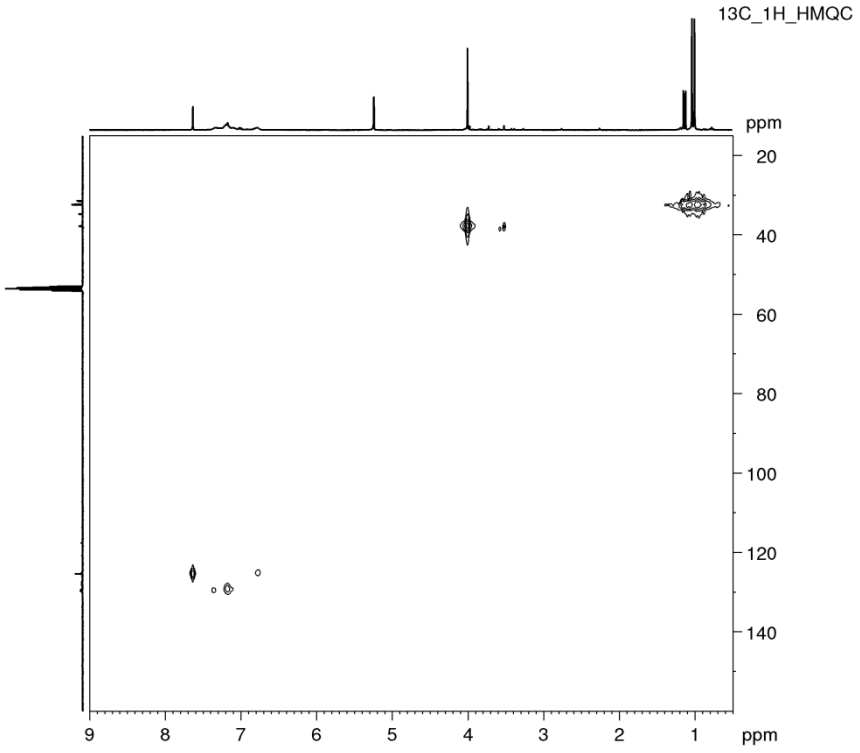

Figure S 39. ^{13}C ^{1}H HMQC spectrum (CD_2Cl_2) of **2b**

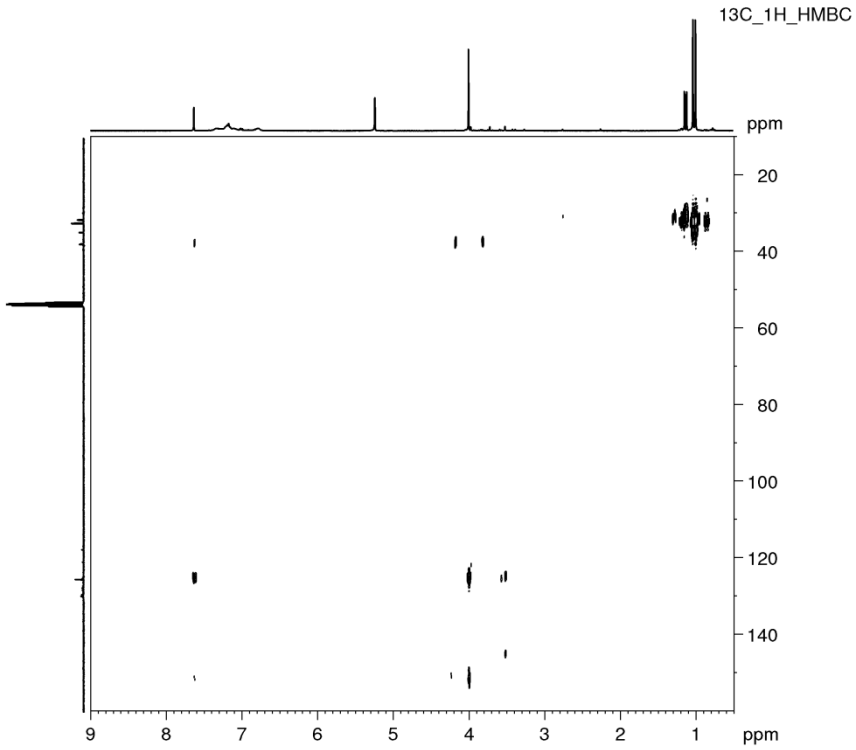

Figure S 40. ^{13}C ^{1}H HMBC spectrum (CD_2Cl_2) of **2b**

NMR spectra of 3a

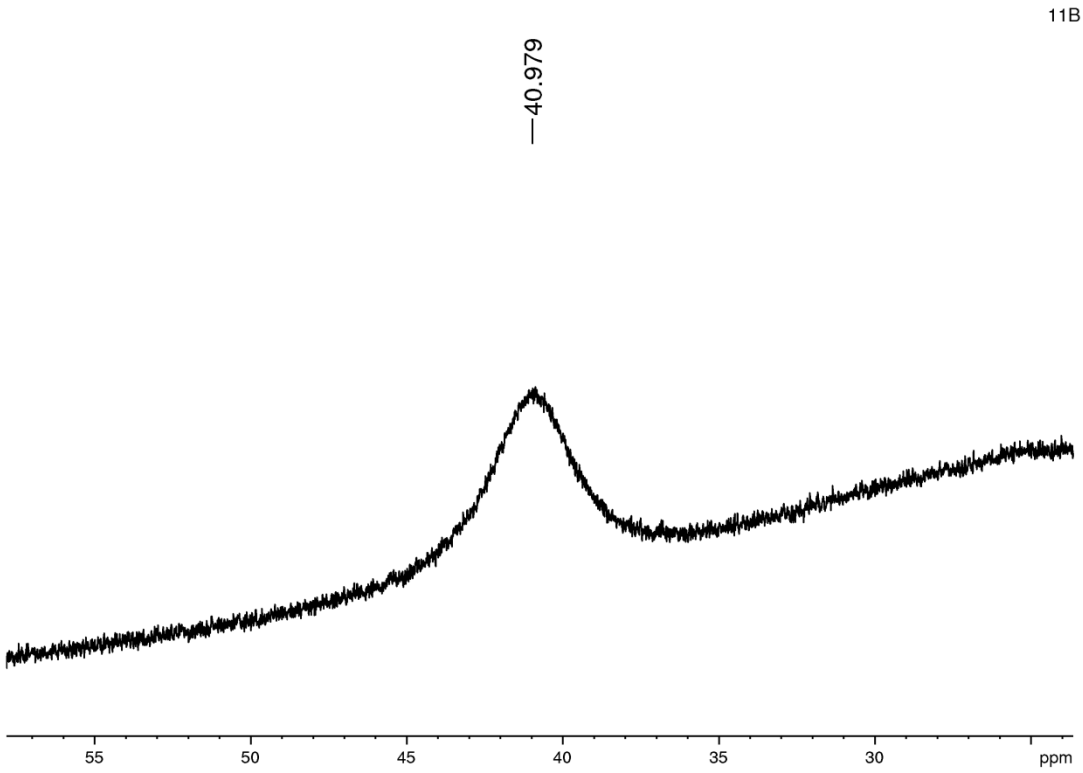

Figure S 41. ^{11}B spectrum (CD_2Cl_2) of **3a**

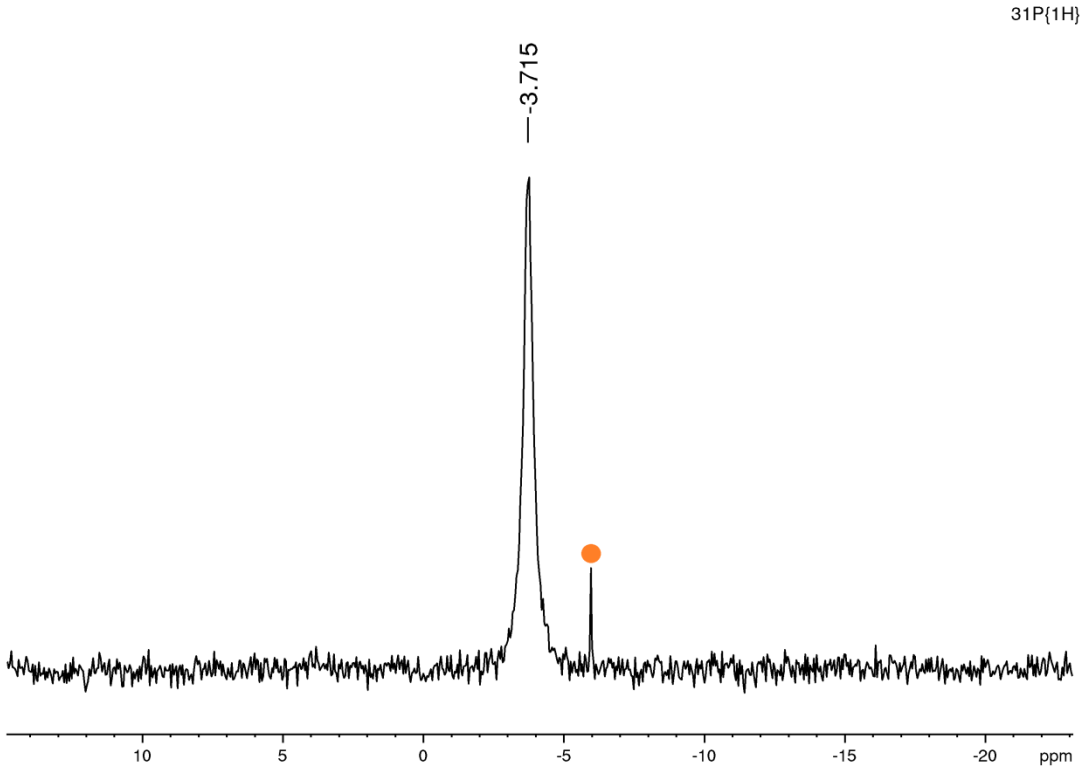

Figure S 42. $^{31}P\{^{1}H\}$ spectrum (CD_2Cl_2) of **3a**

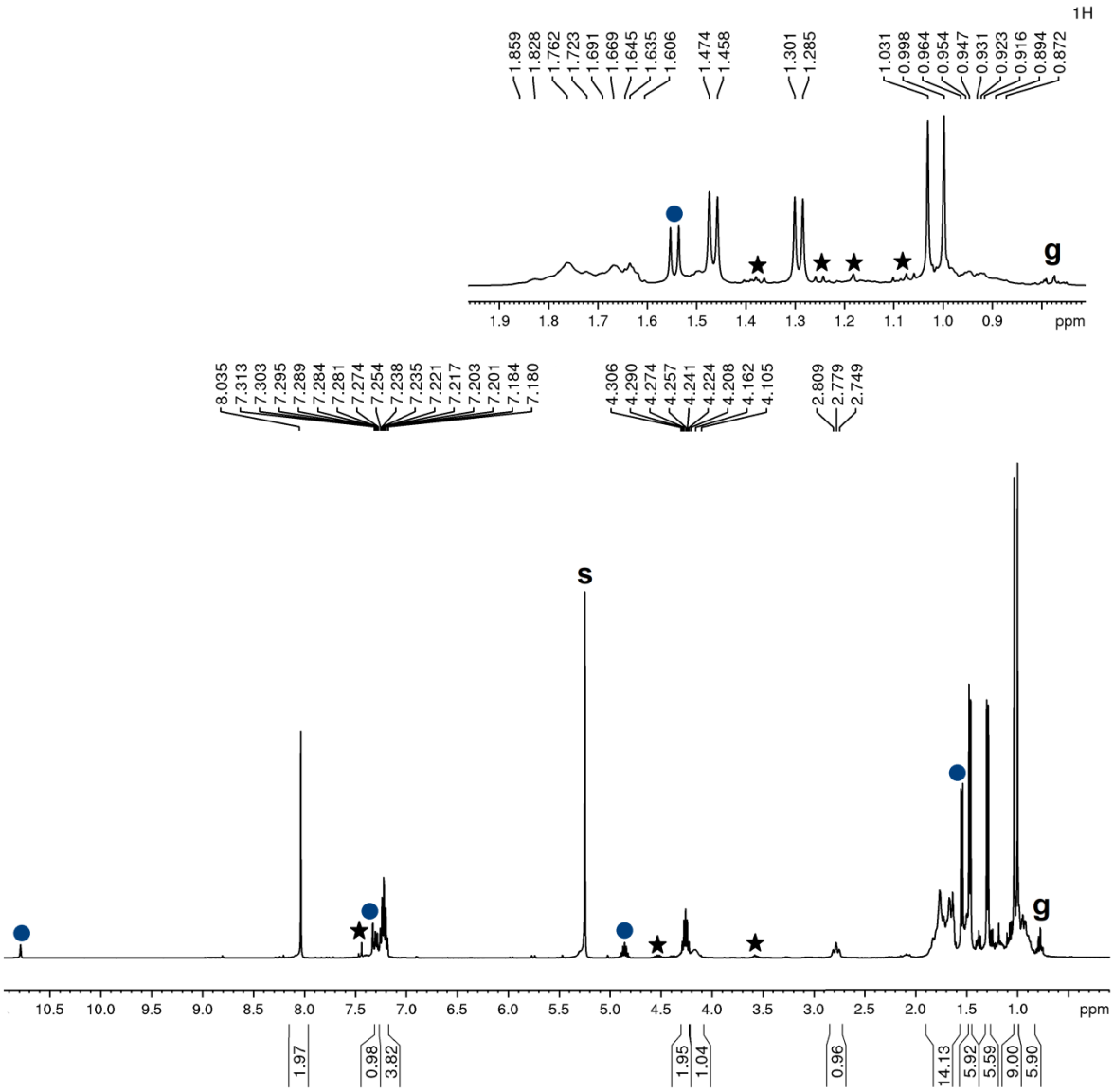

Figure S 43. ^{1}H spectrum (CD_2Cl_2) of **3a**

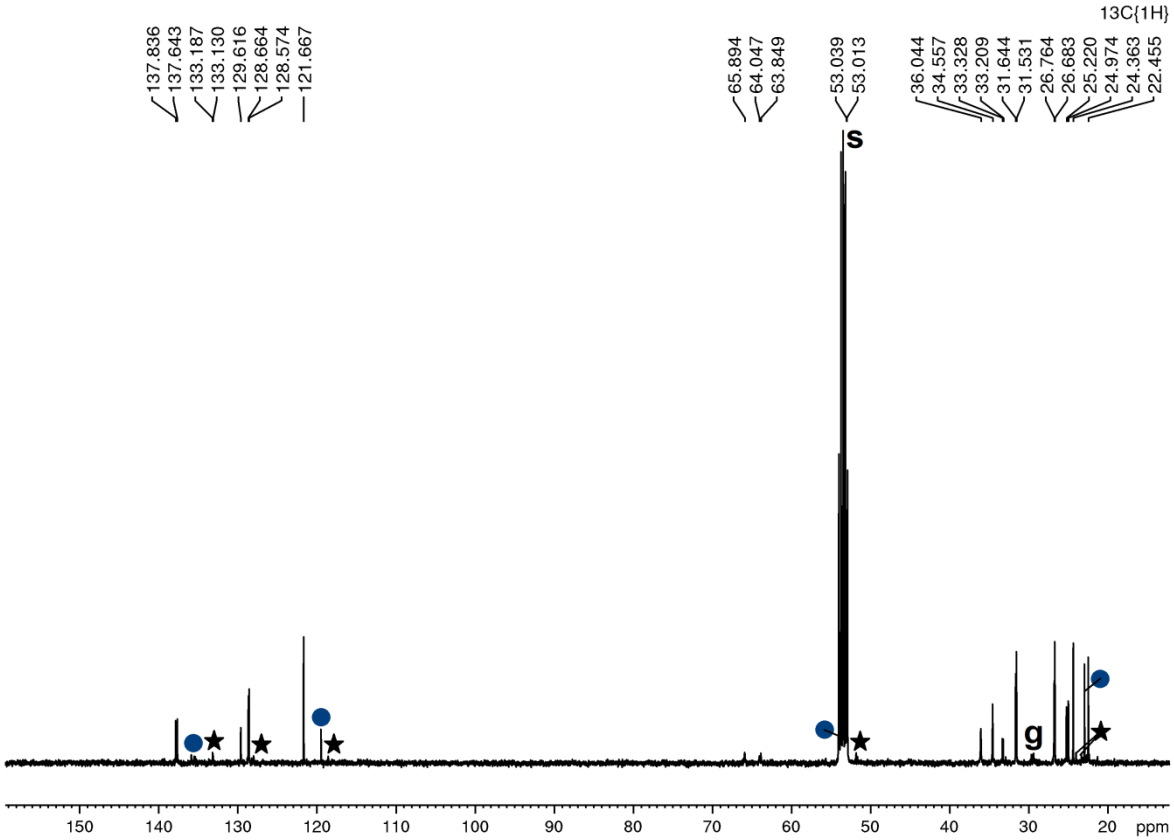

Figure S 44. $^{13}C\{^{1}H\}$ spectrum (CD_2Cl_2) of **3a**

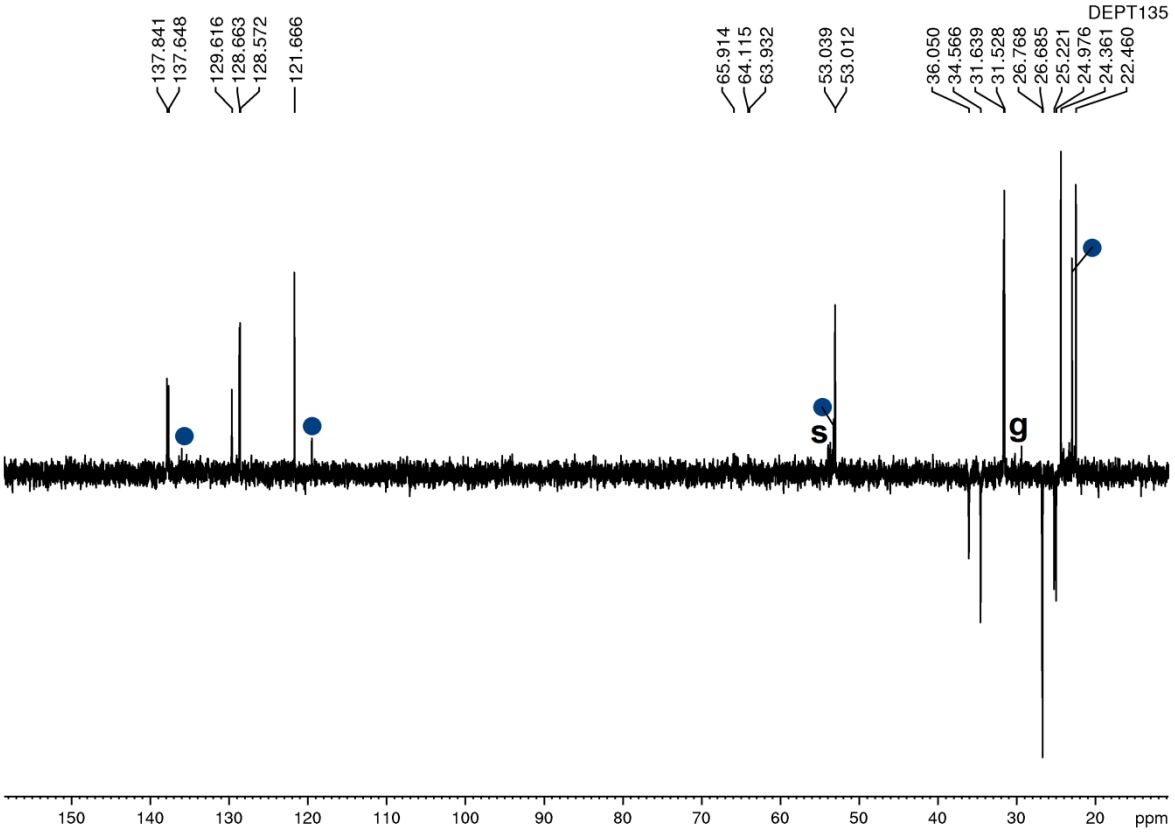

Figure S 45. ^{135}DEPT spectrum (CD_2Cl_2) of **3a**

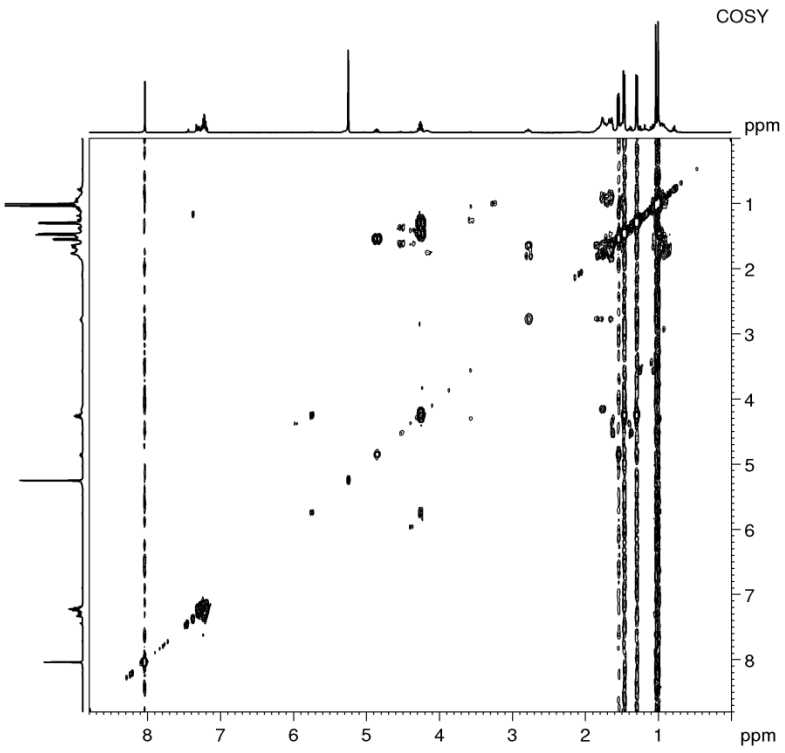

Figure S 46. COSY spectrum (CD_2Cl_2) of **3a**

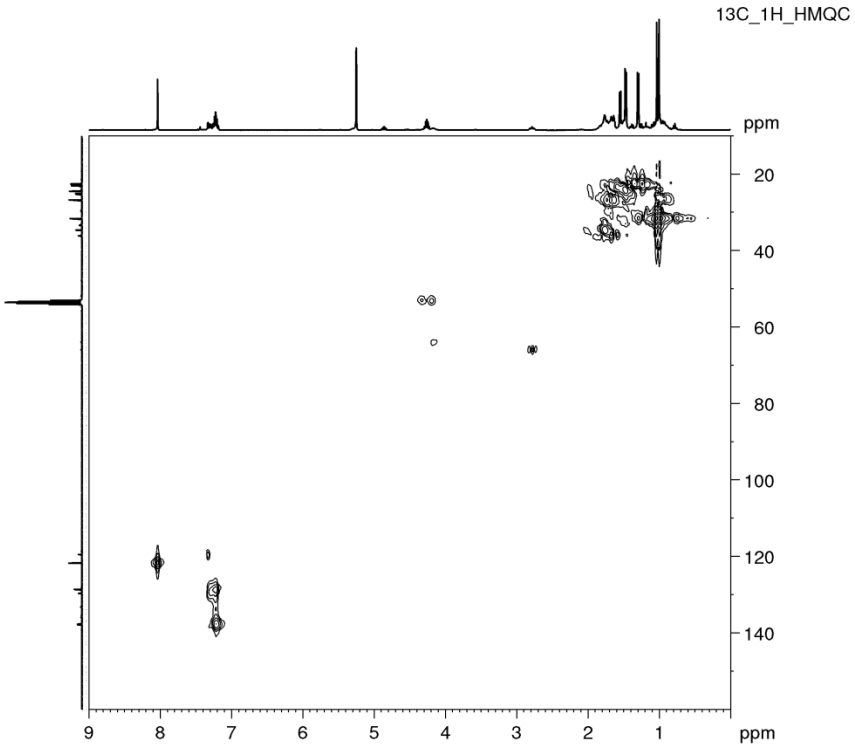

Figure S 47. ^{13}C ^{1}H HMQC spectrum (CD_2Cl_2) of **3a**

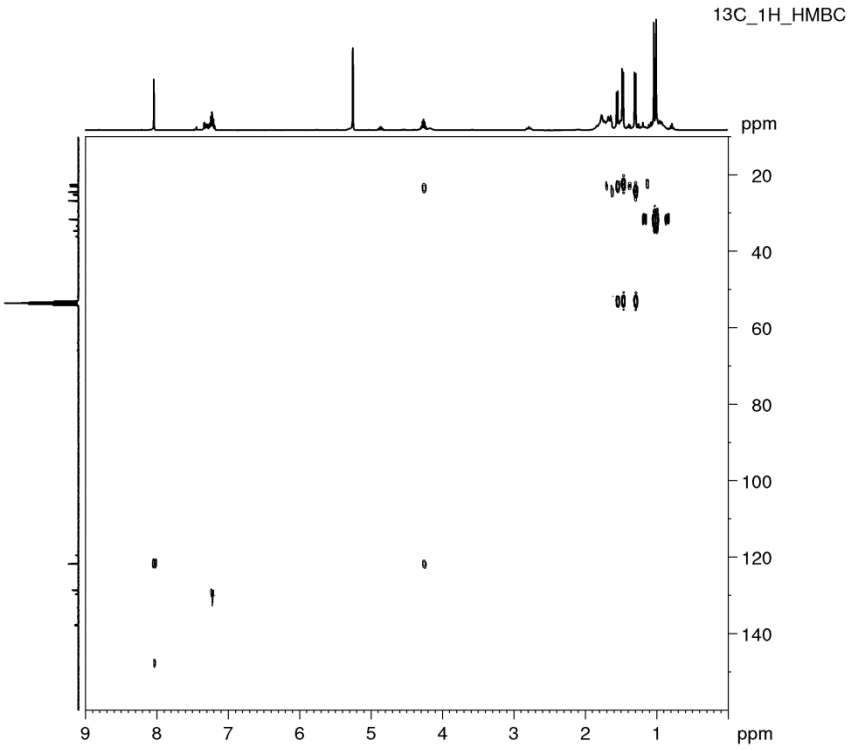

Figure S 48. ^{13}C ^{1}H HMBC spectrum (CD_2Cl_2) of **3a**

NMR spectra of 3b

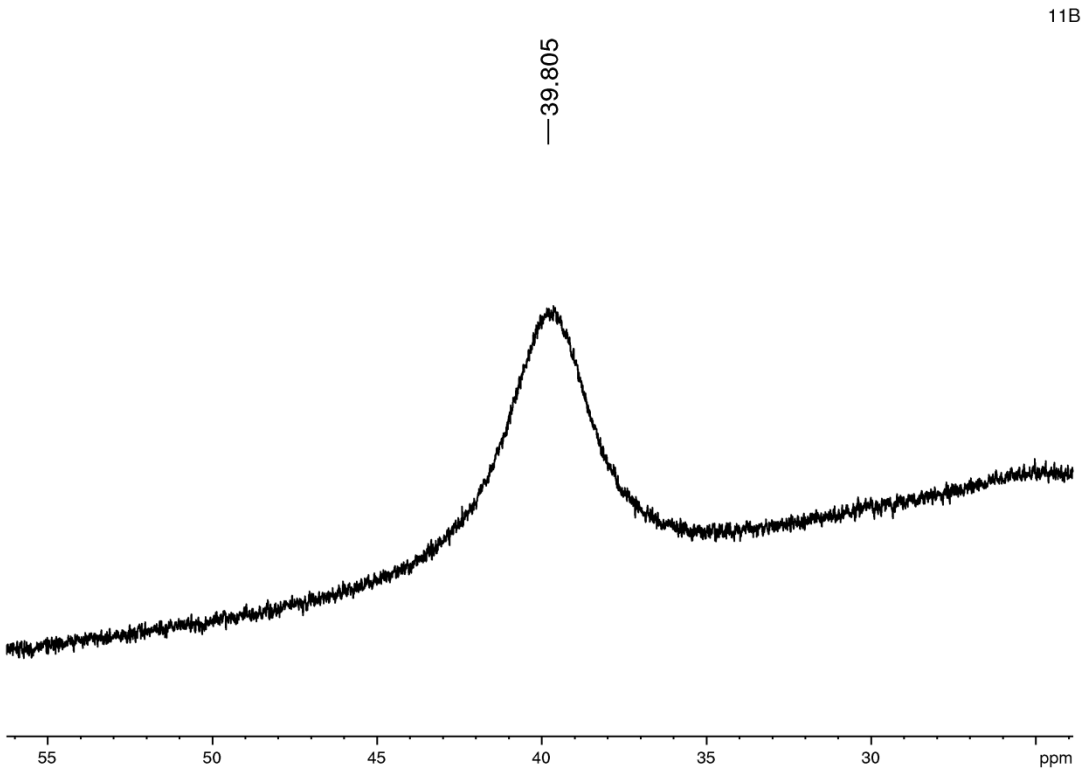

Figure S 49. ^{11}B spectrum (CD_2Cl_2) of **3b**

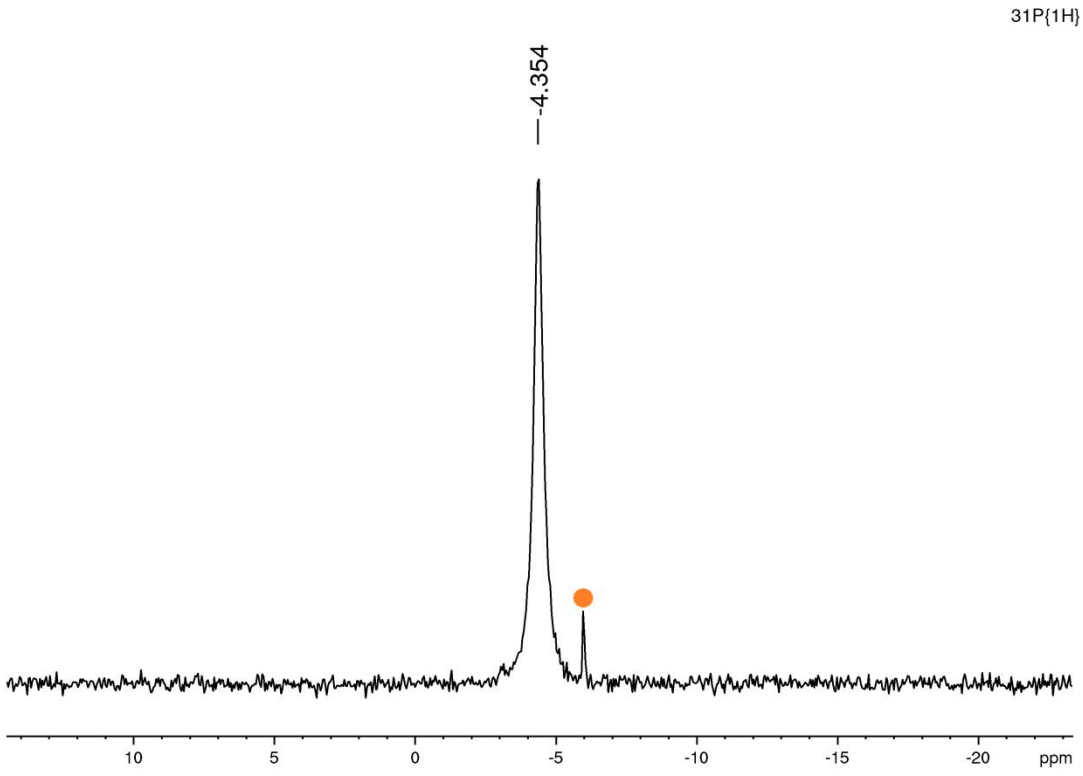

Figure S 50. $^{31}P\{^{1}H\}$ spectrum (CD_2Cl_2) of **3b**

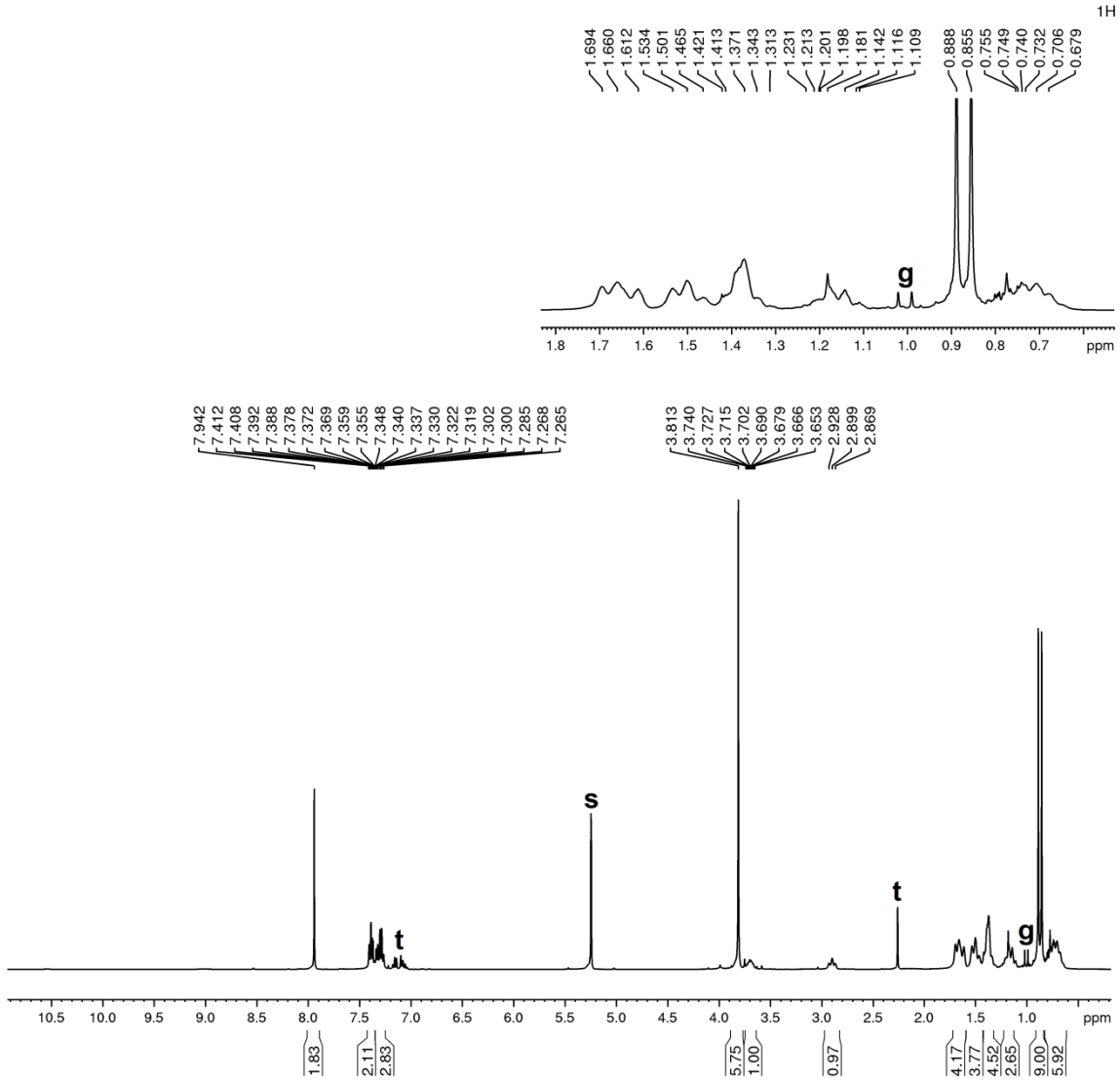

Figure S 51. ^{1}H spectrum (CD_2Cl_2) of **3b**

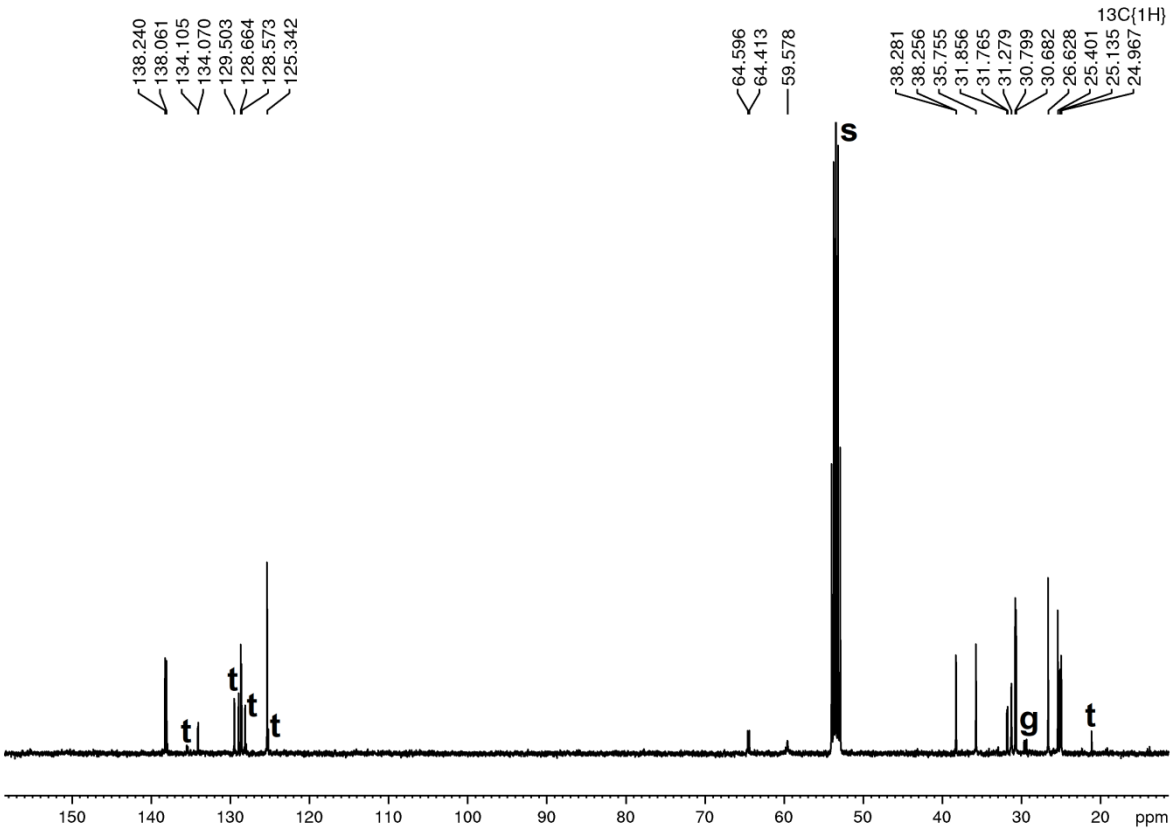

Figure S 52. $^{13}C\{^{1}H\}$ spectrum (CD_2Cl_2) of **3b**

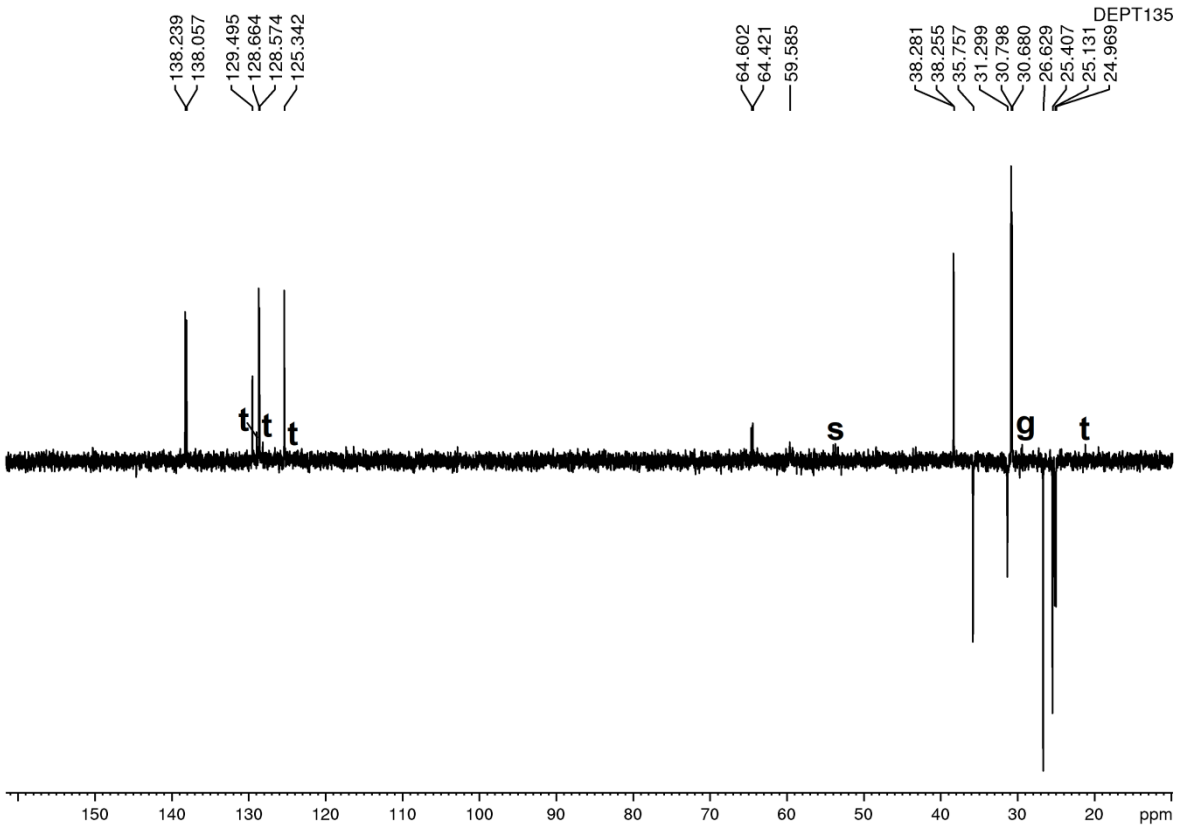

Figure S 53. ^{135}DEPT spectrum (CD_2Cl_2) of **3b**

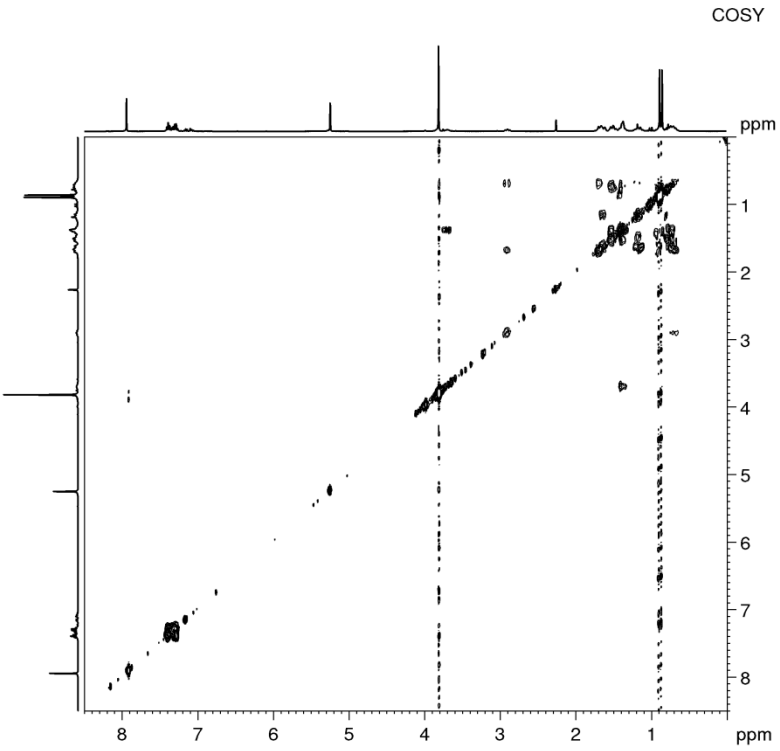

Figure S 54. COSY spectrum (CD_2Cl_2) of **3b**

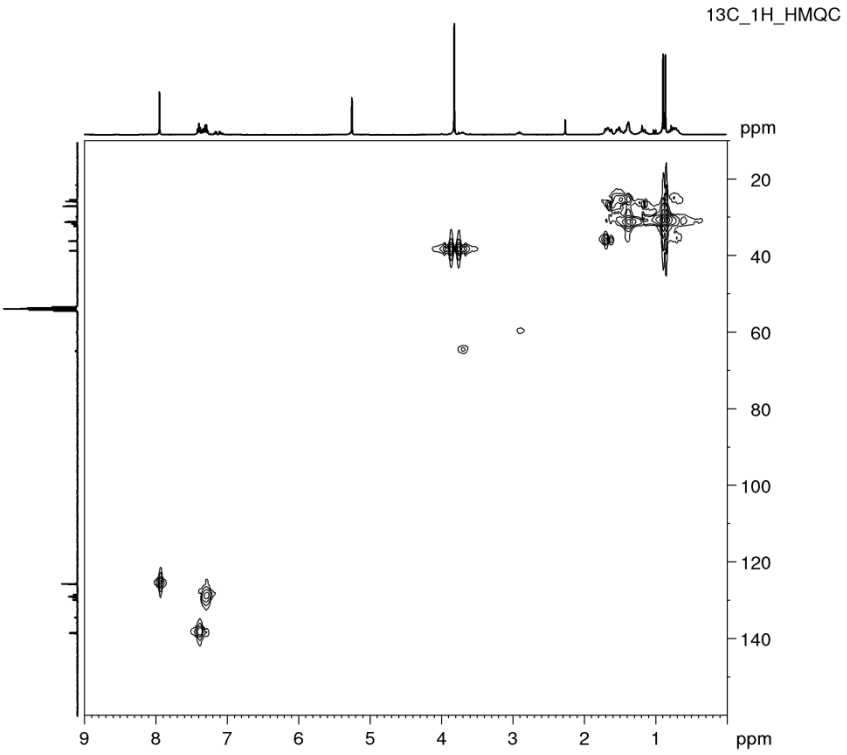

Figure S 55. ^{13}C ^{1}H HMQC spectrum (CD_2Cl_2) of **3b**

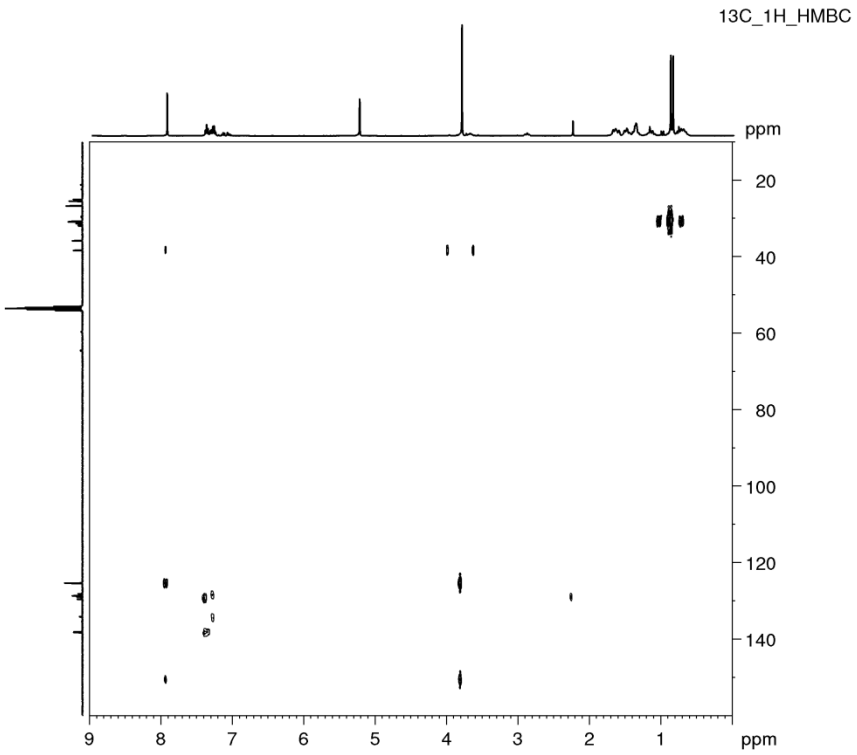

Figure S 56. ^{13}C ^{1}H HMBC spectrum (CD_2Cl_2) of **3b**

Reactivity studies

Reaction of 3a with Li[Al(OC(CF$_3$)$_3$)$_4$]

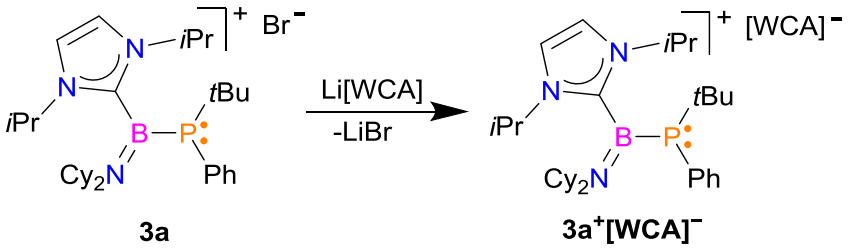

3a **3a$^+$[WCA]$^-$**

[WCA]$^-$ = [Al(OC(CF$_3$)$_3$)$_4$]$^-$

Scheme S 3. Reaction of **3a** with Li[Al(OC(CF$_3$)$_3$)$_4$].

A solution of **3a** (0.147 g, 0.250 mmol) in CH_2Cl_2 (2 mL) was added dropwise to a stirred suspension of Li[Al(OC(CF$_3$)$_3$)$_4$] (0.244 g, 0.250 mmol) in CH_2Cl_2 (3 mL) at -30°C. The mixture was allowed to warm to room temperature and stirred overnight. Progress of the reaction was monitored by ^{11}B, ^{31}P, ^{27}Al, and ^{11}F NMR spectroscopy.

NMR data of reaction mixture

^{11}B NMR (CD_2Cl_2): δ 40.6 (bs, **3a$^+$**).

$^{31}P\{^{1}H\}$ NMR (CD_2Cl_2): δ **-3.8** (bs, **3a**$^{+}$), δ -5.9 (s *t*BuPhPH)

^{27}Al NMR (CD_2Cl_2): δ 34.2 (s, [***Al***$(OC(CF_3)_3)_4]^-$).

NMR spectra of reaction mixture

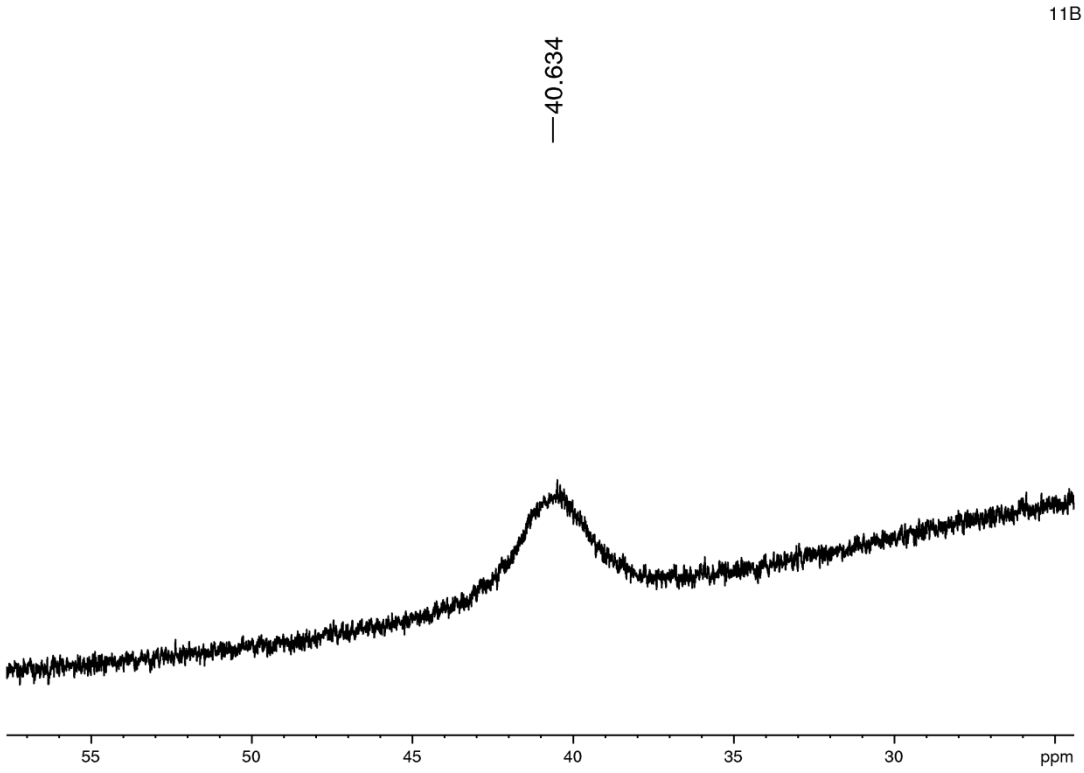

Figure S 57. ^{11}B NMR spectrum. Reaction of **3a** with $Li[Al(OC(CF_3)_3)_4]$

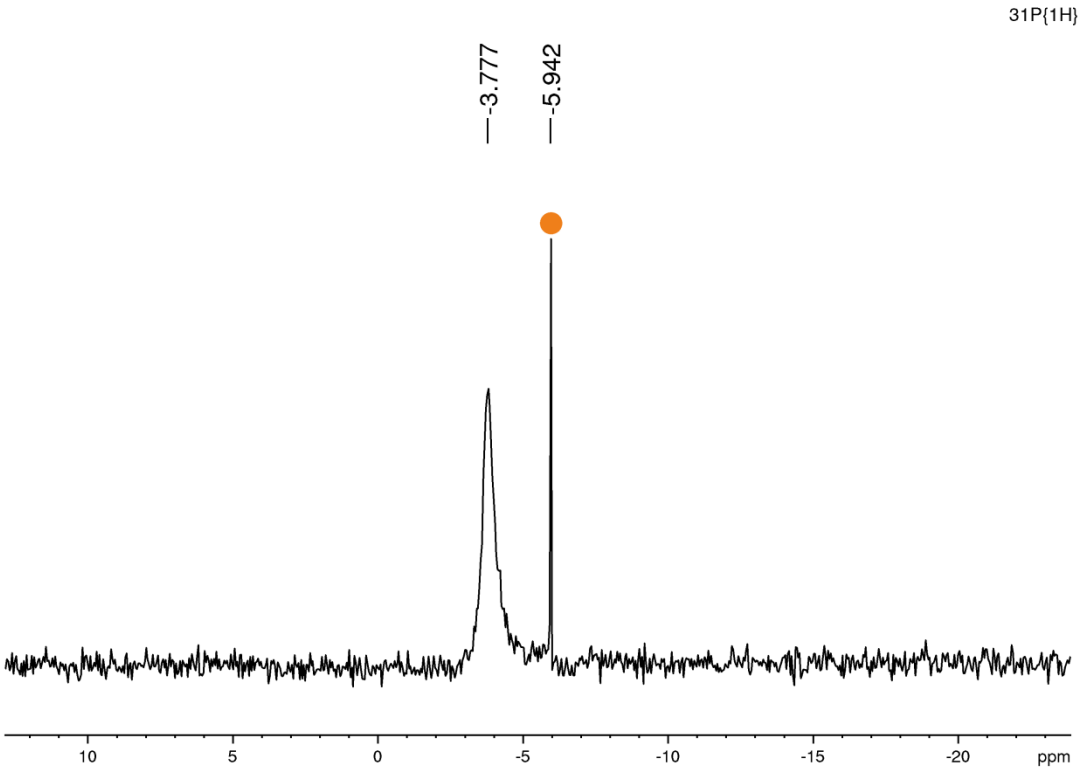

Figure S 58. $^{31}P\{^{1}H\}$ NMR spectrum. Reaction of **3a** with $Li[Al(OC(CF_3)_3)_4]$

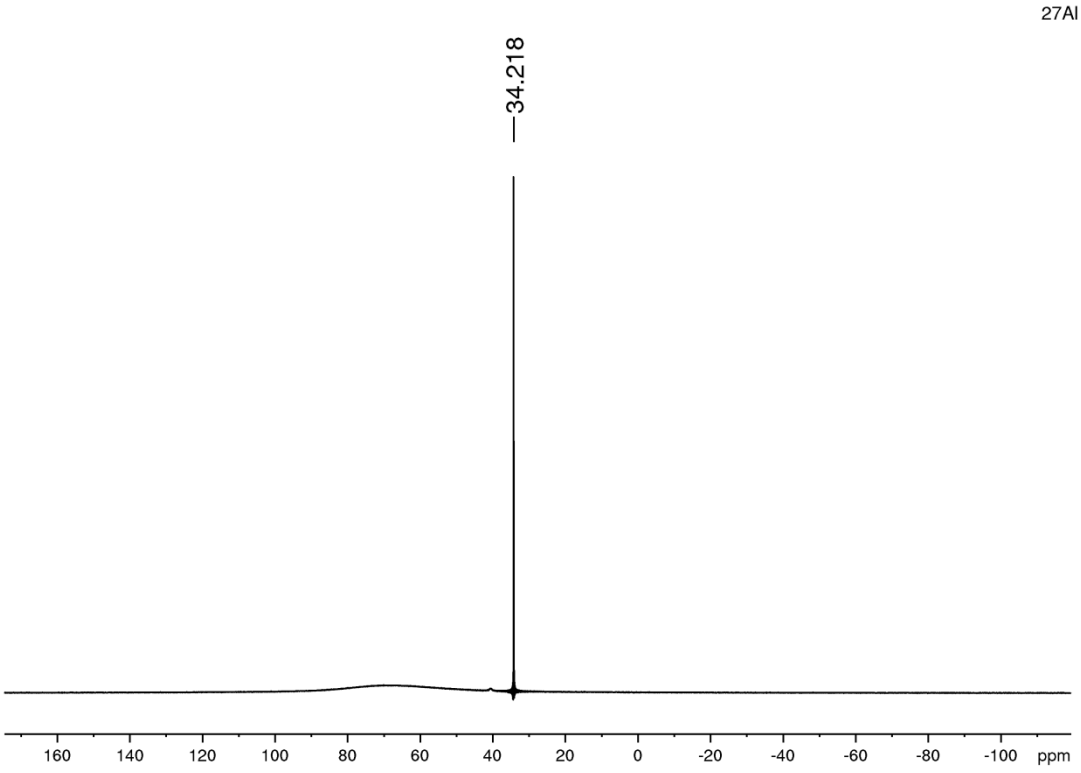

Figure S 59. ^{27}Al NMR spectrum. Reaction of **3a** with $Li[Al(OC(CF_3)_3)_4]$

Reaction of 1 with AuCl·SMe$_2$

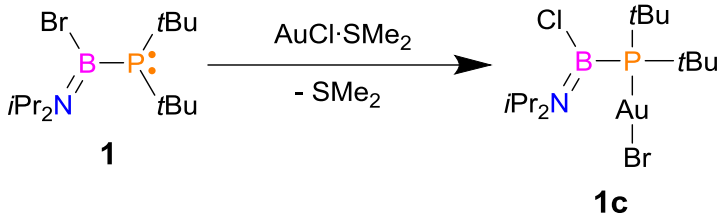

Scheme S 3. Synthesis of **1c**

A solution of (*i*Pr$_2$N)B(Br)P*t*Bu$_2$ (0.084 g, 0.250 mmol) in CH_2Cl_2 (2 mL) was added dropwise to the stirred suspension of AuCl·SMe$_2$ in CH_2Cl_2 (2 mL) at -50°C. The reacting mixture was then warmed up to room temperature and the solvent was evaporated under reduced pressure. Solid residue was re-dissolved in toluene and X-ray quality crystals were obtained from toluene solution layered with petroleum ether at -20°C. Yield 60% (0.085 g, 0.150 mmol). **Elemental analysis** calc. for $C_{14}H_{32}AuBBrClNP$ (568.52 g/mol): C, 29.58; H, 5.673; N, 2.46. Found: C, 29.66; H, 5.650; N, 2.40.

NMR data of 1c

^{11}B NMR (C_6D_6): δ 34.1 (d, $^1J_{PB}$ = 126.5 Hz).

^{31}P{^{1}H} NMR (C_6D_6): δ 32.3 (bm).

^{1}H NMR (C_6D_6): δ 6.02 (dsept, 1 H, $^3J_{HH}$ = 6.6 Hz, $^4J_{PH}$ = 3.7 Hz, C***H***(CH$_3$)$_2$); 2.99 (dsept, 1 H, $^3J_{HH}$ = 7.0 Hz, $^4J_{PH}$ = 2.7 Hz, C***H***(CH$_3$)$_2$); 1.15 (d, 18H, $^3J_{HH}$ = 15.4 Hz, C(C***H***$_3$)$_3$, overlapped with CH(C***H***$_3$)$_2$); 1.15 (d, 6 H, $^3J_{HH}$ = 7.0 Hz, CH(C***H***$_3$)$_2$, overlapped with C(C***H***$_3$)$_3$); 0.93 (d, 6 H, $^3J_{HH}$ = 6.6 Hz, CH(C***H***$_3$)$_2$).

^{13}C{^{1}H} NMR (C_6D_6): δ 53.4 (d, $^3J_{CP}$ = 14.0 Hz, ***C***H(CH$_3$)$_2$); 48.8 (d, $^3J_{CP}$ = 3.8 Hz, ***C***H(CH$_3$)$_2$); 36.2 (d, $^1J_{CP}$ = 22.7 Hz, ***C***(CH$_3$)$_3$); 31.1 (d, $^2J_{CP}$ = 5.7 Hz, C(***C***H$_3$)$_3$); 22.5 (s, CH(***C***H$_3$)$_2$); 20.7 (s, CH(***C***H$_3$)$_2$).

NMR spectra of 1c

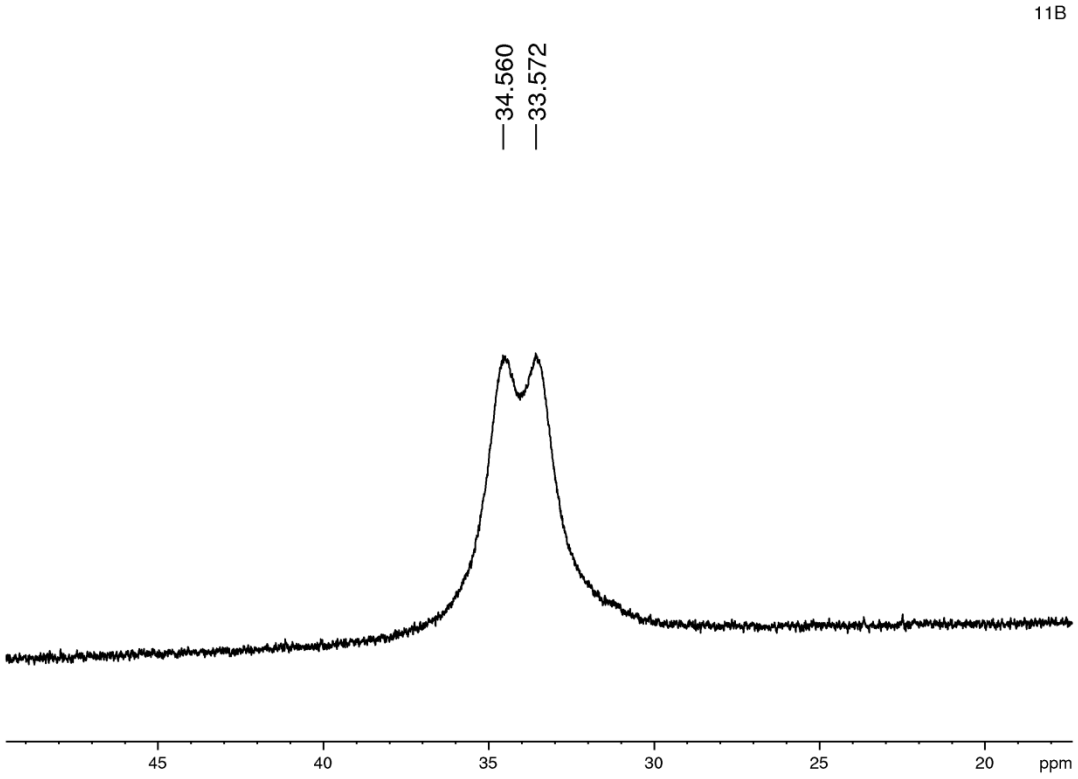

Figure S 60. ^{11}B spectrum (C_6D_6) of **1c**

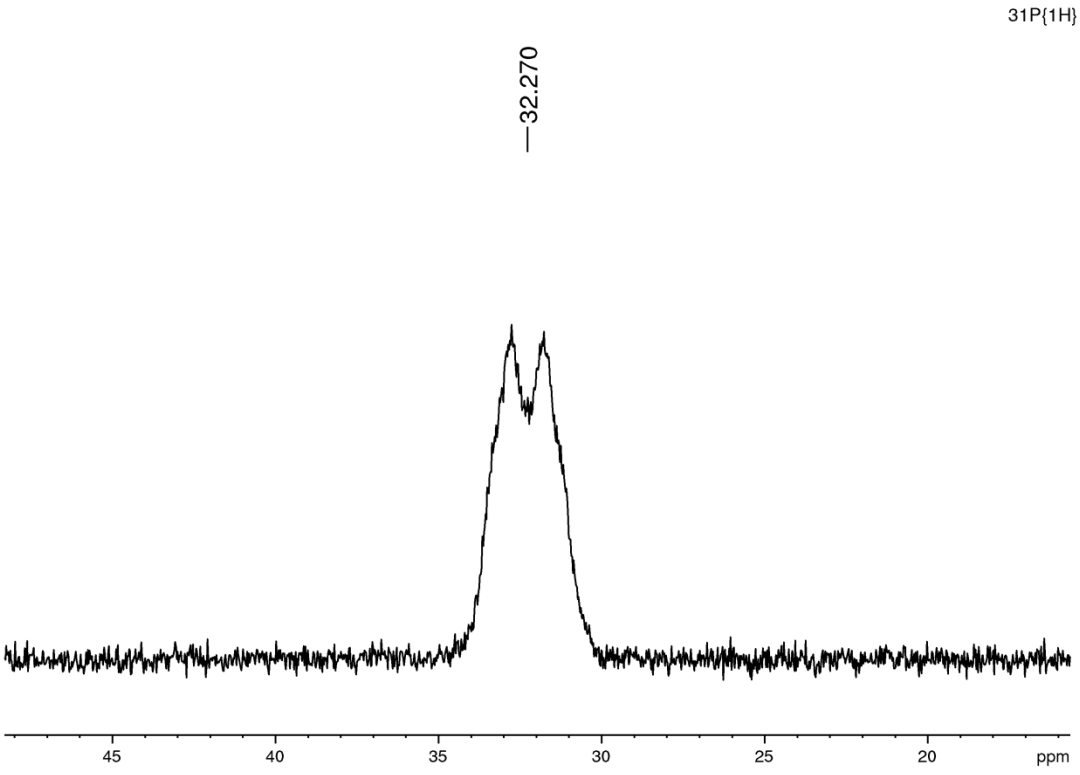

Figure S 61. $^{31}P\{^1H\}$ spectrum (C_6D_6) of **1c**

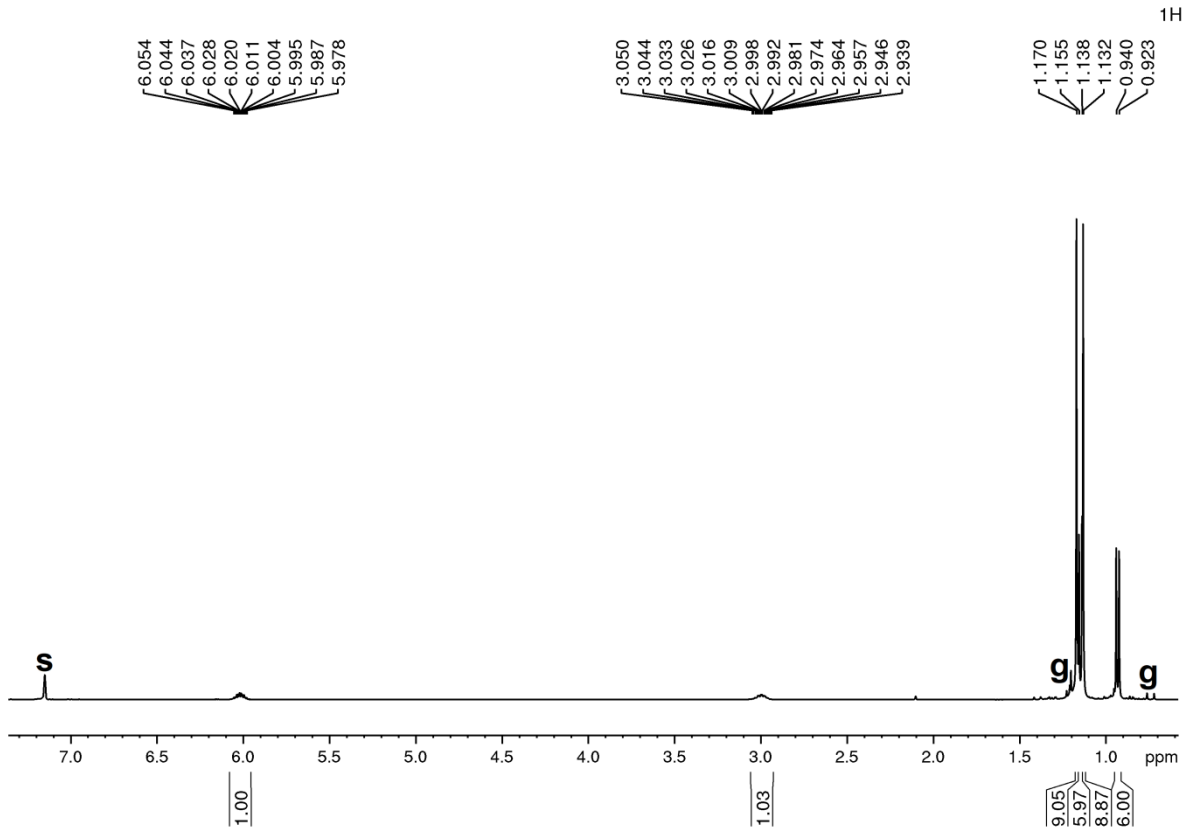

Figure S 62. ^{1}H spectrum (C_6D_6) of **1c**

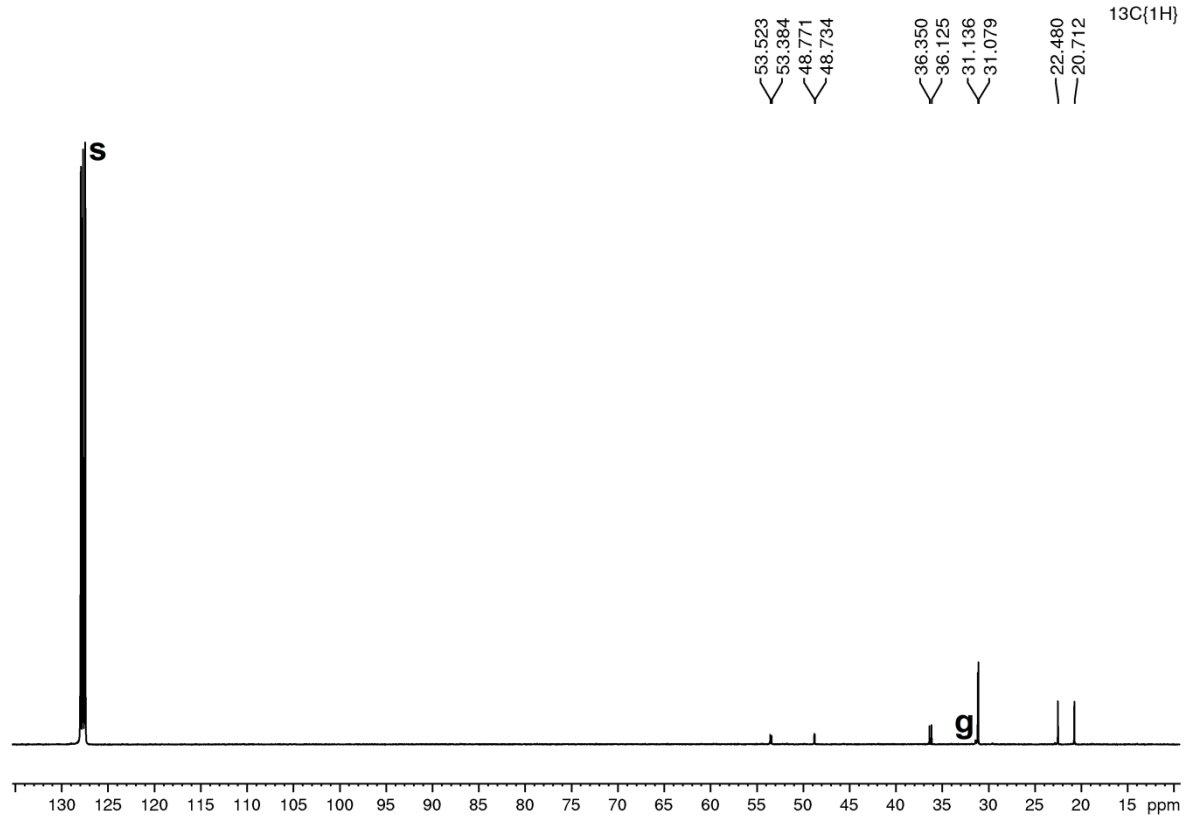

Figure S 63. $^{13}C\{^{1}H\}$ spectrum (C_6D_6) of **1c**

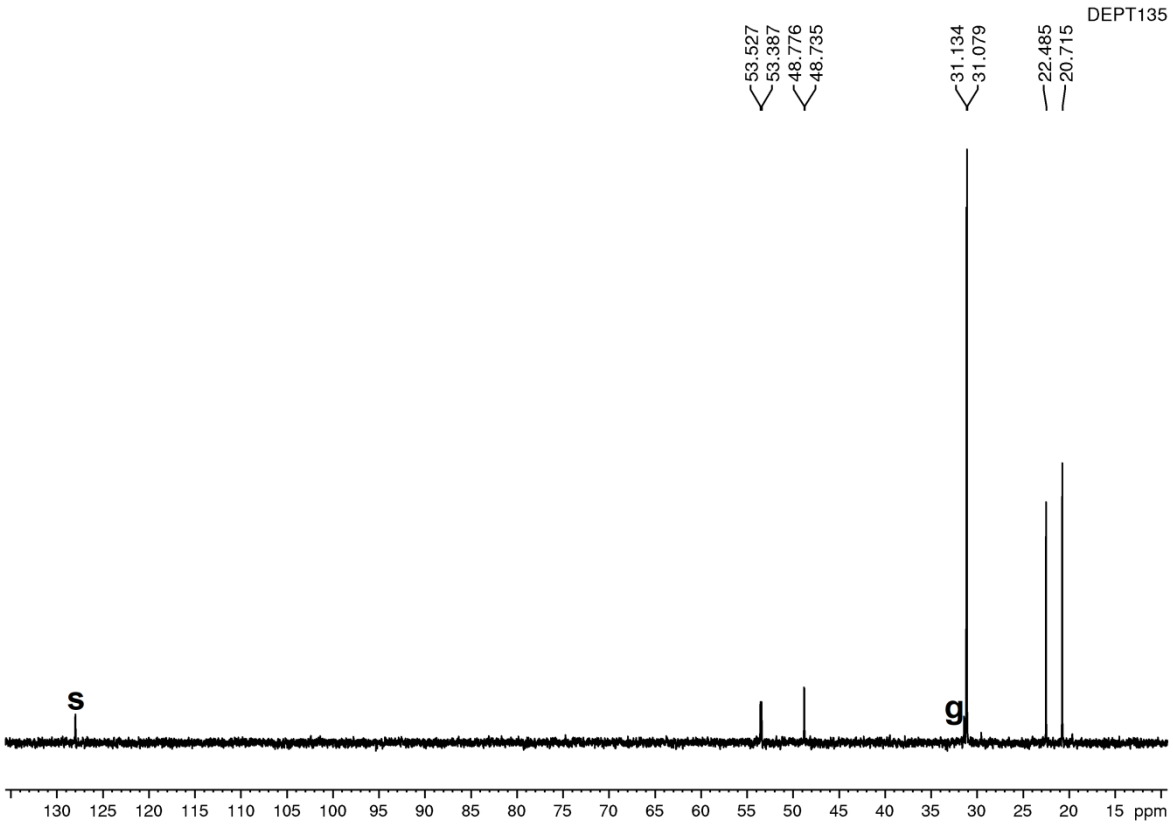

Figure S 64. ^{135}DEPT spectrum (C_6D_6) of **1c**

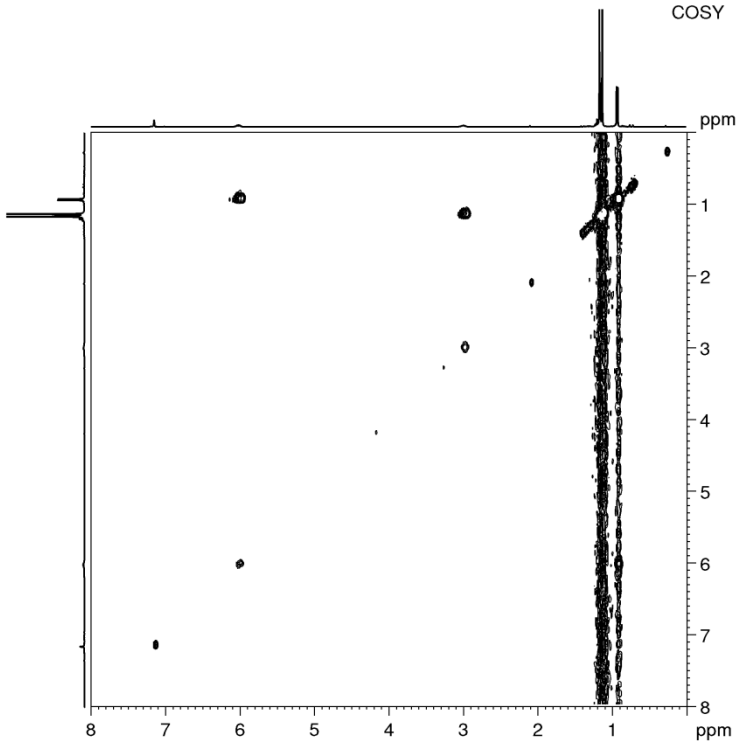

Figure S 65. COSY spectrum (C_6D_6) of **1c**

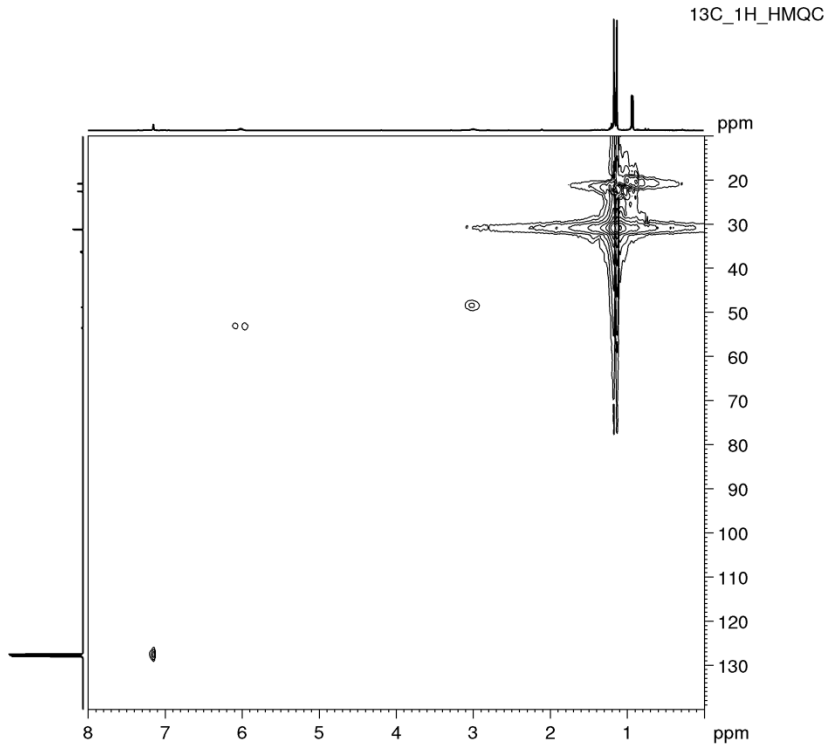

Figure S 66. ^{13}C ^{1}H HMQC spectrum (C_6D_6) of **1c**

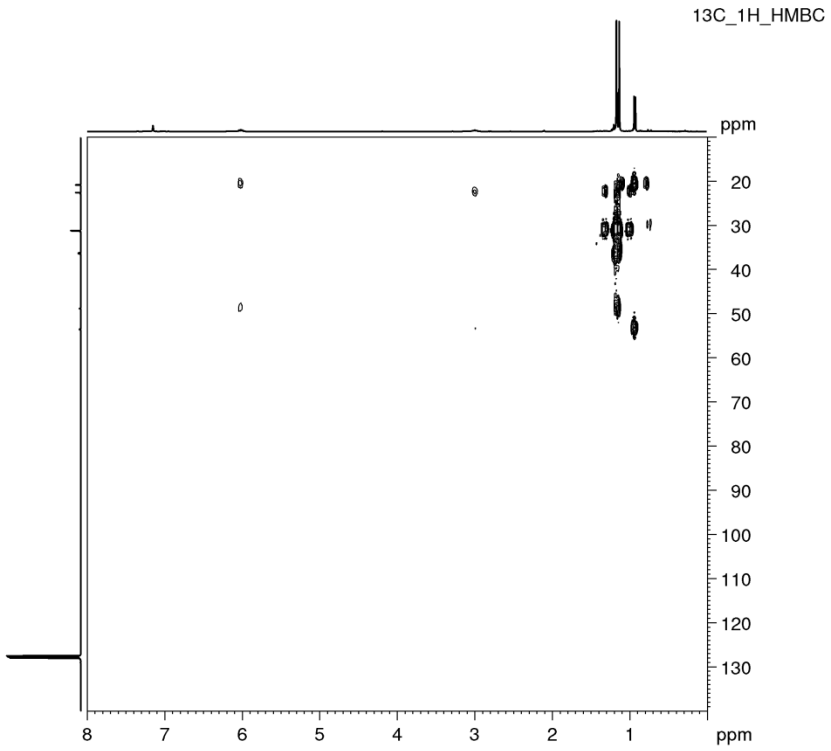

Figure S 67. ^{13}C ^{1}H HMBC spectrum (C_6D_6) of **1c**

Reaction of 1 with AuCl·SMe$_2$ and Li[Al(OC(CF$_3$)$_3$)$_4$]

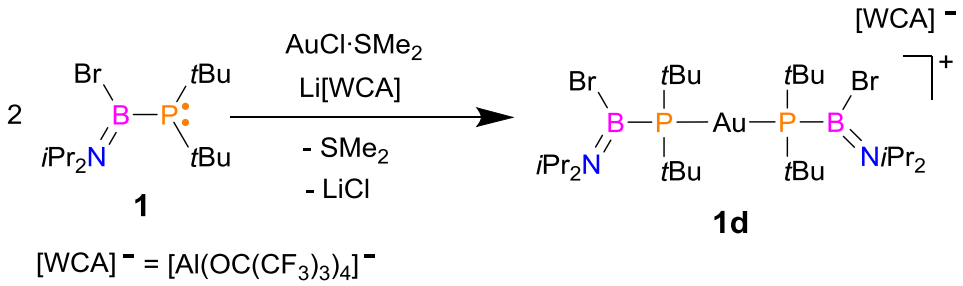

Scheme S 4. Synthesis of **1d**

A solution of (*i*Pr$_2$N)B(Br)P*t*Bu$_2$ (0.168 g, 0.500 mmol) in CH_2Cl_2 (3 mL) was added dropwise to the stirred suspension of Li[Al(OC(CF$_3$)$_3$)$_4$] (0.244g, 0.250 mmol) and AuCl·SMe$_2$ (0.074 g, 0.250 mmol) in CH_2Cl_2 (2 mL) -50°C. The reacting mixture was then warmed up to room temperature and filtrated to remove LiCl. Filtrate was concentrated to 2 mL and layered with petroleum ether. X-ray quality crystals were obtained at -20°C. Yield 57.5% (0.264 g, 0.144 mmol). **Elemental analysis** calc. for $C_{44}H_{64}AlAuB_2Br_2F_{36}N_2O_4P_2$ (1836.26 g/mol): C, 28.78; H, 3.513; N, 1.52. Found: C, 28.96; H, 3.290; N, 1.51.

NMR data of 1d

^{11}B NMR (CD_2Cl_2): δ 32.9 (s).

^{31}P{^{1}H} NMR (CD_2Cl_2): δ 38.4 (s).

^{1}H NMR (CD_2Cl_2): δ 5.53 (bm, 2H, $(H_3C)_2CH$); 3.64 (bm, 2H, $(H_3C)_2CH$); 1.48 (m, overlapped 48H, $C(CH_3)_3$ and $(H_3C)_2CH$); 1.19 (m, overlapped, 12H, $(H_3C)_2CH$).

^{13}C{^{1}H} NMR (CD_2Cl_2): δ 121.2 (q, $^1J_{CF}$ = 292.6 Hz, $OC(CF_3)_3$); 55.9 (m, $CH(CH_3)_2$); 51.1 (m, $CH(CH_3)_2$); 37.8 (m, $C(CH_3)_3$);32.0 (s, $C(CH_3)_3$); 23.0 (s, $CH(CH_3)_2$); 21.4 (s, $CH(CH_3)_2$).

^{27}Al NMR (CD_2Cl_2): δ 34.6 (s, $[Al(OC(CF_3)_3)_4]^-$).

^{19}F NMR (CD_2Cl_2): δ -75.7 (s, $OC(CF_3)_3$).

NMR spectra of 1d

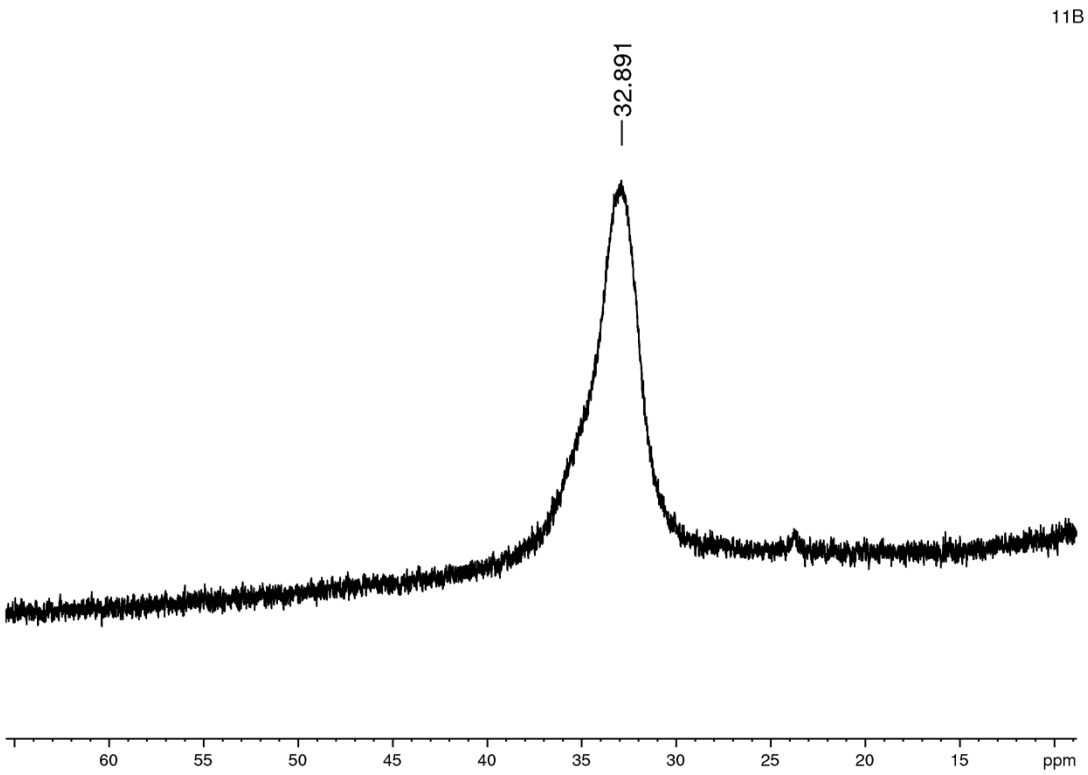

Figure S 68. ^{11}B spectrum (CD_2Cl_2) of **1d**

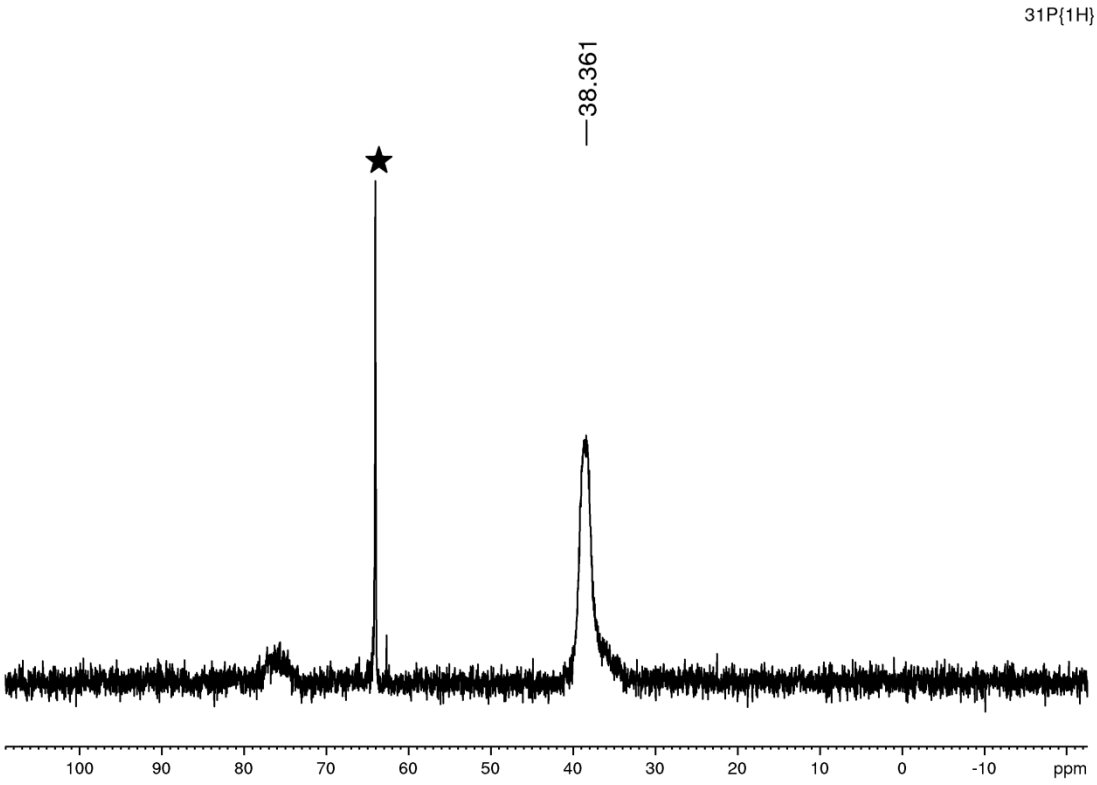

Figure S 69. $^{31}P\{^{1}H\}$ spectrum (CD_2Cl_2) of **1d**

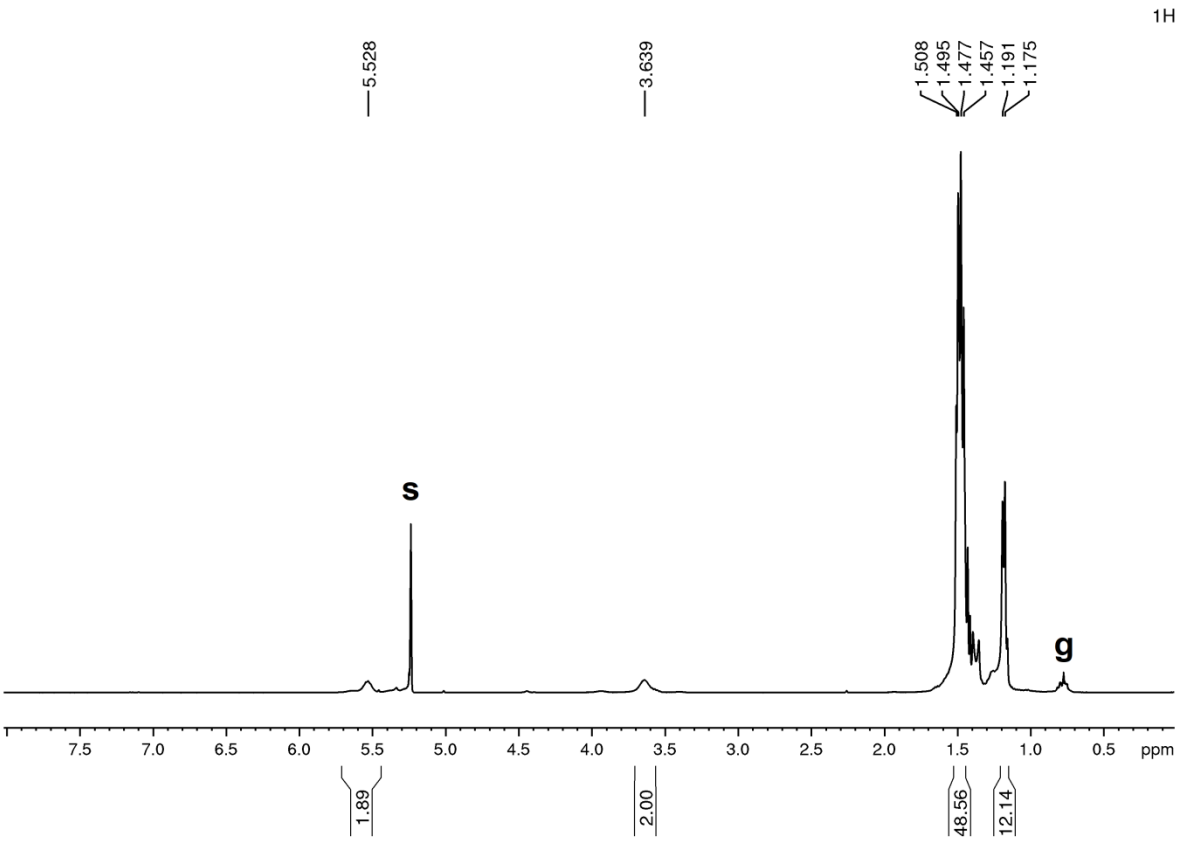

Figure S 70. ^{1}H spectrum (CD_2Cl_2) of **1d**

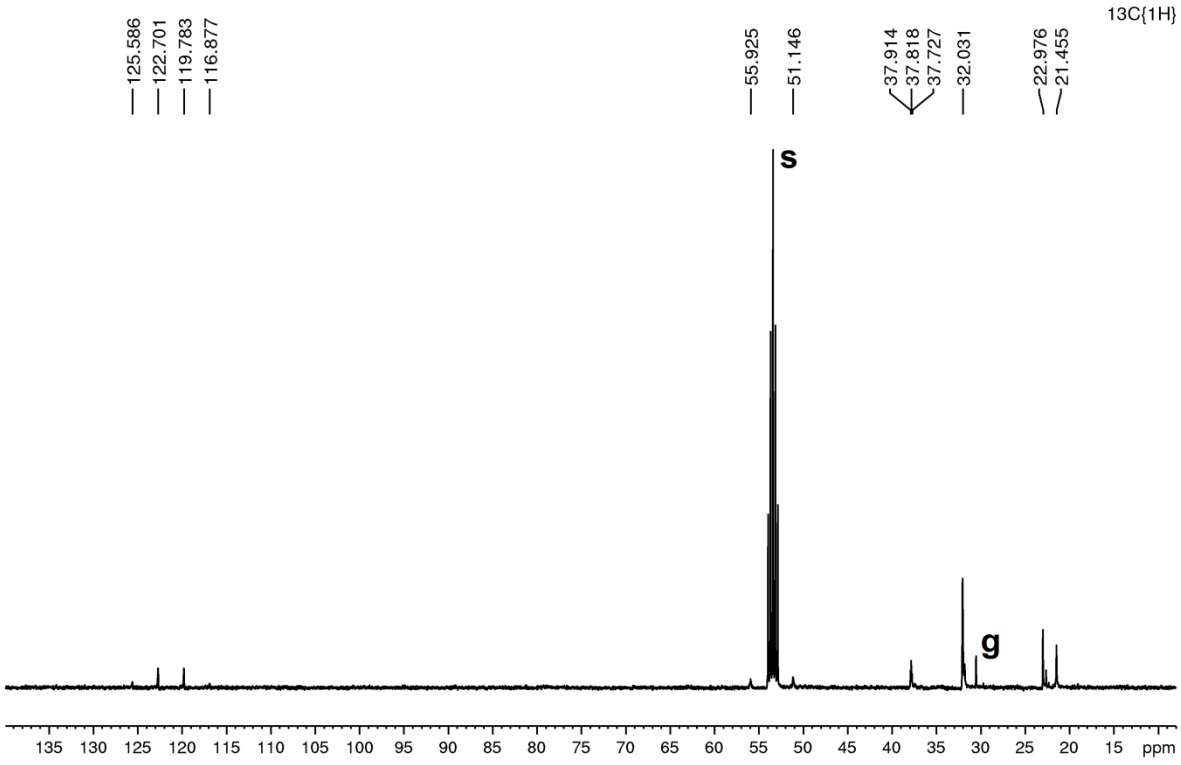

Figure S 71. $^{13}C\{^{1}H\}$ spectrum (CD_2Cl_2) of **1d**

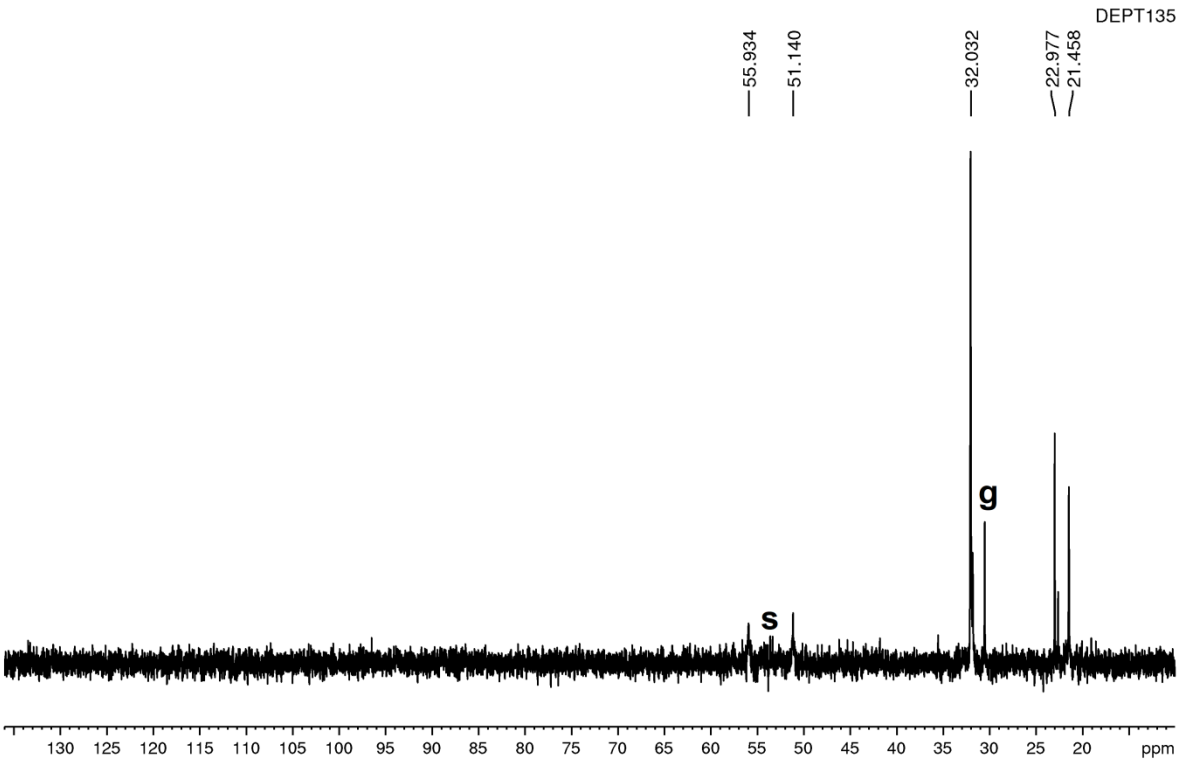

Figure S 72. ^{135}DEPT spectrum (CD_2Cl_2) of **1d**

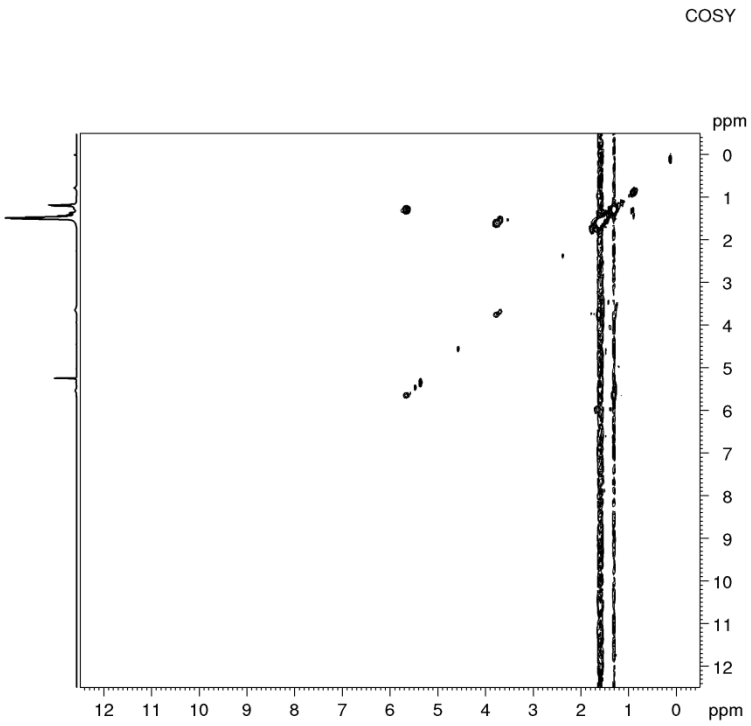

Figure S 73. COSY spectrum (CD_2Cl_2) of **1d**

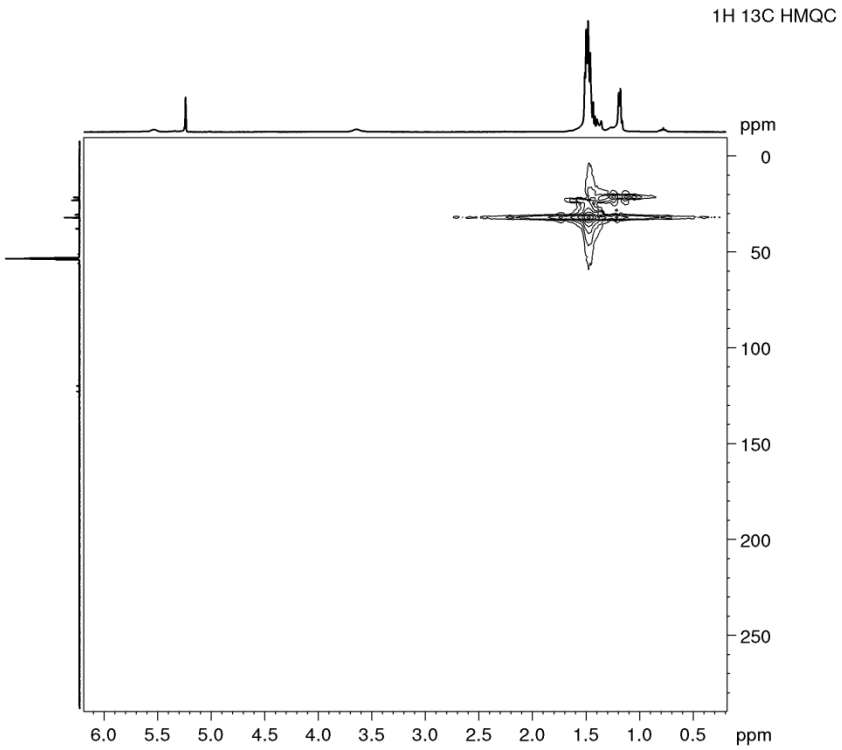

Figure S 74. ^{13}C ^{1}H HMQC spectrum (CD_2Cl_2) of **1d**

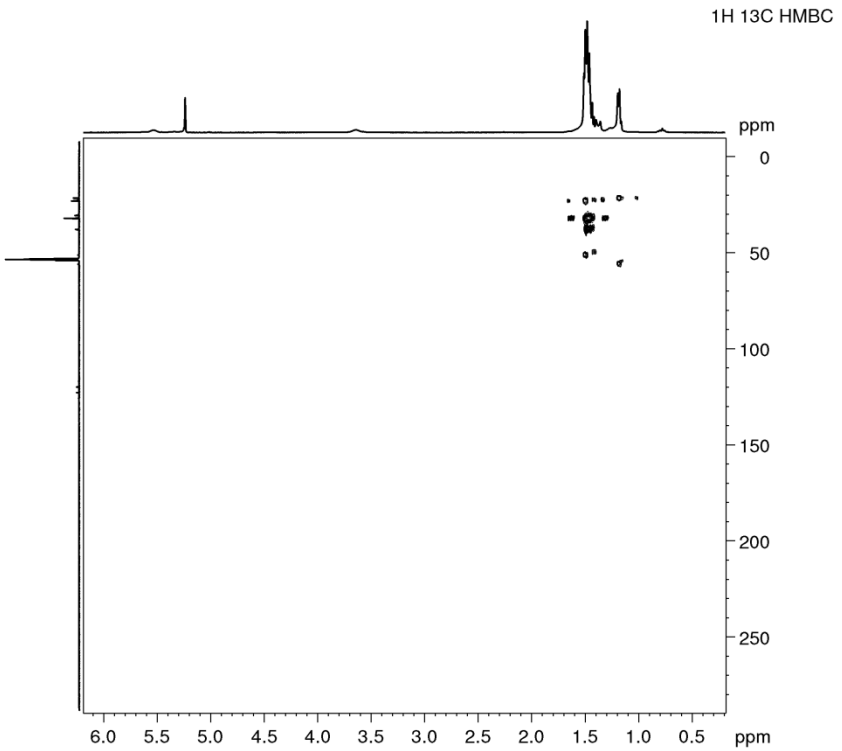

Figure S 75. ^{13}C ^{1}H HMBC spectrum (CD_2Cl_2) of **1d**

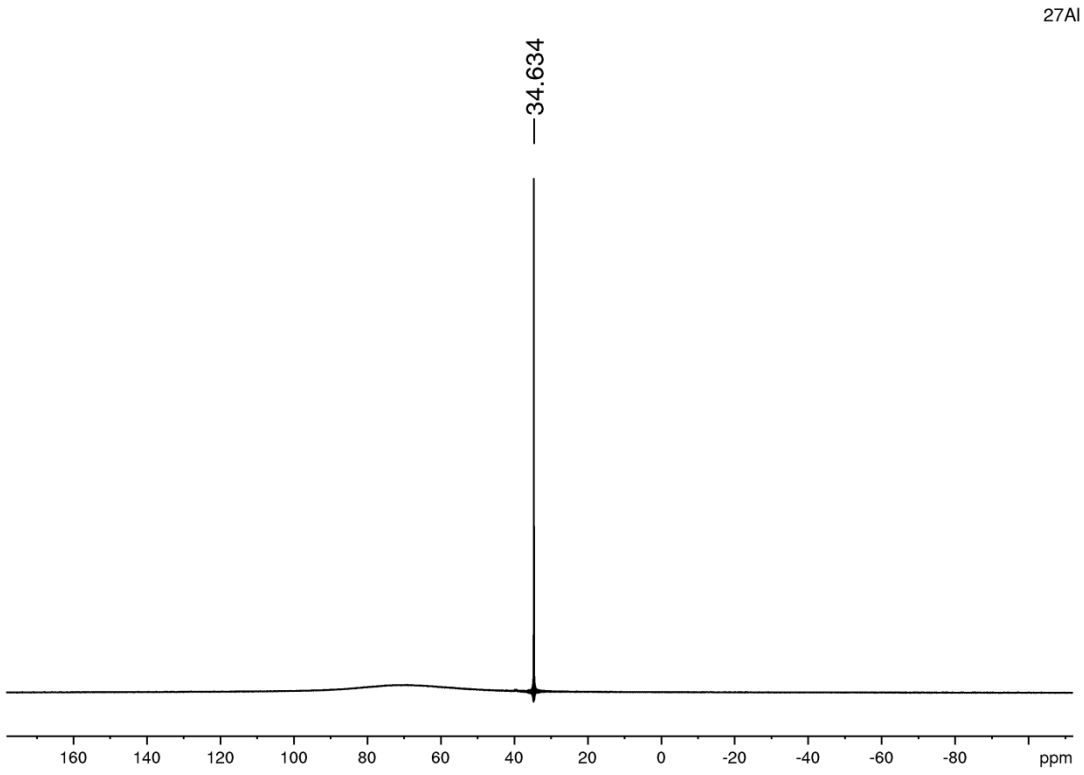

Figure S 76. ^{27}Al spectrum (CD_2Cl_2) of **1d**

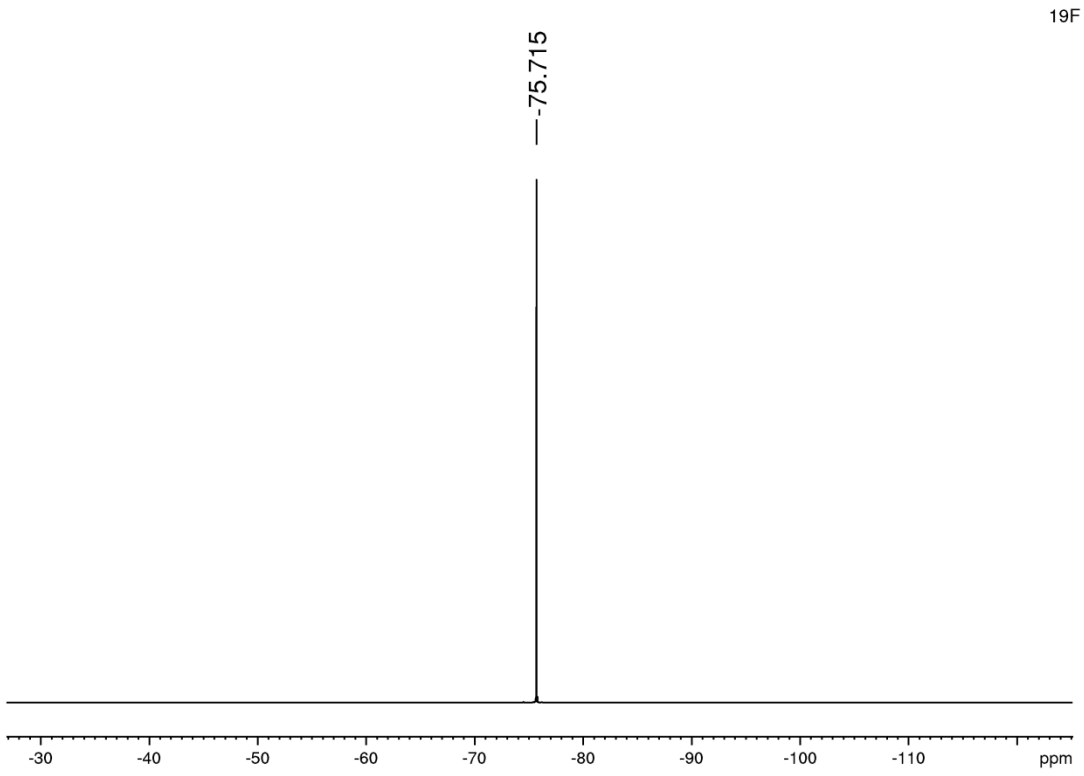

Figure S 77. ^{19}F spectrum (CD_2Cl_2) of **1d**

Reaction of 1a with AuCl·SMe$_2$ and Li[Al(OC(CF$_3$)$_3$)$_4$]

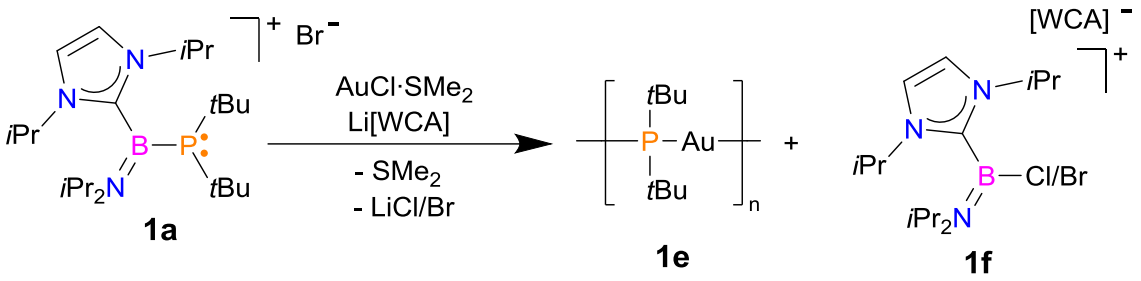

Scheme S 5. Synthesis of **1e** and **1f**

To the suspension of AuCl·SMe$_2$ (0.074 g, 0.250 mmol) in CH_2Cl_2 (2 mL) the solution of **1a** (0.122 g, 0.025 mmol) in CH_2Cl_2 (2 mL) was added dropwise at room temperature. Afterwards, the obtained solution was added to the suspension of Li[Al(OC(CF$_3$)$_3$)$_4$] (0.244 g, 0.250 mmol) in CH_2Cl_2 (2 mL) also at room temperature. The solvent was then evaporated and the residue was partially redissolved in toluene obtaining yellowish solution. Residue insoluble in toluene was redissolved in CH_2Cl_2 (2 mL) and layered with 1 mL of petroleum ether. Storage at -20°C gave suitable orange crystals of **1f**. Yield: 76% (0.224 g, 0.191 mmol, yield for the estimated solid solution 77% 2-Cl and 23% 2-Br, based on ^{1}H NMR). **Elemental analysis** calc. for $C_{31}H_{30}AlBBr_{0.23}Cl_{0.77}F_{16}N_3O_4$ (1276.00 g/mol): C 29.18,; H, 2.449; N, 3.29. Found: C, 28.82; H, 2.240; N, 3.00.

NMR data of reaction mixture

^{11}B NMR (CD_2Cl_2): δ 28.6 (s, **1f-Cl**); 24.8 (s, **1f-Br**).

^{31}P{^{1}H} NMR (CD_2Cl_2): δ 91.7 (s, **1e**).

^{27}Al NMR (CD_2Cl_2): δ 34.9 (s, [***Al***(OC(CF$_3$)$_3$)$_4$]$^-$).

NMR data of 1f

^{11}B NMR (CD_2Cl_2): δ 29.0 (s, **1f-Cl**); 25.3 (s, **1f-Br**).

^{1}H NMR (CD_2Cl_2):

1f-Cl: δ 7.30 (s, 2 H, ***H***C=C***H*** of I*i*Pr$_2$); 4.30 (sept, 2 H, $^3J_{HH}$ = 6.7 Hz, C***H***(CH$_3$)$_2$ of I*i*Pr$_2$); 3.61 (sept, 1 H, $^3J_{HH}$ = 7.0 Hz, C***H***(CH$_3$)$_2$); 3.20 (sept, 1 H, $^3J_{HH}$ = 6.6 Hz, C***H***(CH$_3$)$_2$); 1.55 – 1.43 (m, 18 H, overlapped signals of CH(C***H***$_3$)$_2$ of I*i*Pr$_2$ and CH(C***H***$_3$)$_2$, overlapped also with CH(C***H***$_3$)$_2$ of I*i*Pr$_2$ of 1f-Br); 1.16 (d, 6 H, $^3J_{HH}$ = 6.6 Hz, CH(C***H***$_3$)$_2$).

1f-Br: δ 7.27 (s, 2H, ***H***C=C***H*** of I*i*Pr$_2$); 4.39 (m, 2 H, $^3J_{HH}$ = 6.7 Hz, C***H***(CH$_3$)$_2$ of I*i*Pr$_2$); 3.36 (sept, 1 H, $^3J_{HH}$ = 7.0 Hz, C***H***(CH$_3$)$_2$); 2.86 (sept, 1 H, $^3J_{HH}$ = 6.6 Hz, C***H***(CH$_3$)$_2$); 1.55 – 1.43 (m, 12 H, CH(C***H***$_3$)$_2$ of I*i*Pr$_2$, overlapped with CH(C***H***$_3$)$_2$ of I*i*Pr$_2$ and CH(C***H***$_3$)$_2$ of 1f-Cl); 1.36 (d, 6 H, $^3J_{HH}$ = 7.0 Hz, CH(C***H***$_3$)$_2$); 1.08 (d, 6 H, $^3J_{HH}$ = 6.6 Hz, CH(C***H***$_3$)$_2$).

^{13}C{^{1}H} NMR (CD$_2$Cl$_2$):

1f-Cl: δ 121.2 (q, $^1J_{CF}$ = 292.9 Hz, OC(***C***F$_3$)); 119.9 (s, H***C***=***C***H of I*i*Pr$_2$); 55.1 (s, ***C***H(CH$_3$)$_2$); 53.7 (s, ***C***H(CH$_3$)$_2$ of I*i*Pr$_2$, overlapped with solvent); 48.1 (s, ***C***H(CH$_3$)$_2$); 23.3 (s, CH(***C***H$_3$)$_2$ of I*i*Pr$_2$); 22.6 (s, CH(***C***H$_3$)$_2$); 22.4 (s, CH(***C***H$_3$)$_2$ of I*i*Pr$_2$); 21.2 (s, CH(***C***H$_3$)$_2$). The carbene carbon atom was not detected at the ^{13}C{^{1}H} spectrum.

1f-Br: δ 121.2 (q, $^1J_{CF}$ = 292.9 Hz, OC(***C***F$_3$)); 119.6 (s, H***C***=***C***H of I*i*Pr$_2$); 53.4 (s, ***C***H(CH$_3$)$_2$ of I*i*Pr$_2$, overlapped with solvent); 51.0 (s, ***C***H(CH$_3$)$_2$); 44.6 (s, ***C***H(CH$_3$)$_2$); 23.7 (s, CH(***C***H$_3$)$_2$ of I*i*Pr$_2$); 23.4 (s, CH(***C***H$_3$)$_2$); 22.6 (s, CH(***C***H$_3$)$_2$ of I*i*Pr$_2$); 21.7 (s, CH(***C***H$_3$)$_2$). The carbene carbon atom was not detected at the ^{13}C{^{1}H} spectrum.

^{27}Al NMR (CD$_2$Cl$_2$): δ 34.7 (s, [***Al***(OC(CF$_3$)$_3$)$_4$]$^-$).

^{19}F{^{1}H} NMR (CD$_2$Cl$_2$): δ -75.7 (s, OC(C***F***$_3$)$_3$).

NMR spectra of reaction mixture

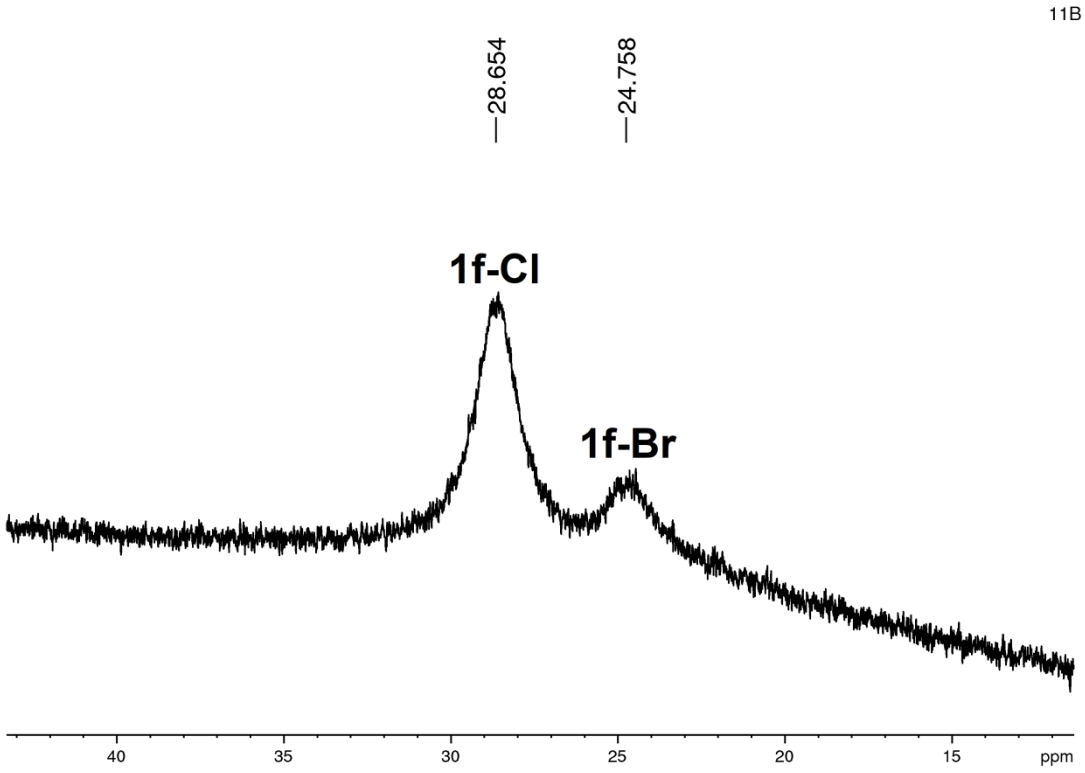

Figure S 78. Reaction of **1a** with AuCl·SMe_2 and Li[Al(OC(CF_3)$_3$)$_4$]: ^{11}B NMR spectrum of reaction mixture

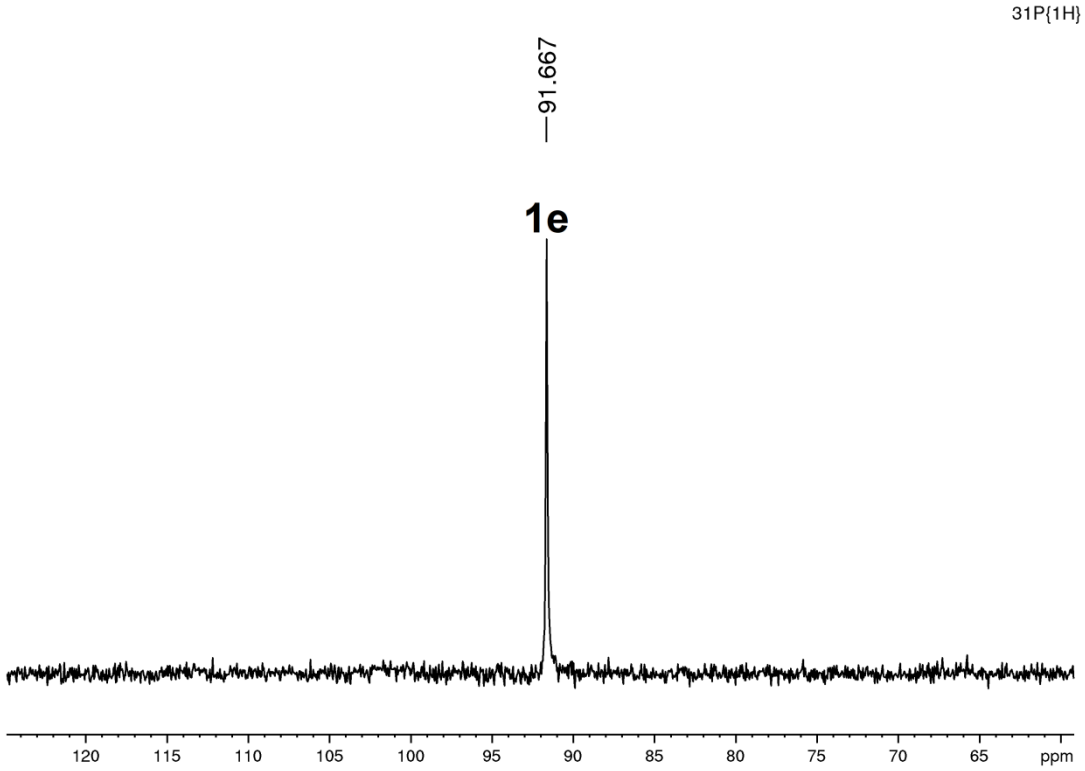

Figure S 79. Reaction of **1a** with AuCl·SMe_2 and Li[Al(OC(CF_3)$_3$)$_4$]: ^{31}P{^{1}H} NMR spectrum of reaction mixture

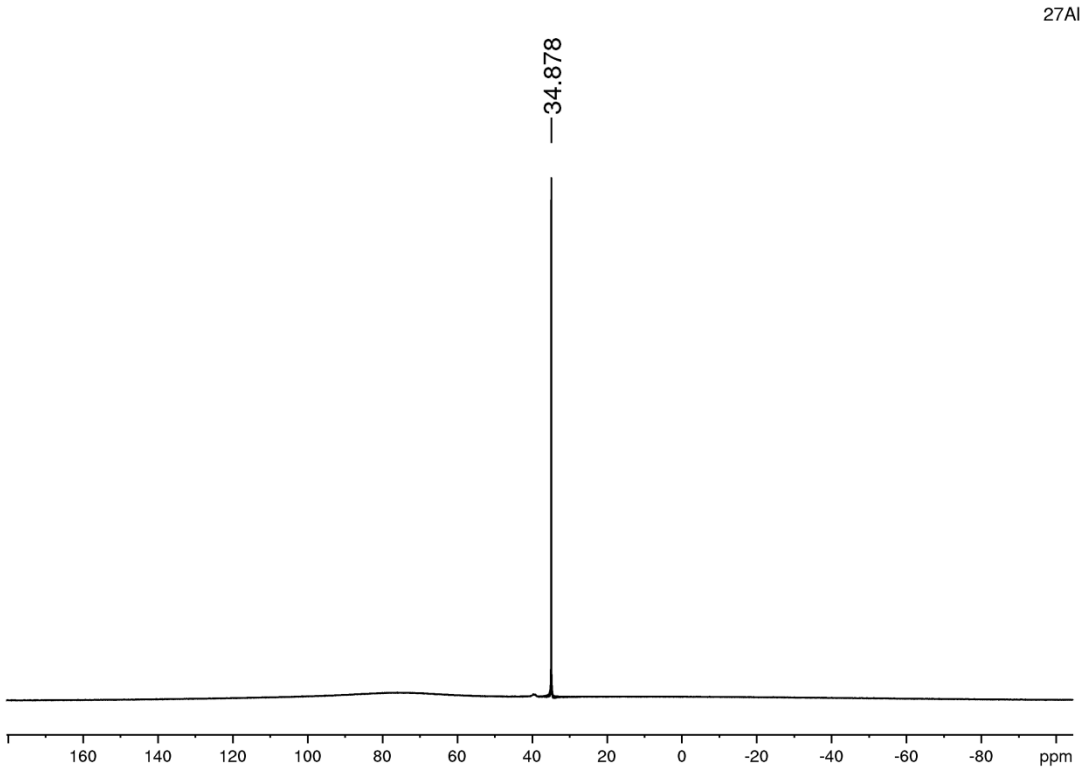

Figure S 80. Reaction of **1a** with AuCl·SMe_2 and Li[Al(OC(CF_3)$_3$)$_4$]: ^{27}Al NMR spectrum of reaction mixture

NMR spectra of 1f

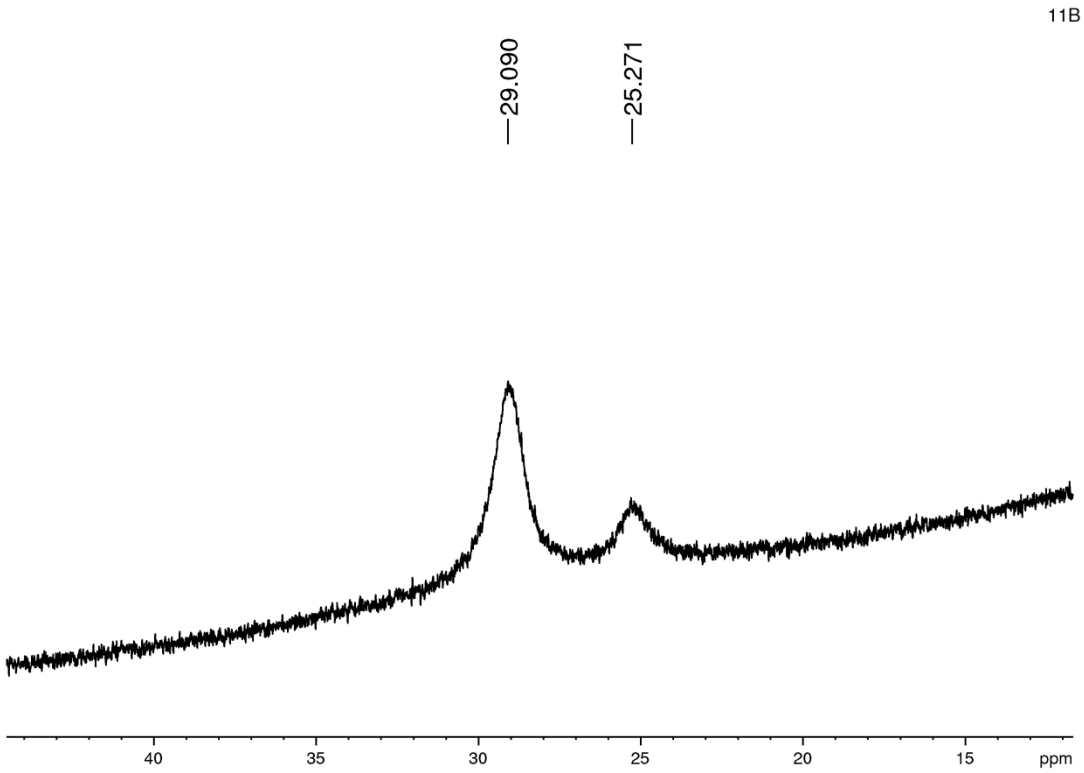

Figure S 81. ^{11}B spectrum (CD_2Cl_2) of **1f**

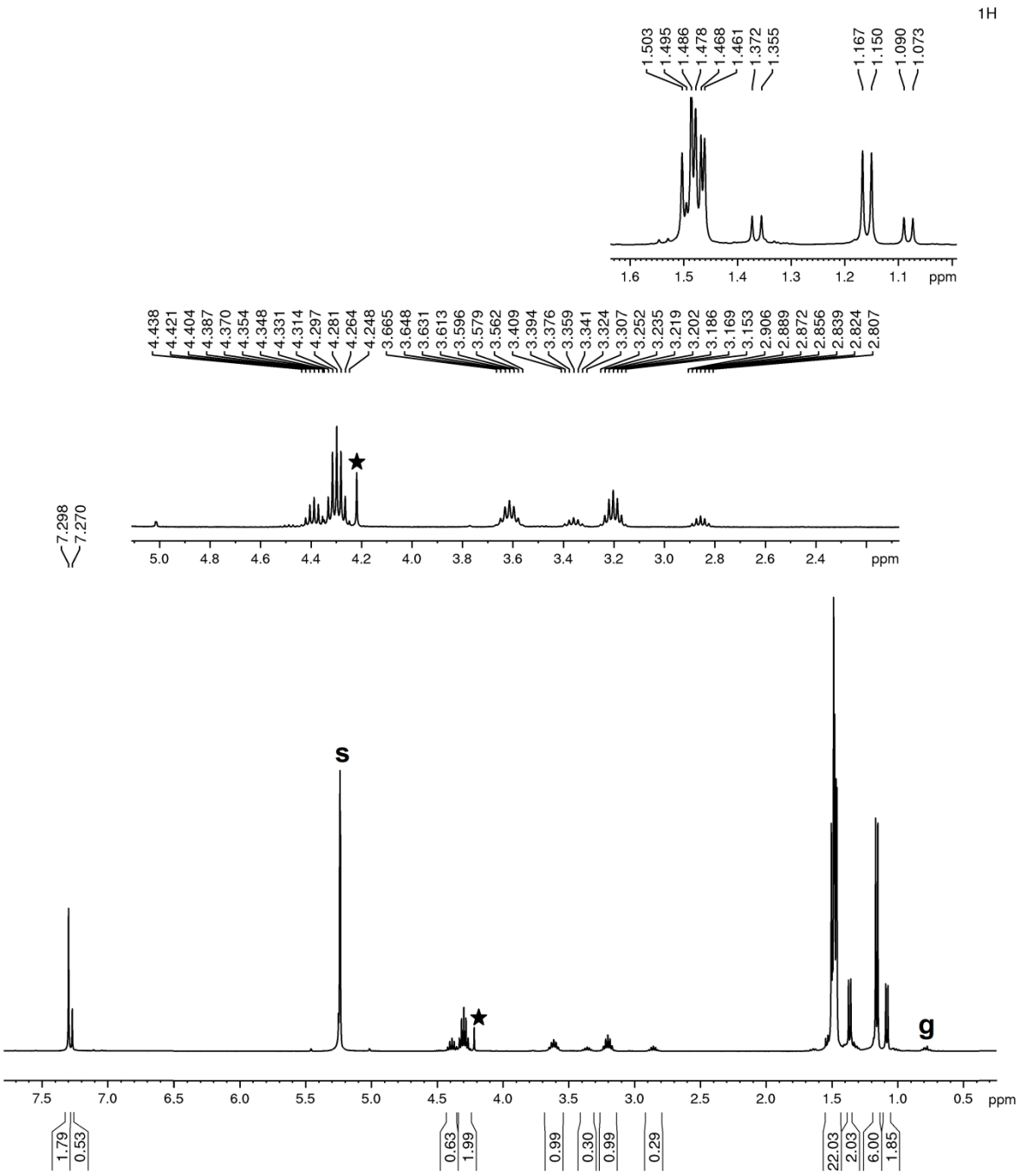

Figure S 82. ^{1}H spectrum (CD_2Cl_2) of **1f**

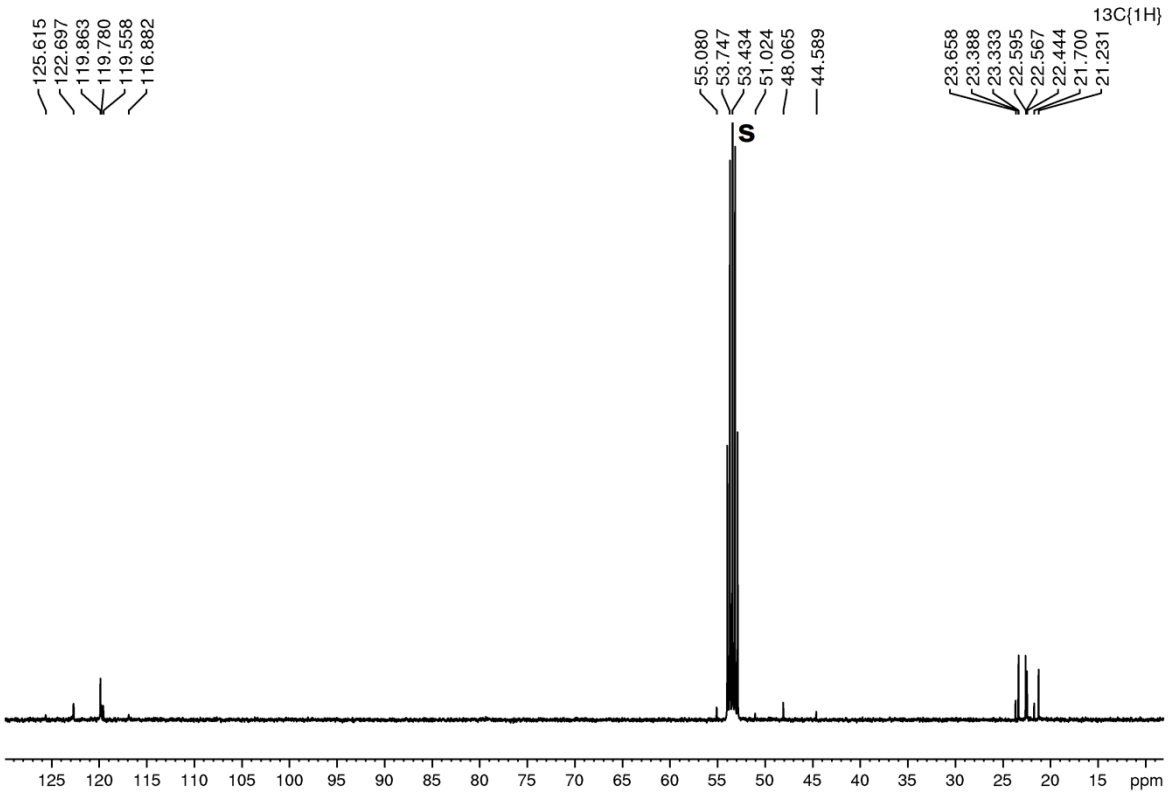

Figure S 83. $^{13}C\{^{1}H\}$ spectrum (CD_2Cl_2) of **1f**

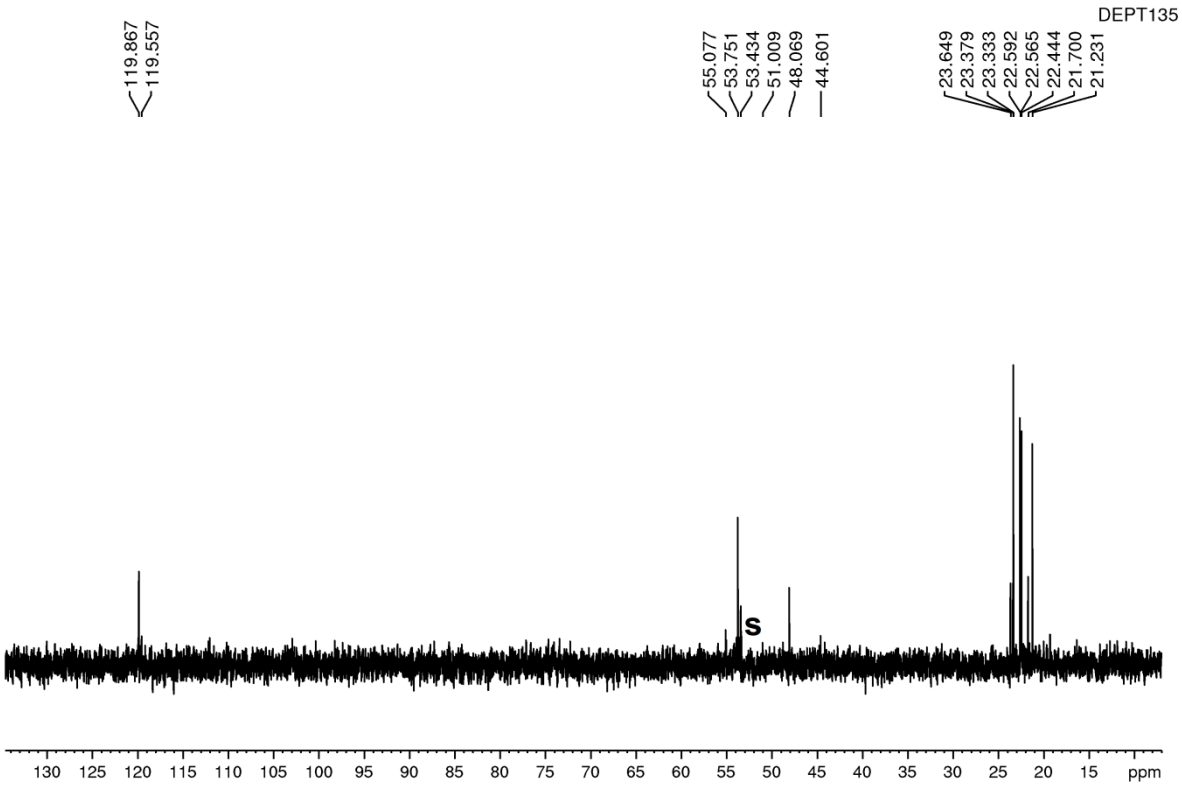

Figure S 84. ^{135}DEPT spectrum (CD_2Cl_2) of **1f**

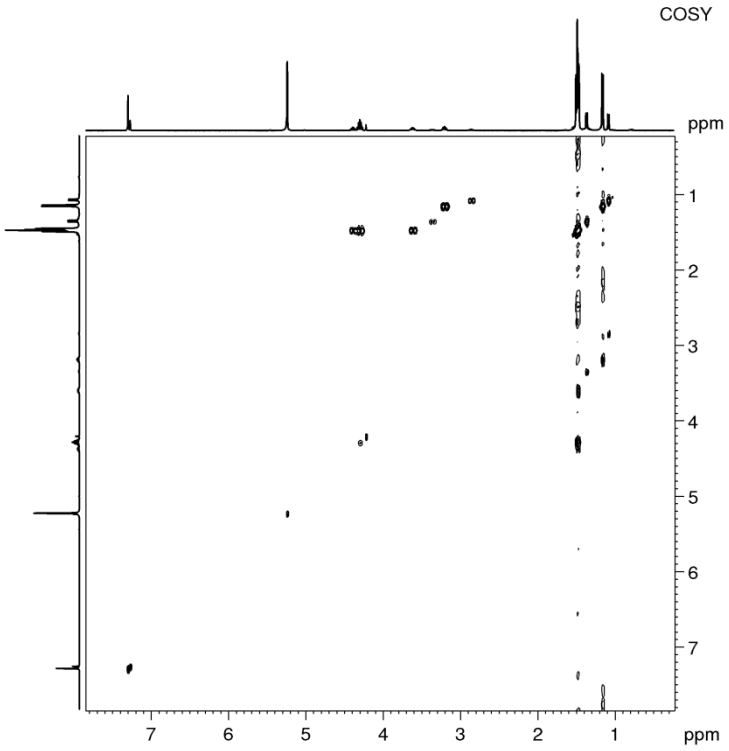

Figure S 85. COSY spectrum (CD_2Cl_2) of **1f**

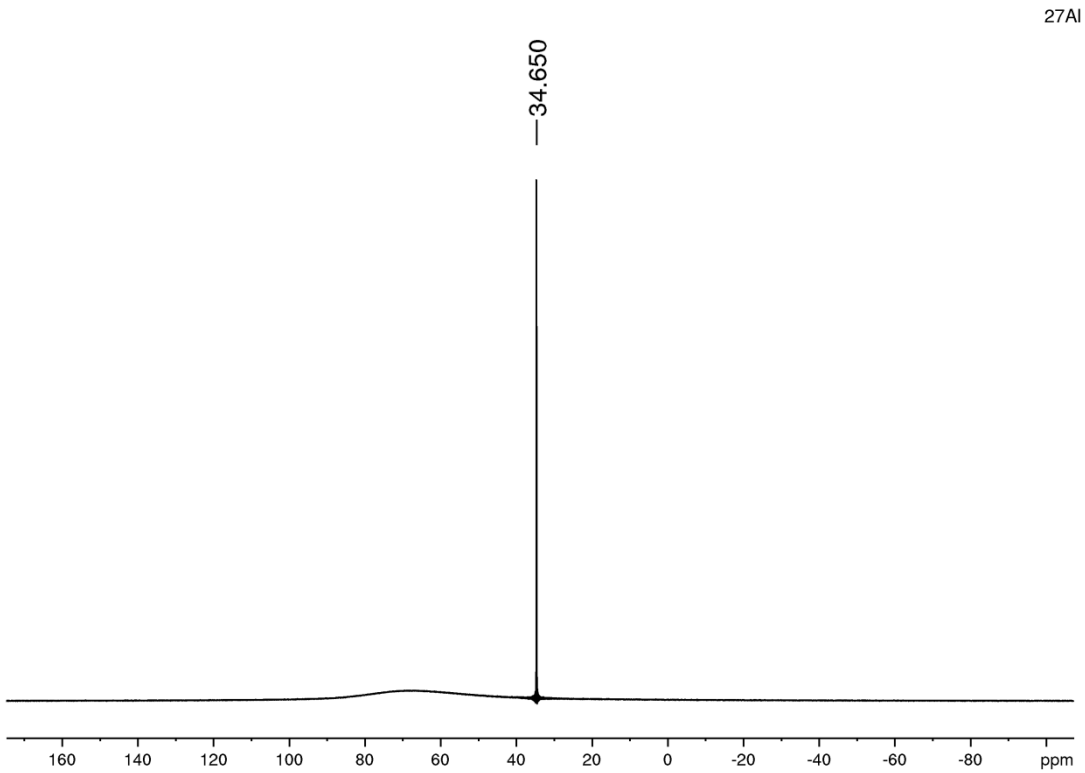

Figure S 86. ^{27}Al spectrum (CD_2Cl_2) of **1f**

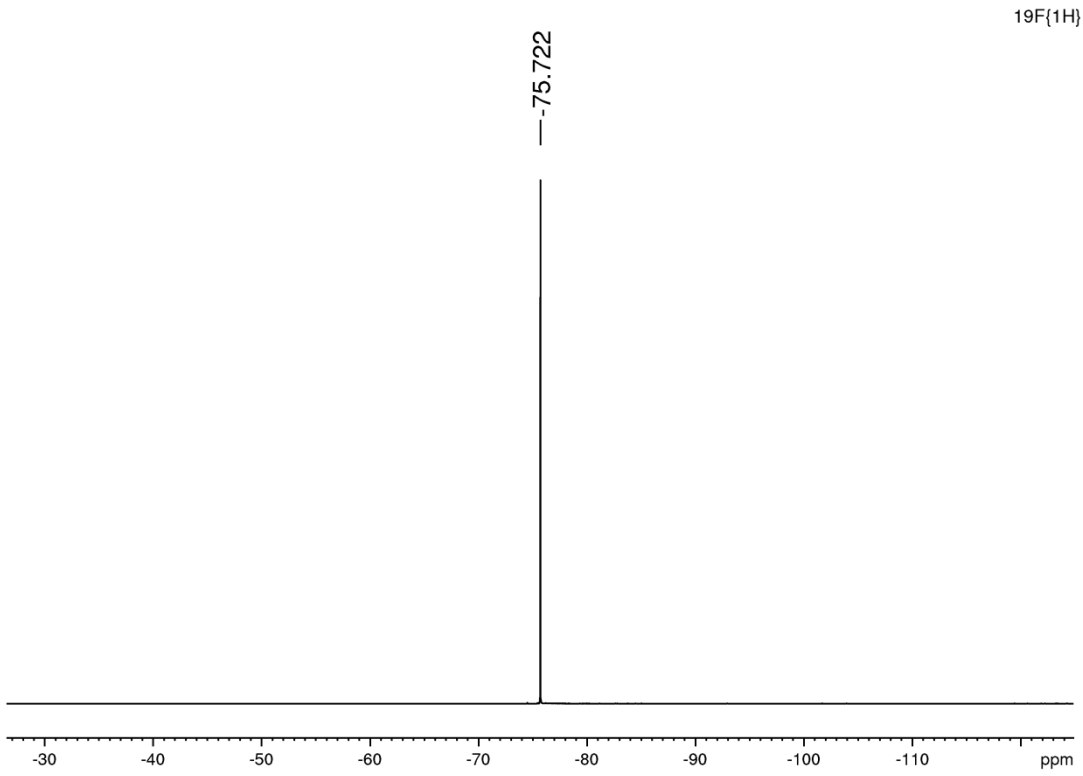

Figure S 87. $^{19}F\{^{1}H\}$ spectrum (CD_2Cl_2) of **1f**

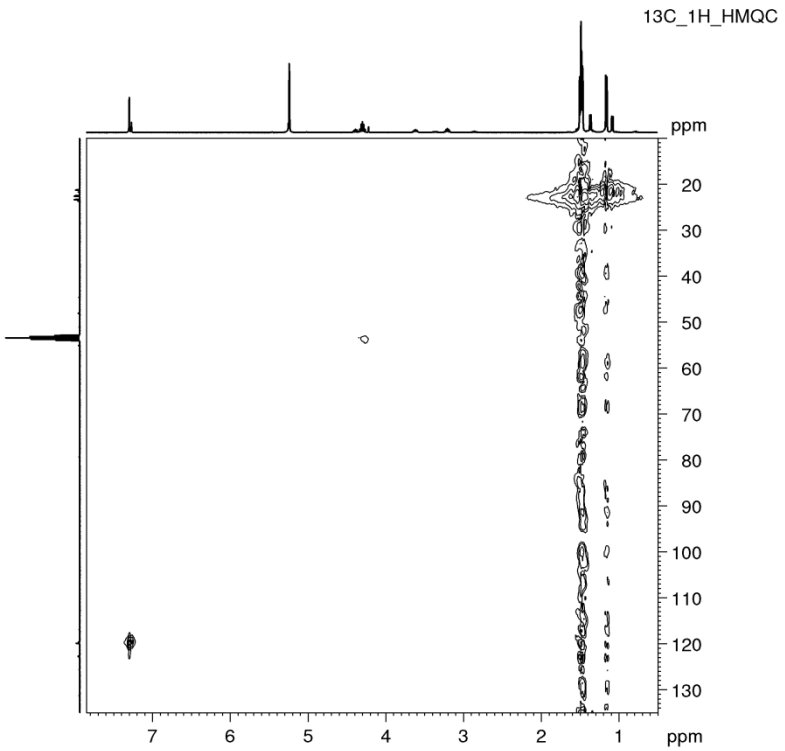

Figure S 88. ^{13}C ^{1}H HMQC spectrum (CD_2Cl_2) of **1f**

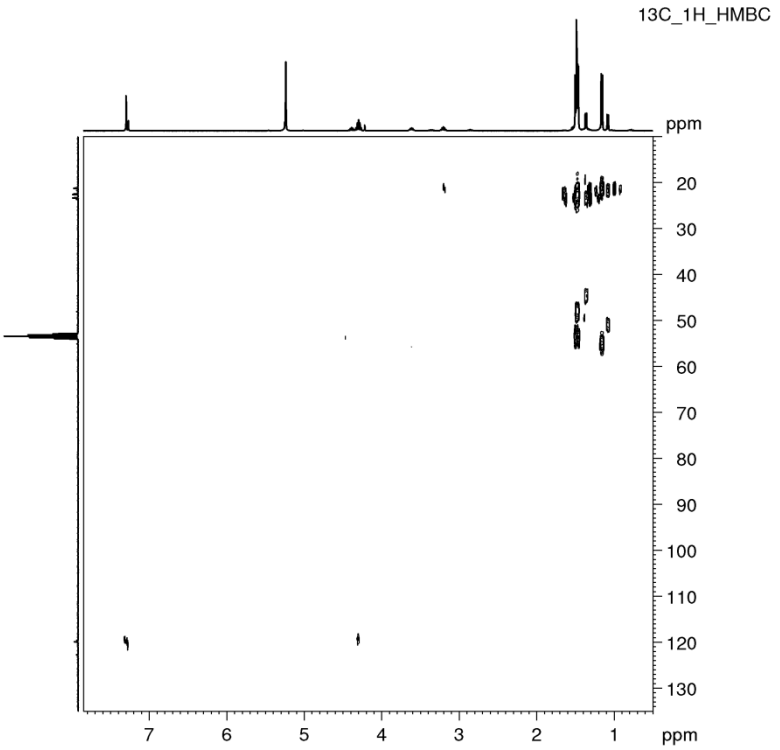

Figure S 89. ^{13}C ^{1}H HMBC spectrum (CD_2Cl_2) of **1f**

Reaction of 1 with Ph_2PCl

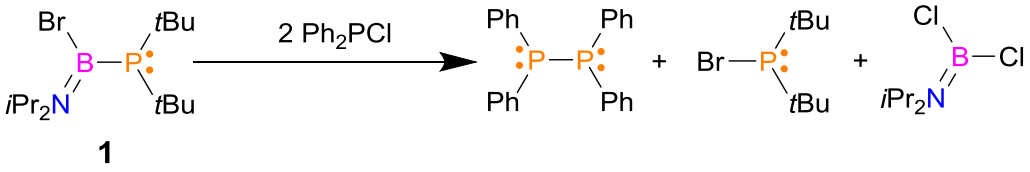

Scheme S 6. Reaction of **1** with Ph_2PCl

A toluene solution of Ph_2PCl (c = 0.1 M, 1 mL) was added dropwise to a stirred solution of **1** (0.034 g, 0.1 mmol) in CH_2Cl_2 (1 mL) at -30°C. The mixture was allowed to warm to room temperature and stirred overnight. Progress of the reaction was monitored by ^{11}B and ^{31}P NMR spectroscopy.

NMR data of reaction mixture

^{11}B NMR (CD_2Cl_2): δ **30.2** (bs, (*i*Pr_2N)BCl_2), 27.8 (bs, (*i*Pr_2N)BClBr), 25.2 (bs, (*i*Pr_2N)BBr_2)

$^{31}P\{^{1}H\}$ NMR (CD_2Cl_2): δ **151.2** (s, *t*Bu_2PBr), 72.1 (s, Ph_2PBr), 33.2 (d, $^{1}J_{PP}$ = 254 Hz, *t*Bu_2PPPh_2), 19.5 (s, *t*Bu_2PH), **-15.3** (s, Ph_2PPPh_2), -26.0 (d, $^{1}J_{PP}$ = 254 Hz, *t*Bu_2PPPh_2)

NMR spectra of reaction mixture

Abbreviations

★	impurity
●	$(i\text{Pr}_2\text{N})\text{BCl}_2$
●	$(i\text{Pr}_2\text{N})\text{BClBr}$
●	$(i\text{Pr}_2\text{N})\text{BBr}_2$
●	Ph_2PBr
●	Ph_2PPPh_2
●	$t\text{Bu}_2\text{PH}$
●	$t\text{Bu}_2\text{PBr}$
●	$t\text{Bu}_2\text{PPPh}_2$

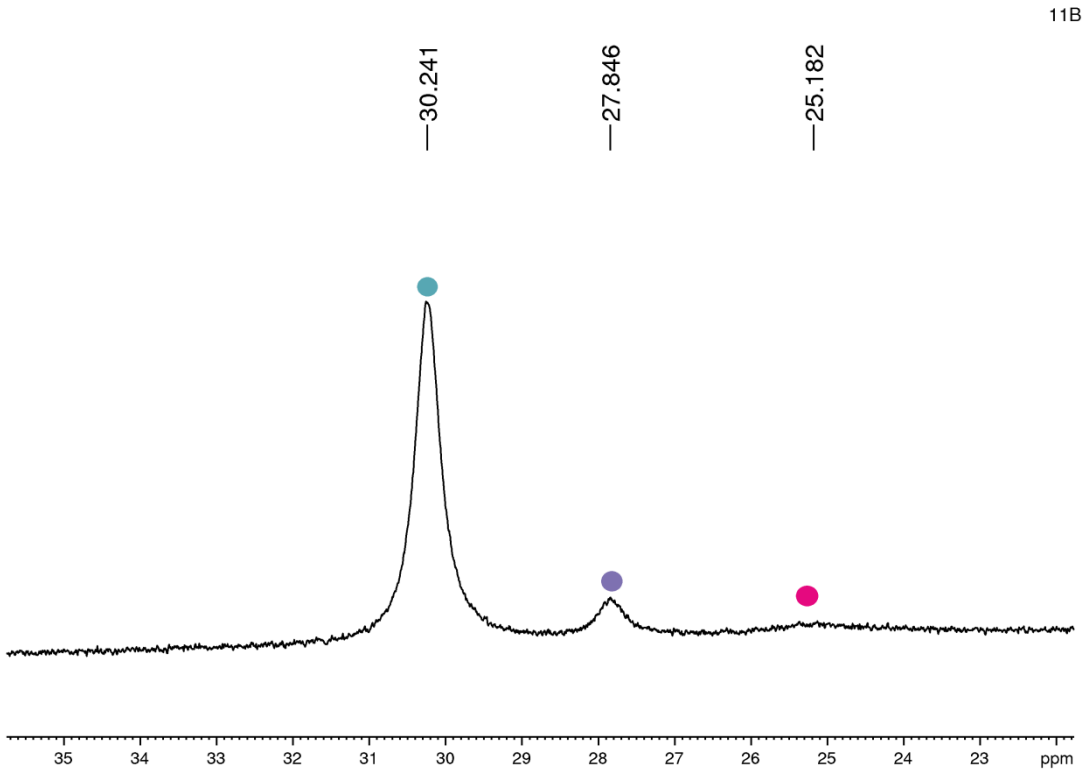

Figure S 90. ^{11}B Reaction of **1** with Ph_2PCl: ^{11}B NMR spectrum of reaction mixture

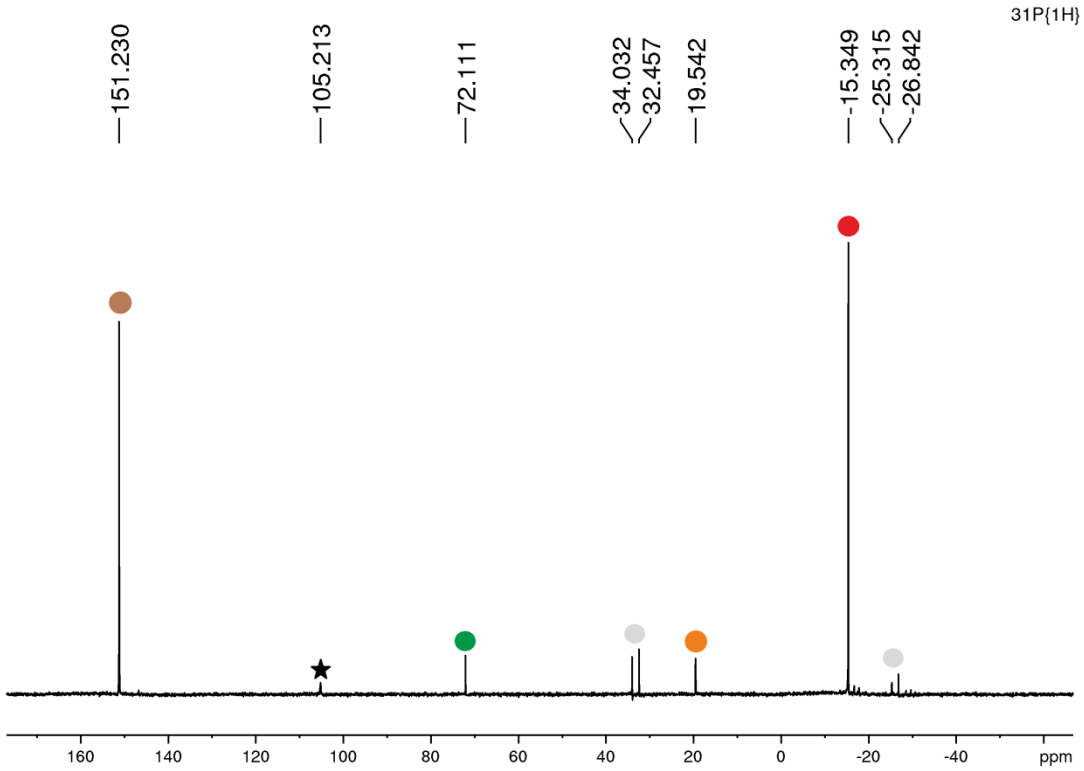

Figure S 91. Reaction of **1** with Ph_2PCl: $^{31}P\{^1H\}$ NMR spectrum of reaction mixture

Reaction of 1a with Ph_2PCl

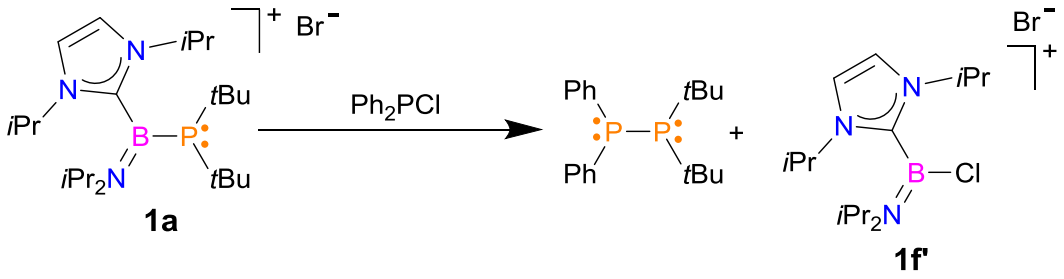

Scheme S 7. Reaction of **1a** with Ph_2PCl

A toluene solution of Ph_2PCl (c = 0.1 M, 1 mL) was added dropwise to a stirred solution of **1a** (0.049 g, 0.1 mmol) in CH_2Cl_2 (1 mL) at -30°C. The mixture was allowed to warm to room temperature and stirred overnight. Progress of the reaction was monitored by ^{11}B and ^{31}P NMR spectroscopy.

^{11}B NMR (CD_2Cl_2): δ **29.4** (bs, **1f'**)

$^{31}P\{^1H\}$ NMR (CD_2Cl_2): δ 146.7 (s, tBu_2PCl), 81.7 (s, Ph_2PCl), 42.0 (s, tBu_2PPtBu_2), **33.2** (d, $^1J_{PP}$ = 254 Hz, tBu_2PPPh_2), 19.5 (s, tBu_2PH), -15.2 (s, Ph_2PPPh_2), **-26.0** (d, $^1J_{PP}$ = 254 Hz, tBu_2PPPh_2)

NMR spectra of reaction mixture

Abbreviations

★	impurity
●	Ph_2PCl
●	Ph_2PPPh_2
●	tBu_2PH
●	tBu_2PCl
●	tBu_2PPPh_2
●	tBu_2PPtBu_2

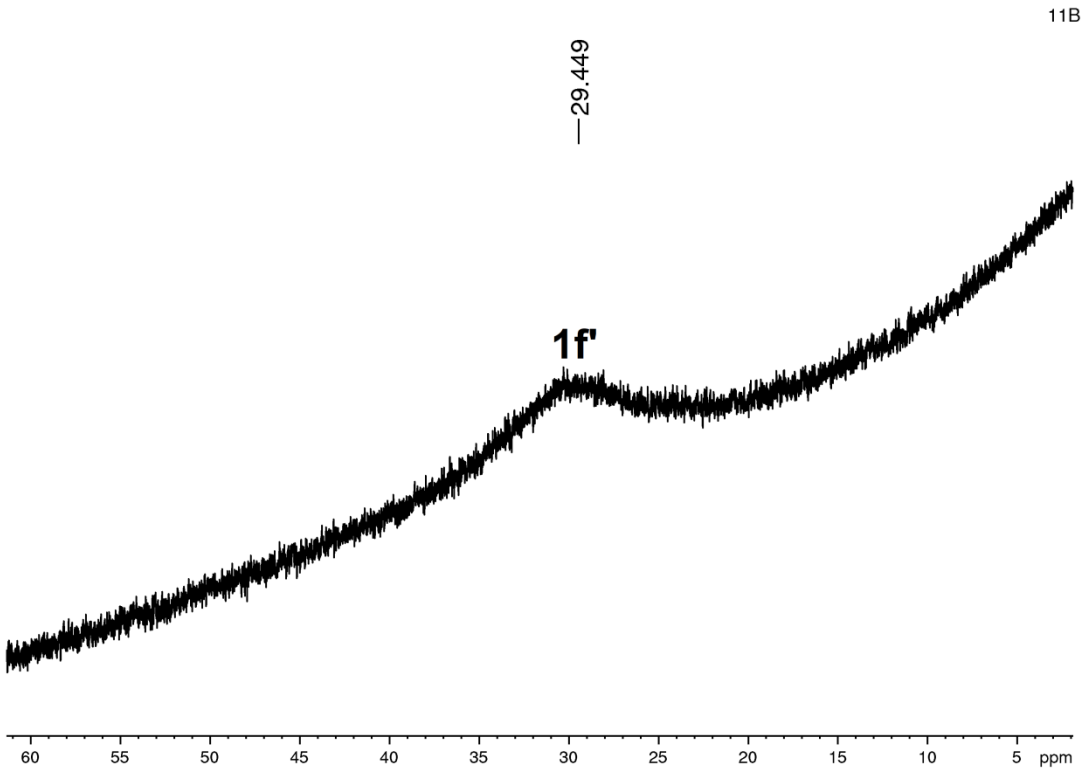

Figure S 92. Reaction of **1a** with Ph_2PCl: ^{11}B NMR spectrum

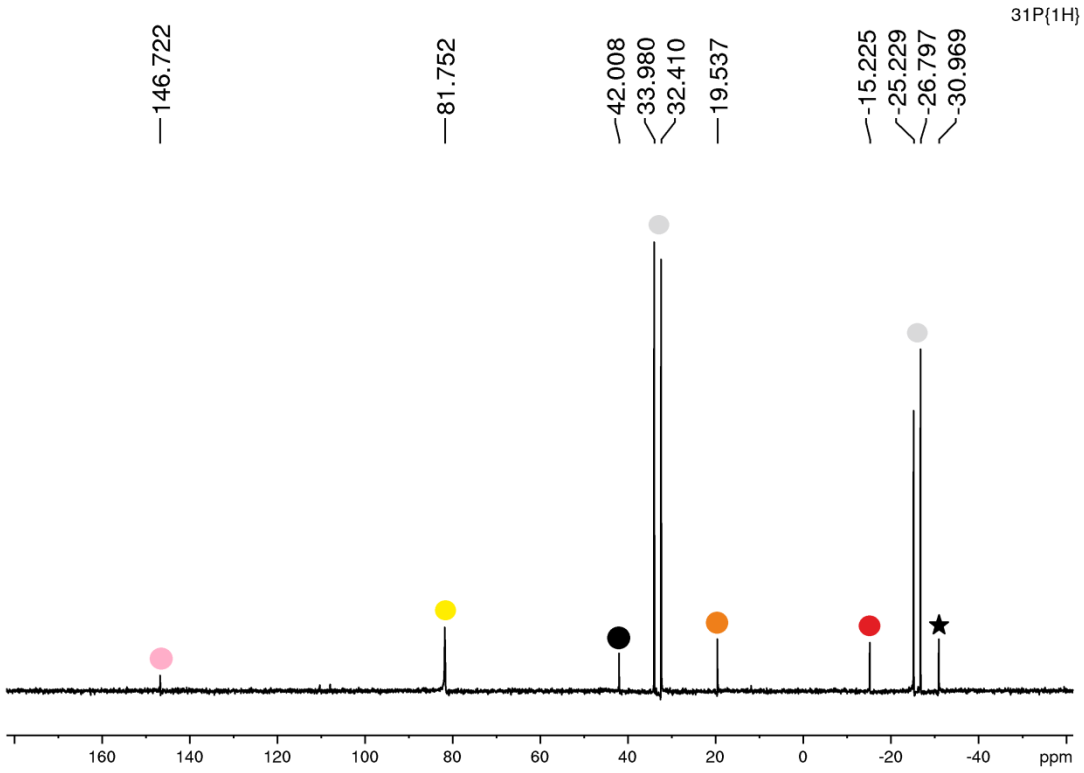

Figure S 93. Reaction of **1a** with Ph_2PCl: $^{31}P\{^1H\}$ NMR spectrum

X-ray structure analysis

X-ray structure analysis details

Diffraction intensity data for all crystals were collected on an IPDS 2T dual beam diffractometer (STOE & Cie GmbH, Darmstadt, Germany) at 120.0(2) K with MoKa radiation of a microfocus X-ray source (GeniX 3D Mo High Flux, Xenocs, Sassenage, 50 kV, 1.0 mA, and λ = 0.71069 Å). Investigated crystals were thermostated under a nitrogen stream at 120 K using the CryoStream-800 device (Oxford CryoSystem, UK) during the entire experiment.

Data collection and data reduction were controlled by using the X-Area 1.75 program (STOE, 2015). Numerical absorption correction was performed for all structures because absorption coefficients were high, m > 0.5 mm^{-1}. The structures were solved using intrinsic phasing implemented in SHELXT and refined anisotropically using the program packages Olex2[7] and SHELX-2015[8,9]. Positions of hydrogen atoms were calculated geometrically taking into account isotropic temperature factors. All H-atoms were refined as riding on their parent atoms with the usual restraints.

Structure **1a** ($C_{23}H_{48}BN_3P^+ \cdot Br^- \cdot CH_2Cl_2$) contains one borenium cation, one bromide anion and one solvate CH_2Cl_2 molecule in the asymmetric unit. P*t*Bu_2 group in the cation turned out to be disordered

over two positions with different spatial orientation and with occupation factors of 0.824(3)/0.176(3). Several restraints were necessary to make refinement stable.

Structure **1c** ($C_{14}H_{32}AuBBrClNP$) contains one molecule of the coordination compound in the asymmetric unit. The structure was solved and refined without any special treatment. However, five B-level warnings were generated by the checkCIF procedure. In our opinion, these warnings are primarily attributed to the presence of the heavy Au atom. We interpret them as artifacts because it is likely that the electron density map has not been modelled accurately. No real atom can be placed at the site where a density of 3.25 e is reported or in close vicinity of Au. We were unable to construct any disorder model to explain this phenomenon. Additionally, there are no indications of any additional atoms in the NMR spectra or elemental analysis, and their presence would not make chemical sense. We also attempted other unsuccessful approaches to explain this behavior, such as using TwinRotMat to detect twinning. However, the diffraction pattern suggests some form of modulation or the formation of a superstructure, which may have contributed to this anomaly.

Structure **1d** exhibit high degree of disorder which is located mainly in the aluminate anion. The $[Al(OC(CF_3)_3)_4]^-$ anion has many modes of deformation which makes it difficult to model. Without any disorder model at the flexible anions, the R_1 indices rise well above 20%. Structure **1d** ($2(C_{16}AlF_{36}O_4^-)\cdot 2(C_{28}H_{64}AuB_2Br_2N_2P_2^+)\cdot 3(C_7H_8)$) contains two positive and two negative ions and three toluene molecules in the asymmetric unit. One anion with Al1 was refined as fully ordered but the other aluminate molecule is strongly disordered. Perfluoroalkoxy group with O5 atom was refined as disordered over two positions with occupation factors of 0.696(16)/0.304(16); group starting from O6 with s.o.f of 0.515(13)/0.485(13); group linked to O8 was also refined in a similar way with occupation factors of 0.574(11)/0.426(11). Lots of restraints were necessary to make refinement stable. We left nine F atoms isotropic due to hard to model, strong disorder in the weakly coordinating anion: $[Al(OC(CF_3)_3)_4]^-$. The present study is not focused on conformation of this anion. The cations are placed in the well-defined positions with relatively small displacement ellipsoids for all atoms.

Asymmetric unit of structure **2** $C_{20}H_{28}BBrNP$ contains one molecule. The structure was solved and refined without any special treatment.

Deposition numbers **2282790** (for **1a**), **2282791** (for **1c**), **2282792** (for **1d**) and **2282793** (for **2**) contain the supplementary crystallographic data for this paper. These data are provided free of charge by the joint Cambridge Crystallographic Data Centre and Fachinformationszentrum Karlsruhe www.ccdc.cam.ac.uk/structures.

Table S 1. Crystal data and structure refinement for **1a**, **1c**, **1d**, and **2**

	1a	**1c**	**1d**	**2**
CCDC deposition No	2282790	2282791	2282792	2282793
Chemical formula	$C_{23}H_{48}BN_3P^+ \cdot Br^- \cdot CH_2Cl_2$	$C_{14}H_{32}AuBBrClNP$	$2(C_{16}AlF_{36}O_4^-) \cdot 2(C_{28}H_{64}AuB_2Br_2N_2P_2^+) \cdot 3(C_7H_8)$	$C_{20}H_{28}BBrNP$
M_r [g·mol^{-1}]	573.26	568.51	3948.99	404.12
Crystal system	Monoclinic	Monoclinic	Monoclinic	Monoclinic
Space group	$P2_1/n$	$P2_1/c$	$P2_1/c$	$P2_1/c$
Temperature [K]	120	120	120	120
a [Å] b [Å] c [Å]	17.2597(4) 10.7727(2) 18.5283(5)	11.9513(11) 9.9691(9) 17.3494(15)	24.8390(11) 23.5598(8) 26.1742 (12)	12.3679(9) 12.3039(8) 14.0443 (11)
α [°] β [°] γ [°]	90 113.564(2) 90	90 92.402(7) 90	90 91.128(4) 90	90 105.345(6) 90
V [Å^3]	3157.76(13)	2065.3(3)	15314.2(11)	2061.0(3)
Z	4	4	4	4
Radiation type λ [Å]	Mo $K\alpha$ 0.71073	Mo $K\alpha$ 0.71073	Mo $K\alpha$ 0.71073	Mo $K\alpha$ 0.71073
Calculated density [g·cm^{-1}]	1.206	1.828	1.713	1.302
μ [mm^{-1}]	1.54	9.26	3.15	2.07
Crystal size [mm]	0.43 × 0.16 × 0.05	0.26 × 0.14 × 0.11	0.32 × 0.21 × 0.15	0.35 × 0.29 × 0.09
F(000)	1216	1096	7800	840
R_{int}	0.042	0.063	0.040	0.057
No. of measured, independent and observed [$I > 2\sigma(I)$] reflections	39054 8543 7337	13321 4274 4041	158079 33063 24985	22427 3917 3024
$R[F^2 > 2\sigma(F^2)]$	0.056	0.057	0.064	0.037
$wR(F^2)$	0.139	0.150	0.138	0.092
S	1.12	1.08	1.17	1.00
No. of reflections	8543	4274	33063	3917
No. of parameters	347	191	2066	223
No. of restraints	17	0	137	0
$\Delta>_{max}$ [e·Å^{-3}] $\Delta>_{min}$ [e·Å^{-3}]	1.78 -1.37	3.43 -2.79	2.33 -1.17	0.54 -0.23

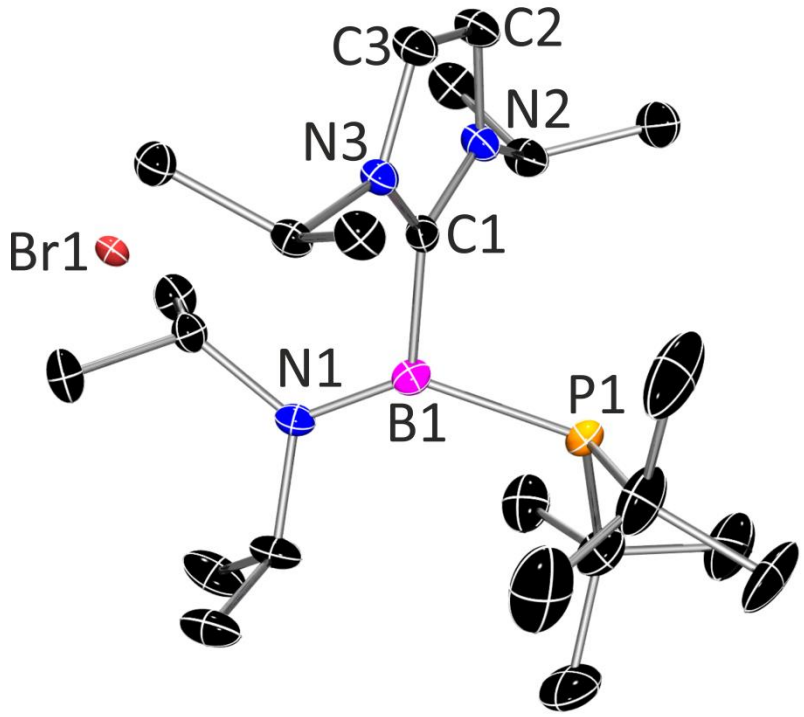

Figure S 94. Molecular structure of **1a**. The thermal ellipsoids are shown at the 40% probability level. The solvent molecule (CH_2Cl_2) and hydrogen atoms are omitted for clarity. Important bond distances [Å]: B1 – P1 1.991(3); B1 – N1 1.390(4); B1 – C1 1.604(4); C1 – N2 1.355(4); C1 – N3 1.358(3); N2 – C2 1.377(4); N3 – C3 1.382(4); C2 – C3 1.355(4). Important angles [°]: N1 – B1 – P1 135.6(2), P1 – B1 – C1 105.99(19), C1 – B1 – N1 117.6(3); B1 – P1 – C10 115.52(16), C10 – P1 – C14 111.8(3), C14 – P1 – B1 104.6(3); B1 – C1 – N2 126.5(2), N2 – C1 – N3 105.7(2), N3 – C1 – B1 127.8(2); B1 – N1 – C18 120.3(3), C18 – N1 – C21 119.3(2), C21 – N1 – B1 120.3(2); C1 – N2 – C2 110.5(2), C2 – N2 – C4 123.8(2), C4 – N2 – C1 125.4(2); C1 – N3 – C3 109.8(2), C3 – N3 – C7 123.1(2), C7 – N3 – C1 126.8(2).

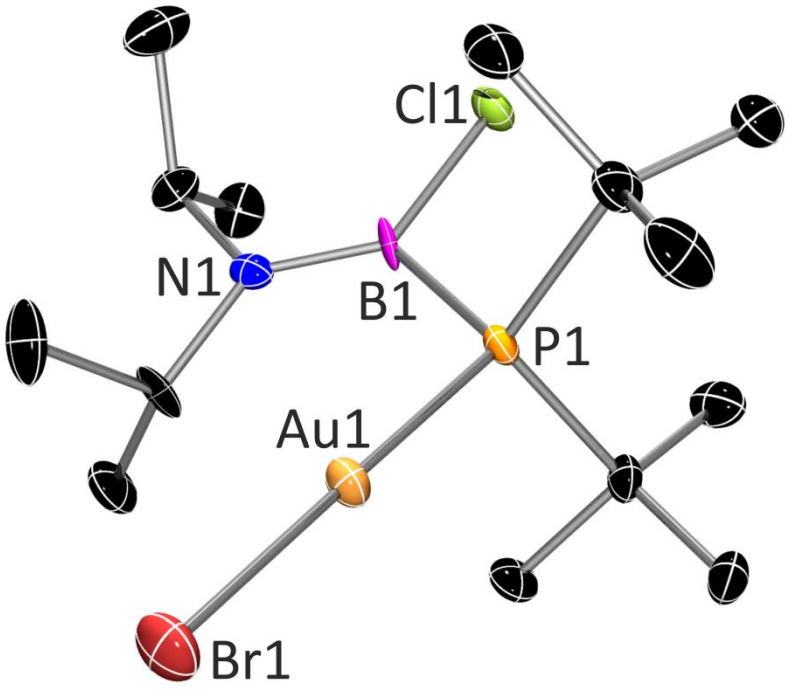

Figure S 95. Molecular structure of **1c**. The thermal ellipsoids are shown at the 40% probability level. Hydrogen atoms are omitted for clarity. Important bond distances [Å]: Au1 – P1 2.268(2); B1 – P1 1.981(9); B1 – N1 1.37(1); B1 – Cl1 1.828(9); Au1 – Br1 2.408(1). Important angles [°]: P1 – Au1 – Br1 178.62(5); N1 – B1 – P1 126.3(6), P1 – B1 – Cl1 114.2(5), Cl1 – B1 – N1 119.5(6); B1 – P1 – Au1 115.0(3), Au1 – P1 – C1 106.1(3), C1 – P1 – C5 114.4(4),

C5 – P1 – Au1 109.8(3), C5 – P1 – B1 104.1(4), B1 – P1 – C1 107.6(4); B1 – N1 – C9 123.0(7), C9 – N1 – C12 111.8(7), C12 – N1 – B1 125.1(7).

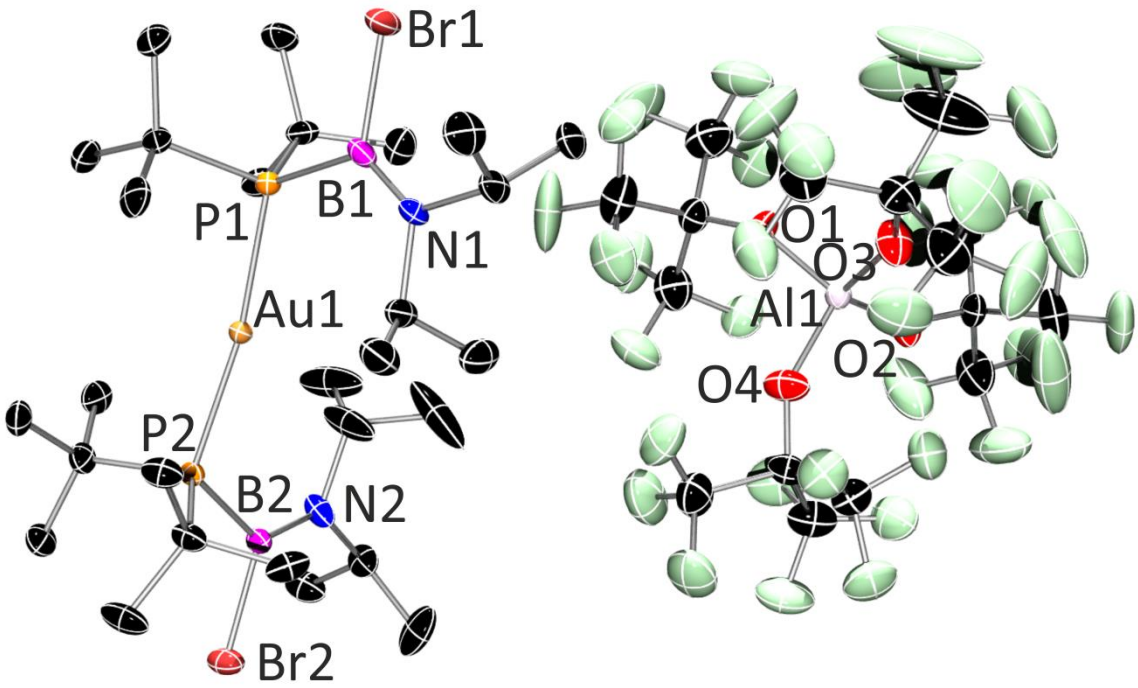

Figure S 96. Molecular structure of **1d**. The thermal ellipsoids are shown at the 40% probability level. The solvent molecules (toluene) and hydrogen atoms are omitted for clarity. Important bond distances [Å]: Au1- P1 2.3487(18); Au1 – P2 2.3455(18); B1 – P1 1.965(9); B2 – P2 1.985(9); B1 – N1 1.366(11); B2 – N2 1.370(10); B1 –Br1 1.971(9); B2 – Br2 1.965(8). Important angles [°]: P1 – Au1 – P2 171.55(6); N1 – B1 – P1 127.2(6), P1 – B1 – Br1 113.0(5), Br1 – B1 – N1 119.9(6); N2 –B2 – P2 127.2(6), P2 – B2 – Br2 113.2(4), Br2 – B2 – N2 119.6(6); B1 – P1 – Au1 118.3(3), Au1 – P1 – C7 107.5(2), C7 – P1 – C11 113.6(4), C11 – P1 – Au1 103.8(2), C11 – P1 – B1 107.5(4), B1 – P1 – C7 106.3(4); B2 – P2 – Au1 118.8(2), Au1 – P2 – C21 104.8(3), C21 – P2 – C25 113.6(4), C25 – P2 – Au1 105.7(2), C25 – P2 – B2 108.2(4), B2 – P2 – C21 106.0(4); B1 – N1 – C1 126.3 (6), C1 – N1 – C4 110.9(6), C4 – N1 – B1 122.7(6); B2 – N2 – C15 125.9(7); C15 – N2 – C18 112.7(6), C18 – N2 – B2 121.4(7).

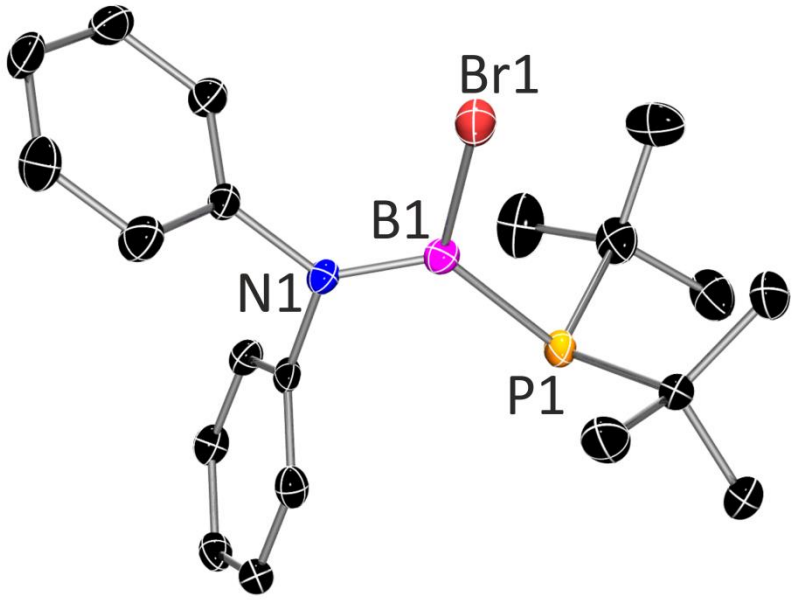

Figure S 97. Molecular structure of **2**. The thermal ellipsoids are shown at the 40% probability level. Hydrogen atoms are omitted for clarity. Important bond distances [Å]: B1–Br1 1.960(3); B1–P1 1.936(3); B1–N1 1.393(4). Important angles [°]: P1–B1–N1 119.9(2), N1–B1–Br1 115.7(2), Br1–B1–P1 124.34(16); B1–P1–C1 105.57(13), C1–P1–C5 111.78(13), C5–P1–B1 101.13(13); B1–N1–C9 124.8(2), C9–N1–C15 112.61(19), C15–N1–B1 122.6(2).

DFT calculations

General methods

The equilibrium structures of all systems investigated in this work were calculated using density functional theory (DFT) method, ωB97xD[10] hybrid functional, with the 6-311++G(d,p)[11] Pople's basis set of triple-zeta quality. The corresponding harmonic frequencies were computed at the same level of theory. The Gibbs free energies of the resulted structures were estimated using ωB97xD/6-311++G(d,p) electronic energies with zero-point energy corrections, thermal corrections and entropy contributions (at T=298.15 K). The effects of surrounding solvent molecules (dichloromethane) were obtained using the polarizable continuum model (the integral equation formalism variant: IEFPCM).[12] The Natural Bond Orbital analysis were performed with the Gaussian NBO 7 module.[13] All calculations were completed with Gaussian16 (Rev.C.01) software.[14]

Cartesian coordinates

The Cartesian coordinates of all systems investigated in this contribution.

1

P	1.177055000	-0.045296000	-0.643774000
N	-1.873979000	-0.060724000	-0.059105000
C	-2.658498000	-0.305970000	-1.315600000
H	-1.915879000	-0.340142000	-2.117400000
B	-0.549649000	-0.041777000	-0.148416000
C	-2.605663000	0.125245000	1.229697000
H	-3.631540000	-0.188691000	1.034474000
C	2.006802000	-1.587810000	0.057486000
C	-2.605250000	1.595924000	1.631472000
H	-1.591877000	1.933452000	1.866408000
H	-3.222382000	1.730448000	2.522077000
H	-3.004794000	2.226652000	0.836346000
C	1.797033000	1.984832000	1.281110000
H	0.758271000	2.010937000	1.617875000
H	2.229287000	2.977580000	1.443022000
H	2.342142000	1.279227000	1.907237000
C	-2.017471000	-0.777988000	2.306203000
H	-2.032615000	-1.823088000	1.990656000
H	-2.603739000	-0.684584000	3.222079000
H	-0.986563000	-0.493023000	2.542081000
C	1.896591000	1.643592000	-0.210062000
C	-3.347709000	-1.662948000	-1.241299000
H	-2.624059000	-2.456025000	-1.042826000
H	-3.831833000	-1.866837000	-2.198308000
H	-4.118738000	-1.687533000	-0.467456000
C	-3.613312000	0.846301000	-1.594633000
H	-4.389550000	0.925236000	-0.829723000
H	-4.107305000	0.668500000	-2.551865000
H	-3.076925000	1.795172000	-1.655237000
C	3.362640000	1.658588000	-0.663212000
H	3.978880000	0.975834000	-0.074026000
H	3.762004000	2.666885000	-0.520235000
H	3.466012000	1.400371000	-1.719932000
C	1.085502000	2.658118000	-1.029944000
H	1.160756000	2.467906000	-2.102839000
H	1.477669000	3.660045000	-0.832072000
H	0.027204000	2.660484000	-0.749723000
C	2.565182000	-1.387436000	1.468446000
H	3.372797000	-0.653164000	1.488923000
H	2.981958000	-2.339125000	1.813497000
H	1.792571000	-1.079715000	2.175550000
C	3.137499000	-1.972013000	-0.909957000
H	2.754414000	-2.172444000	-1.913259000
H	3.622379000	-2.881008000	-0.541693000
H	3.900292000	-1.193748000	-0.980376000
C	0.940878000	-2.692555000	0.063246000
H	0.170058000	-2.510274000	0.816971000
H	1.424505000	-3.642708000	0.307543000

1a

15	-1.615239000	-0.776155000	0.001481000
7	0.304057000	1.640313000	-0.393173000
7	1.486436000	-1.758222000	-1.024266000
7	2.267799000	-0.786368000	0.736375000
6	1.285593000	-0.725358000	-0.188098000
6	2.585480000	-2.478093000	-0.621764000
1	2.937177000	-3.345131000	-1.153025000
6	3.072043000	-1.872702000	0.485143000
1	3.917481000	-2.122493000	1.102184000
6	0.743571000	-2.018322000	-2.277434000
1	-0.081915000	-1.306955000	-2.273053000
6	1.646451000	-1.737371000	-3.473005000
1	2.047453000	-0.722155000	-3.431207000
1	1.067281000	-1.842745000	-4.392202000

1	2.481274000	-2.441795000	-3.516858000
6	0.167281000	-3.425654000	-2.265042000
1	0.954144000	-4.184308000	-2.261064000
1	-0.434115000	-3.572791000	-3.164034000
1	-0.472020000	-3.565469000	-1.391458000
6	2.522743000	0.187016000	1.822039000
1	1.752130000	0.950403000	1.707836000
6	2.394522000	-0.469451000	3.191324000
1	1.405443000	-0.898690000	3.347468000
1	2.565734000	0.284908000	3.961387000
1	3.141142000	-1.256843000	3.320671000
6	3.895794000	0.822874000	1.623714000
1	4.693297000	0.100473000	1.814376000
1	4.015093000	1.646726000	2.329529000
1	4.016467000	1.214009000	0.612537000
6	-3.211782000	0.082956000	-0.575009000
6	-3.898461000	1.110100000	0.337176000
1	-4.144713000	0.690149000	1.313289000
1	-4.840167000	1.419947000	-0.129402000
1	-3.317507000	2.016744000	0.504643000
6	-4.225588000	-1.047962000	-0.850134000
1	-3.791927000	-1.827041000	-1.481892000
1	-5.091196000	-0.627615000	-1.373901000
1	-4.591085000	-1.513624000	0.065116000
6	-2.871163000	0.706869000	-1.938274000
6	-1.689288000	-1.256800000	1.836595000
1	-2.116558000	0.743456000	2.609820000
6	-0.688270000	2.656602000	0.024497000
1	-1.585109000	2.069990000	0.184822000
6	-0.357594000	3.286509000	1.382727000
1	-0.052219000	2.527463000	2.105290000
1	-1.257131000	3.772179000	1.770751000
1	0.423976000	4.043523000	1.318793000
6	-1.024696000	3.734300000	-1.004674000
1	-0.222996000	4.465605000	-1.120400000
1	-1.909164000	4.273915000	-0.656694000
1	-1.253237000	3.317747000	-1.985895000
6	1.577246000	2.058722000	-1.036484000
1	2.238756000	1.195939000	-0.948567000
6	1.407013000	2.297134000	-2.540537000
1	0.845418000	1.480707000	-3.000727000
1	2.393258000	2.343206000	-3.009671000
1	0.891995000	3.233468000	-2.756193000
6	2.295811000	3.225635000	-0.363250000
1	1.783798000	4.176446000	-0.515250000
1	3.290567000	3.317783000	-0.806119000
1	2.419691000	3.066243000	0.708605000
5	0.032389000	0.285654000	-0.179165000
6	-0.642972000	-2.365496000	2.046069000
1	-0.898233000	-3.254828000	1.465122000
1	-0.617714000	-2.645413000	3.105133000
1	0.366295000	-2.065697000	1.765359000
6	-3.051789000	-1.869767000	2.189372000
1	-3.864061000	-1.143262000	2.156732000
1	-3.004078000	-2.258273000	3.212460000
1	-3.302094000	-2.703439000	1.528817000
6	-1.408392000	-0.073324000	2.769227000
1	-0.402997000	0.325914000	2.613875000
1	-1.483726000	-0.388107000	3.816637000
1	-2.124313000	1.495090000	-1.868795000
1	-3.776466000	1.139583000	-2.376626000
1	-2.495856000	-0.051449000	-2.632227000

References

1 N. Szynkiewicz, A. Ordyszewska, J. Chojnacki and R. Grubba, *RSC Adv.*, 2019, **9**, 27749–27753.

2 K. Kaniewska-Laskowska, K. Klimsiak, N. Szynkiewicz, J. Chojnacki and R. Grubba, *Chem. Commun.*, 2022, **58**, 10068–10071.

3 I. Krossing, *Chem. - A Eur. J.*, 2001, **7**, 490–502.

4 T. Schaub, M. Backes and U. Radius, *Organometallics*, 2006, **25**, 4196–4206.

5 J. Messelberger, A. Grünwald, S. J. Goodner, F. Zeilinger, P. Pinter, M. E. Miehlich, F. W. Heinemann, M. M. Hansmann and D. Munz, *Chem. Sci.*, 2020, **11**, 4138–4149.

6 S. Burling, B. M. Paine, D. Nama, V. S. Brown, M. F. Mahon, T. J. Prior, P. S. Pregosin, M. K. Whittlesey and J. M. J. Williams, *J. Am. Chem. Soc.*, 2007, **129**, 1987–1995.

7 O. V Dolomanov, L. J. Bourhis, R. J. Gildea, J. A. K. Howard and H. Puschmann, *J. Appl. Crystallogr.*, 2009, **42**, 339–341.

8 G. M. Sheldrick, *Acta Cryst. A*, 2015, **71**, 3–8.

9 G. M. Sheldrick, *Acta Cryst. C*, 2015, **71**, 3–8.

10 J. Da Chai and M. Head-Gordon, *Phys. Chem. Chem. Phys.*, 2008, **10**, 6615–6620.

11 R. Krishnan, J. S. Binkley, R. Seeger and J. A. Pople, *J. Chem. Physicsournal Chem. Phys.*, 1980, **72**, 650–654.

12 S. Miertuš, E. Scrocco and J. Tomasi, *Chem. Phys.*, 1981, **55**, 117–129.

13 E. D. Glendening, J. K. Badenhoop, A. E. Reed, J. E. Carpenter, J. A. Bohmann, C. M. Morales, P. Karafiloglou, C. R. Landis and F. Weinhold, *NBO 7.0.*, Theoretical Chemistry Institute, University of Wisconsin, Madison, 2018.

14 M. J. Frisch, G. W. Trucks, H. B. Schlegel, G. E. Scuseria, M. A. Robb, J. R. Cheeseman, G. Scalmani, V. Barone, B. Mennucci, G. A. Petersson, H. Nakatsuji, M. Caricato, X. Li, H. P. Hratchian, A. F. Izmaylov, J. Bloino, G. Zheng, J. L. Sonnenberg, M. Hada, M. Ehara, K. Toyota, R. Fukuda, J. Hasegawa, M. Ishida, T. Nakajima, Y. Honda, O. Kitao, H. Nakai, T. Vreven, J. A. Montgomery, Jr., J. E. Peralta, F. Ogliaro, M. Bearpark, J. J. Heyd, E. Brothers, K. N. Kudin, V. N. Staroverov, R. Kobayashi, J. Normand, K. Raghavachari, A. Rendell, J. C. Burant, S. S. Iyengar, J. Tomasi, M. Cossi, N. Rega, J. M. Millam, M. Klene, J. E. Knox, J. B. Cross, V. Bakken, C. Adamo, J. Jaramillo, R. Gomperts, R. E. Stratmann, O. Yazyev, A. J. Austin, R. Cammi, C. Pomelli, J. W. Ochterski, R. L. Martin, K. Morokuma, V. G. Zakrzewski, G. A. Voth, P. Salvador, J. J. Dannenberg, S. Dapprich, A. D. Daniels, Ö. Farkas, J. B. Foresman, J. V. Ortiz, J. Cioslowski and D. J. Fox,

Gaussian 16, Gaussian, Inc., Wallingford CT, 2016.